Title
Distinct functional programming in human fetal and adult monocytes

Permalink
https://escholarship.org/uc/item/4mz4351g

Author
Krow-Lucal, Elisabeth

Publication Date
2014

Peer reviewed|Thesis/dissertation

Distinct functional programming in human fetal and adult monocytes

by

Elisabeth Krow-Lucal

DISSERTATION

Submitted in partial satisfaction of the requirements for the degree of

DOCTOR OF PHILOSOPHY

in

Biomedical Sciences

in the

GRADUATE DIVISION

of the

UNIVERSITY OF CALIFORNIA, SAN FRANCISCO

Acknowledgements

I would like to thank my thesis advisor, Mike McCune, for all the support and love over the years. I never would have imagined I would have a PI who cared just as much about my happiness outside of the lab as in it. I have been truly lucky to have worked for him and been a part of his lab. I would also like to thank my lab family, in particular, the members of the first ever McCune Lab Gradical, Maggie, Chris, Ivan and Avantika. Without your help and support, I never would have gotten to this point. I'd also like to thank all of the other lab members in the McCune lab including Yelena, Louise, Rick, Gabe, Paul, Wes, Becca, Din, and Samson. I'd also like to especially thank Trevor Burt, who started as my postdoc and then had his own lab. Without Trevor's help and support, this project never would have been born. He is one of the smartest kindest people I have ever met and I'm so grateful that I was able to work on this project with him. I'd also like to thank the BMS Program staff, especially Lisa and Monique; their help has been completely invaluable and they are the best.

I would like to thank all of my friends who have stuck by me through this process, especially my housemates, the Minty House girls, Tali, Anna, and Lindsay. I'd also like to thank my soccer friends for keeping me sane and giving me something to do outside of science. Thanks Anya, Martha, Emily, Kierra, Toni, and Chris. And, of course I'd like to thank my friends Ashley and Katrina for listening to me whine and complain, never letting me give up and always having faith in me.

And finally, I would like to thank my family. Thank you for nodding and smiling and encouraging me even when you had no idea what I was talking about. You have

always been there for me through thick and thin, good times and bad. Thank you Mom, Dad, Aunt Judy, Uncle David, Sam, and Kasia. I love you guys.

Distinct functional programming in human fetal and adult monocytes

Elisabeth Krow-Lucal

Abstract:

Immune development *in utero* and early in life represents a critical period in human health. Until this point, most studies have been conducted using model organisms which may or may not mirror the actual developmental events found in humans. In this dissertation we strove to elucidate and understand the inherent differences between the fetal immune system and the adult, with a particular emphasis on the myeloid compartment. We extended these studies to look at the response to cytokines *in utero* as well as the potential response to HIV *in utero*, as well as whether these fetal phenotypes persisted after birth in both the myeloid and lymphoid compartment.

To carry out these studies we developed *in vitro* flow cytometry assays to phenotypically characterize cell surface markers and the phosphorylation responses present in the JAK/STAT pathways. We also developed a high-throughput qPCR genetic signature to assess umbilical cord blood for fetal and adult transcripts. We have shown that human fetal and adult classical monocytes have distinct baseline transcriptional and signaling programs as well as that transcriptional and signaling differences in fetal monocytes underlie stronger responses to cytokine stimulation. Further, we have identified and validated a genetic signature to query umbilical cord blood for the presence of fetal-like classical monocyte and naïve T cells. And finally we have demonstrated that fetal classical monocytes may more strongly induce HIV

restriction factors in response to IFNγ than adult and have a stronger canonical and

non-canonical STAT response to IFNα/β. These studies shed light, for the first time, on

many of the immune mechanisms at play both during normal development *in utero* as

well as in the case of infection.

TABLE OF CONTENTS

Chapter V:

LIST OF TABLES

LIST OF FIGURES

CHAPTER II

CHAPTER III

<u>**CHAPTER IV**</u>

Chapter 1

Introduction

Introduction

Pregnancy poses a challenge to normal mechanisms of immune recognition and rejection. Both the mother and the fetus are exposed to allogeneic cells. In the case of the mother, these cells are fetal cells carrying paternal antigens, while in the case of the fetus, they are maternal cells expressing non-inherited maternal alloantigens[1,2]. Adaptive immune recognition of these alloantigens could result in a graft-versus rejection and as such there are extensive mechanisms in place to inhibit adaptive responses including poor antigen presentation[3], non-canonical MHC expression, and unique placental and decidual immunomodulatory cell populations [4]. The reader is referred to several excellent reviews on this subject[4-7].

Studies of the fetal-maternal interface have been primarily carried out in mice, due to the inherent challenges in studying this in humans. However, there are some discrepancies between mouse and human immune development that make it challenging to fully understand the unique mechanisms present. In mice, mature $\alpha\beta$ T cells colonize peripheral lymphoid organs during very late gestation and do not fully populate the periphery until after birth[8]. In contrast, mature human $\alpha\beta$ T cells can be found in the periphery as early as 10-12 gestational weeks[5,9]. Thus early hypotheses posited that *in utero* tolerance was maintained by a passive or inert fetal immune system (similar to that found in the mouse). However, current research suggests that there exist distinct fetal programs both in the T and myeloid compartments that contribute to the unique environment *in utero*, both in mice and in humans.

Fetal T cell development and function

Early work in quail chick embryos identified that thymic T cell development occurs in waves of restricted T cells. Each of these waves of T cells can be identified by unique TCRs and are generated by differential stem cell colonization of thymic tissue[10]. These waves appear to be developmentally regulated as they wax and wane according to embryonic gestational age[10]. Further work in mice has identified discrete TCR ($\gamma\delta$) utilization during fetal and neonatal development as compared to the adult TCR ($\alpha\beta$)[11-15]. The fetal-derived $\gamma\delta$ T cells have limited TCR diversity, suggesting a distinct and limited antigen recognition repertoire[12]. Furthermore, these cells appear to localize to specific tissues including the epithelium[16] and the intestine[17]. This localization and restricted TCR repertoire suggest that these fetal-derived cells may play a unique role in barrier sites and, as they are developmentally restricted, may be important for promoting tolerance to skin and gut microbiota in early life.

Because of their distinct TCR repertoire and anatomical location, multiple fetal-derived functional populations have been characterized in mice including dendritic epidermal T cells (DETCs) and non-DETC $\gamma\delta$ T cell populations found in the dermis[18,19]. DETCs are the first T cells and seed the epidermis early in development[20]. They have been implicated in inhibition of inflammatory skin conditions[21], protection against cutaneous malignancies[22,23], and wound repair[24,25]. Non-DETC $\gamma\delta$ T cell populations have been shown to be primary producers of IL-17[18,19] in the skin, and may play a role in response to infection.

These functions may be indicative of a fetal-specific program, ontologically geared towards appropriate development and maintenance of *in utero* tolerance. Work

in humans has demonstrated that, while fetal T cells are capable of recognizing and responding to alloantigen *in utero*[1], these cells preferentially differentiate into T regulatory (Treg) cells, capable of suppressing immune responses[1,26]. Further, these studies show that the fetal T cells are derived from a fetal hematopoietic stem/progenitor cell (HSPC) which gives rise to distinct downstream progeny than an adult HSPC.

Taken together, these data suggest that there are developmentally restricted windows of T cell development in which fetal T cells, functionally distinct from their adult counterparts, arise from discrete stem cells and seed specific anatomical locations.

Fetal myeloid development and function

The discovery of distinct stem cells giving rise to fetal or adult downstream progeny, further highlights the potential differences between the fetal and adult immune system, not just in T cells but also in other lymphoid and myeloid cells. There has been extensive work in human and mouse models elucidating the pathways of regulation of fetal as compared to adult hemoglobin in red blood cells[27-30]. Further work in mice has shown the presence of fetal-derived B1 cells, with distinct innate-like functions as compared to the adult B2 cells[31-36]. Because of the multi-lineage potential of HSPCs, it therefore suggested the presence of fetal-derived, tissue-restricted myeloid cells.

In mice, the first hematopoietic progenitors are derived from the extra-embryonic yolk sac and lead to primitive hematopoiesis (E7.0-E9.0)[37,38]. "Definitive hematopoiesis" occurs independently in the aorta, gonads, and mesonephros (AGM) region [37,38]. At E10.5, progenitors colonize the fetal liver, the major site of hematopoiesis early in

development[38]. These waves of hematopoiesis promote egress of various monocyte and macrophage populations that then give rise to various tissue-resident myeloid populations including microglia[39], Langerhans cells[40] and cardiac macrophages[41].

Microglia are the resident macrophage population in the brain and are associated with brain inflammatory diseases. Studies have shown that microglia arise from primitive myeloid progenitors (before E8.0), and are not repopulated by circulating monocyte precursors in the adult. Whether or not these fetal-derived cells have distinct functions from an equivalent adult counterpart remains unknown.

Langerhans cells (LCs) are found in the epidermis of both human and mouse skin. Recent work has demonstrated that LCs are derived from a yolk sac macrophage population during early embryogenesis and then replaced by fetal liver monocytes late in embryogenesis[40]. LCs were originally described as pro-inflammatory antigen presenting cells[42], however, in recent years it has become evident that they are essential for induction of Tregs after infection[43], UV irradiation[44], and glucocorticosteroid stimulation[45]. In humans, LCs are able to induce IL-22, but not IL-17, producing T cells[46], potentially suggesting a role in barrier maintenance as opposed to inflammatory processes. LCs also have a limited toll-like receptor repertoire, including low TLR2, TLR4 and TLR5 expression, leading to attenuated responses to both Gram-positive and Gram-negative bacteria, while leaving viral responses completely intact[47]. Similar to the limited TCR repertoire, this suggests that LCs may be playing a role in tolerization to the skin microbiome.

Recent work is highlighting that other fetal-derived populations exist in various organs including lung, liver, spleen, and kidney[41]. Furthermore, it has been shown that

these populations persist and replicate *in situ*, rather than being replaced by the circulating adult monocyte pool[40,41,48-50]. Thus, these functionally distinct fetal-derived myeloid populations persist into adulthood and can affect immunological outcomes throughout the life of the organism.

Models of immune development

Fetal-derived lymphoid and myeloid cells colonize specific anatomical locations and have distinct functions from their adult counterparts. Many of these functions seem tied to barrier integrity and induction of tolerogenic mechanisms. Ontologically, this could be a developmental program designed to allow *in utero* tolerance to non-inherited maternal alloantigens as well as to promote tolerance to commensal bacteria. These distinct functions, as well as the identification of a fetal HSPC[26], suggest that immune maturation in humans may proceed in a layered fashion[51], with a fetal system that predominates *in utero* and an adult system that predominates later in life.

In this scenario, the immune system at birth represents an admixture of fetal and adult-like cells. Developmentally this could represent itself either as an admixture of fetal and adult cells, independently and irrevocably derived from fetal and adult HSPCs, or it could represent a gradient of fetal cells maturing into adult cells, such that there are some purely fetal and some purely adult cells and some that are neither fetal nor adult but some transitional stage in between. Differences in environmental factors, including *in utero* infection, preterm labor, stochastic developmental events, etc. could then potentially alter the relative frequency of fetal-like cells present at birth. These differences at birth, resulting in either in a skewing towards an excessively adult or fetal

phenotype, could then affect the neonatal response to such immunological insults as vaccination, infection, and/or development of atopic disease.

In the studies presented in this thesis, we have examined the functional properties of fetal myeloid cells from mid-gestation human fetuses. We have addressed unanswered questions about the phenotype of fetal and adult bone marrow monocytes. We have identified distinct signaling responses and downstream functional programs in fetal cells and used high throughput qPCR technologies to identify whether phenotypically fetal cells persist after birth. Finally, we have identified potentially unique fetal mechanisms important in responding to *in utero* HIV infection. These findings elucidate important developmental concerns including the potential response and role of fetal cells to preterm labor, as well as *in utero* infection.

References

1. Mold JE, Michaelsson J, Burt TD, Muench MO, Beckerman KP, et al. Maternal Alloantigens Promote the Development of Tolerogenic Fetal Regulatory T Cells in Utero. Science. 2008;322:1562-1565.

2. Stevens A, Nelson JL. Maternal and fetal microchimerism: implications for human diseases. NeoReviews. 2002;3:e11-e19.

3. Erlebacher A, Vencato D, Price KA, Zhang D, Glimcher LH. Constraints in antigen presentation severely restrict T cell recognition of the allogeneic fetus. J Clin Invest. 2007;117:1399-1411.

4. Erlebacher A. Immunology of the maternal-fetal interface. Annu Rev Immunol. 2013;31:387-411.

5. Mold JE, McCune JM. Immunological tolerance during fetal development: from mouse to man. Adv Immunol. 2012;115:73-111.

6. Munoz-Suano A, Hamilton AB, Betz AG. Gimme shelter: the immune system during pregnancy. Immunological reviews. 2011;241:20-38.

7. Erlebacher A. Mechanisms of T cell tolerance towards the allogeneic fetus. Nat Rev Immunol. 2013;13:23-33.

8. Friedberg SH, Weissman IL. Lymphoid tissue architecture II. Ontogeny of peripheral T and B cells in mice: Evidence against Peyer's patches as the site of generation of B cells. The Journal of Immunology. 1974;113:1477-1492.

9. Haynes BF, Martin ME, Kay HH, Kurtzberg J. Early events in human T cell ontogeny. Phenotypic characterization and immunohistologic localization of T cell precursors in early human fetal tissues. The Journal of experimental medicine. 1988;168:1061-1080.

10. Coltey M, Bucy RP, Chen CH, Cihak J, Lösch U, et al. Analysis of the first two waves of thymus homing stem cells and their T cell progeny in chick-quail chimeras. J Exp Med. 1989;170:543-557.

11. Bonyhadi M, Weiss A, Tucker PW, Tigelaar RE, Allison JP. Delta is the Cx-gene product in the γ/δ antigen receptor of dendritic epidermal cells. Nature. 1987;330:574-576.

12. Ito K, Bonneville M, Takagaki Y, Nakanishi N, Kanagawa O, et al. Different gamma delta T-cell receptors are expressed on thymocytes at different stages of development. Proceedings of the National Academy of Sciences. 1989;86:631-635.

13. Houlden BA, Cron RQ, Coligan JE, Bluestone JA. Systematic development of distinct T cell receptor-gamma delta T cell subsets during fetal ontogeny. The Journal of Immunology. 1988;141:3753-3759.

14. Francis Elliott J, Rock EP, Patten PA, Davis MM, Chien Y-H. The adult T-cell receptor 5-chain is diverse and distinct from that of fetal thymocytes. Nature. 1988;331:627-631.

15. Heilig JS, Tonegawa S. Diversity of murine gamma genes and expression in fetal and adult T lymphocytes. Nature. 1986;322:836-840.

16. Leandersson K, Jaensson E, Ivars F. T cells developing in fetal thymus of T-cell receptor alpha-chain transgenic mice colonize gammadelta T-cell-specific epithelial niches but lack long-term reconstituting potential. Immunology. 2006;119:134-142.

17. Bonneville M, Janeway CA, Ito K, Haser W, Ishida I, et al. Intestinal intraepithelial lymphocytes are a distinct set of γδ T cells. Nature. 1988;336:479-481.

18. Gray EE, Suzuki K, Cyster JG. Cutting edge: Identification of a motile IL-17-producing gammadelta T cell population in the dermis. J Immunol. 2011;186:6091-6095.

19. Sumaria N, Roediger B, Ng LG, Qin J, Pinto R, et al. Cutaneous immunosurveillance by self-renewing dermal gammadelta T cells. J Exp Med. 2011;208:505-518.

20. Havran WL, Allison JP. Developmentally ordered appearance of thymocytes expressing different T-cell antigen receptors. Nature. 1988;335:443-445.

21. Girardi M, Lewis J, Glusac E, Filler RB, Geng L, et al. Resident skin-specific γδ T cells provide local, nonredundant regulation of cutaneous inflammation. The Journal of experimental medicine. 2002;195:855-867.

22. Girardi M, Glusac E, Filler RB, Roberts SJ, Propperova I, et al. The distinct contributions of murine T cell receptor (TCR)gammadelta+ and TCRalphabeta+ T cells to different stages of chemically induced skin cancer. J Exp Med. 2003;198:747-755.

23. Girardi M, Oppenheim DE, Steele CR, Lewis JM, Glusac E, et al. Regulation of cutaneous malignancy by gammadelta T cells. Science. 2001;294:605-609.

24. Sharp LL, Jameson JM, Cauvi G, Havran WL. Dendritic epidermal T cells regulate skin homeostasis through local production of insulin-like growth factor 1. Nat Immunol. 2005;6:73-79.

25. Jameson J, Ugarte K, Chen N, Yachi P, Fuchs E, et al. A role for skin gammadelta T cells in wound repair. Science. 2002;296:747-749.

26. Mold JE, Venkatasubrahmanyam S, Burt TD, Michaëlsson J, Rivera JM, et al. Fetal and adult hematopoietic stem cells give rise to distinct T cell lineages in humans. Science. 2010;330:1695-1699.

27. Wilber A, Nienhuis AW, Persons DA. Transcriptional regulation of fetal to adult hemoglobin switching: new therapeutic opportunities. Blood. 2011;117:3945-3953.

28. Wilber A, Tschulena U, Hargrove PW, Kim YS, Persons DA, et al. A zinc-finger transcriptional activator designed to interact with the gamma-globin gene promoters enhances fetal hemoglobin production in primary human adult erythroblasts. Blood. 2010;115:3033-3041.

29. Rochette J, Dodé C, Leturcq F, Krishnamoorthy R. Level and composition of fetal hemoglobin expression in normal newborn babies are not dependent on β cluster DNA haplotype. American journal of hematology. 1990;34:223-224.

30. Sankaran VG, Xu J, Byron R, Greisman HA, Fisher C, et al. A Functional Element Necessary for Fetal Hemoglobin Silencing. N Engl J Med. 2011;365:807-814.

31. Kantor AB. The development and repertoire of B-1 cells (CD5 B cells). Immunol Today. 1991;12:389-391.

32. Griffin DO, Holodick NE, Rothstein TL. Human B1 cells in umbilical cord and adult peripheral blood express the novel phenotype CD20+ CD27+ CD43+ CD70-. J Exp Med. 2011;208:67-80.

33. Montecino-Rodriguez E, Dorshkind K. B-1 B cell development in the fetus and adult. Immunity. 2012;36:13-21.

34. Montecino-Rodriguez E, Dorshkind K. Formation of B-1 B Cells from Neonatal B-1 Transitional Cells Exhibits NF-κB Redundancy. J Immunol. 2011;187:5712-5719.

35. Hayakawa K, Hardy RR, Herzenberg LA, Herzenberg LA. Progenitors for Ly-1 B cells are distinct from progenitors for other B cells. J Exp Med. 1985;161:1554-1568.

36. Herzenberg LA, Stall AM. Conventional and Ly-1 B-cell lineages in normal and mu transgenic mice. Cold Spring Harb Symp Quant Biol. 1989;54 Pt 1:219-225.

37. Lichanska AM, Hume DA. Origins and functions of phagocytes in the embryo. Experimental hematology. 2000;28:601-611.

38. Orkin SH, Zon LI. Hematopoiesis: an evolving paradigm for stem cell biology. Cell. 2008;132:631-644.

39. Ginhoux F, Greter M, Leboeuf M, Nandi S, See P, et al. Fate mapping analysis reveals that adult microglia derive from primitive macrophages. Science. 2010;330:841-845.

40. Hoeffel G, Wang Y, Greter M, See P, Teo P, et al. Adult Langerhans cells derive predominantly from embryonic fetal liver monocytes with a minor contribution of yolk sac-derived macrophages. J Exp Med. 2012;209:1167-1181.

41. Epelman S, Lavine KJ, Beaudin AE, Sojka DK, Carrero JA, et al. Embryonic and Adult-Derived Resident Cardiac Macrophages Are Maintained through Distinct Mechanisms at Steady State and during Inflammation. Immunity. 2014;40:91-104.

42. Romani N, Brunner PM, Stingl G. Changing views of the role of Langerhans cells. J Invest Dermatol. 2012;132:872-881.

43. Kautz-Neu K, Noordegraaf M, Dinges S, Bennett CL, John D, et al. Langerhans cells are negative regulators of the anti-Leishmania response. J Exp Med. 2011;208:885-891.

44. Obhrai JS, Oberbarnscheidt M, Zhang N, Mueller DL, Shlomchik WD, et al. Langerhans cells are not required for efficient skin graft rejection. J Invest Dermatol. 2008;128:1950-1955.

45. Stary G, Klein I, Bauer W, Koszik F, Reininger B, et al. Glucocorticosteroids modify Langerhans cells to produce TGF-β and expand regulatory T cells. J Immunol. 2011;186:103-112.

46. Fujita H, Nograles KE, Kikuchi T, Gonzalez J, Carucci JA, Krueger JG. Human Langerhans cells induce distinct IL-22-producing CD4+ T cells lacking IL-17 production. Proceedings of the National Academy of Sciences. 2009;106:21795-21800.

47. van der Aar AM, Sylva-Steenland RM, Bos JD, Kapsenberg ML, de Jong EC, Teunissen MB. Cutting edge: loss of TLR2, TLR4, and TLR5 on Langerhans cells abolishes bacterial recognition. The Journal of Immunology. 2007;178:1986-1990.

48. Schulz C, Gomez Perdiguero E, Chorro L, Szabo-Rogers H, Cagnard N, et al. A lineage of myeloid cells independent of Myb and hematopoietic stem cells. Science. 2012;336:86-90.

49. Yona S, Kim KW, Wolf Y, Mildner A, Varol D, et al. Fate Mapping Reveals Origins and Dynamics of Monocytes and Tissue Macrophages under Homeostasis. Immunity. 2012.

50. Hashimoto D, Chow A, Noizat C, Teo P, Beasley MB, et al. Tissue-resident macrophages self-maintain locally throughout adult life with minimal contribution from circulating monocytes. Immunity. 2013;38:792-804.

51. Herzenberg LA, Herzenberg LA. Toward a layered immune system. Cell. 1989;59:953-954.

Chapter 2

Distinct functional programming of human fetal and adult monocytes

This chapter was published as:

Krow-Lucal, E. R., Kim, C.C., Burt, T.D. & McCune, J.M. Distinct functional

programming of human fetal and adult monocytes. *Blood* (2014).

Abstract: Preterm birth affects one out of nine infants born in the United States and is the leading cause of long-term neurological handicap and infant mortality, accounting for 35% of all infant deaths in 2008[1]. Although cytokines including IFNγ[2], IL-10[3], IL-6, IL-1, and TNF[4] are produced in response to *in utero* infection and are strongly associated with the onset or prevention of preterm labor, little to nothing is known about how human fetal immune cells respond to these cytokines. Here, we demonstrate that fetal and adult CD14$^+$16$^-$ classical monocytes are distinct from one another, both in terms of basal transcriptional profiles and in their phosphorylation of signal transducers and activators of transcription (STATs) in response to inflammatory stimuli. Compared to adult monocytes, fetal monocytes phosphorylate both canonical and non-canonical STATs and respond more strongly to multiple cytokines (e.g., IFNγ, IL-6, and IL-4). We show evidence for a potential mechanism to explain these differences in STAT phosphorylation by demonstrating a higher ratio of SOCS3 to IL-6 receptor in adult monocytes, relative to fetal monocytes. In addition, IFNγ signaling results in up-regulation of antigen presentation and co-stimulatory machinery in adult but not fetal monocytes. These findings represent the first evidence that the immune response in primary human fetal monocytes is functionally distinct from the adult, providing a foundation for understanding how these cells respond to cytokines implicated in development[2,3], *in utero* infections, and in the pathogenesis of preterm labor[2].

15

Introduction: Human gestation poses a unique and poorly understood challenge to normal mechanisms of immune recognition and rejection. The mother and her fetus are exposed to genetically distinct cells that bi-directionally cross the placenta[5,6] and each must learn to tolerate the other while simultaneously remaining responsive to pathogens. Previous studies have shown that the mother employs multiple strategies to maintain immune tolerance of her fetus[3]. The fetal immune system also appears to play an active role in maintaining pregnancy[7]. In contrast, production of inflammatory cytokines (e.g., IFNγ, IL-6, TNFα, and IL-1) in response to bacterial infection characterizes the fetal inflammatory response syndrome (FIRS) which is associated with spontaneous abortion or preterm labor[2,8-12].

The fetal immune system actively contributes to tolerance of maternal antigens[5,13]. Upon stimulation with non-inherited maternal alloantigens, fetal naïve CD4$^+$ T cells preferentially differentiate into CD4$^+$CD25$^+$FoxP3$^+$ T regulatory cells (Tregs) that specifically mediate tolerance of those antigens[5] and that may also prevent harmful inflammatory responses against the mother. It is well-recognized that the mouse has a developmentally-limited fetal hematopoietic stem cell (HSC) population that gives rise to unique hematopoietic lineages[14,15], including B-1 B cells, which generate 'natural' antibodies[16-18]. Human fetal T cells[13] and erythrocytes[19] also appear to arise from distinct fetal progenitors. Since HSCs have multi-lineage potential, we hypothesized that human fetal myeloid cells (specifically, fetal monocytes) arising from these cells would also have distinct functional characteristics compared to their adult counterparts.

16

Materials and Methods:

Isolation of bone marrow monocytes. Fetal bone marrow was obtained from 18-22 gestational week specimens obtained under the auspices of CHR-approved protocols from the Department of Obstetrics, Gynecology and Reproductive Science, San Francisco General Hospital. Fetal samples were obtained after elective termination of pregnancy. Samples were excluded in the case of (1) known maternal infection, (2) intrauterine fetal demise, and/or (3) known or suspected chromosomal abnormality. Fetal monocytes were isolated from femurs by bisection and mechanical dispersion of marrow in RPMI-1640 (Sigma Aldrich). Adult bone marrow samples were obtained from healthy donors (AllCells, LLC. and Lonza Group Ltd.). Both adult and fetal mononuclear cells were isolated by density centrifugation of a Ficoll-Hypaque gradient (Amersham Biosciences). All samples, both fetal and adult, were viably cryopreserved prior to use.

Flow cytometry. Mononuclear cell preparations were incubated in FACS staining buffer (PBS with 2% FBS and 2 mM EDTA) with fluorochrome-conjugated, anti-human surface antibodies. Antibodies used for phenotyping included: CD3 APC (BW264/56, Miltenyi), CD20 ECD (B9E9, Beckman Coulter), CD14 qDot605 (Tuk4, Invitrogen), CD16 Pacific Blue (3G8, BD Biosciences), HLA-DR PE-Cy7 (G46-6, BD Biosciences), CX3CR1 APC (2A9-1, Biolegend), CCR2 PerCP-Cy5.5 (K036C2, Biolegend), CD11c Alexa700 (Bly6, BD Biosciences), CD11b APC-Cy7 (ICRF44, BD Biosciences). All cells were stained with a live/dead marker (Amine-Aqua/AmCyan; Invitrogen) to exclude dead cells from the analysis. For intracellular STAT staining, cells were first stained with CD14 and CD16, prior to fixation/permeabilization and subsequent STAT staining according to the

manufacturer's protocol (BD Biosciences, Cytofix Buffer and Permeabilization Buffer III). Intracellular antibodies used included: STAT1 (pY701) Alexa488 (4a, BD Biosciences), STAT3 (pY705) PE-CF594 (4/P-STAT3, BD Biosciences), STAT5 (pY694) AlexaFluor 647 (47/STAT5(pY694), BD Biosciences), and STAT6 (pY641) PerCP-Cy5.5 (18/p-Stat6, BD Biosciences).

For IL-6 receptor and SOCS3 staining, cells were first stained with a live/dead marker, HLA-DR, CD14, CD16, and IL-6R APC (UV4, Biolegend) prior to fixation/permeabilization according to the manufacturer's protocol (BD Biosciences, Cytofix/Cytoperm Buffer). Cells were then stained with a rabbit polyclonal anti-SOCS3 (Abcam, ab16030) and then a donkey anti-rabbit AI488 secondary (Abcam, ab150069).

All data were acquired with an LSRII flow cytometer (BD Biosciences) and analyzed with FlowJo (Treestar) software.

Fluorescence activated cell sorting (FACS). For basal gene expression microarrays, mononuclear cells were stained with the appropriate antibodies and filtered through 70 µM mesh filters (Falcon). The stained cells were subsequently sorted by FACS (FACS Aria, BD Biosciences) directly into RLT buffer (Qiagen). Purity was assessed by reanalyzing a small fraction of sorted cells. For IFNγ stimulation experiments, cells were incubate for 4 hours in sterile serum free cell culture media (SF X-VIVO 20, Lonza Group Ltd.) and appropriate amounts of IFNγ. The cells were subsequently stained with the appropriate surface markers, filtered, and sorted by FACS into sterile PBS. These

cells were then re-sorted to a purity of greater than 99% directly into RNAqueous Micro

lysis buffer (Ambion – Life Technologies).

RNA preparation for microarray analysis – basal gene expression microarray.

RNA was isolated according to the manufacturer's protocol (Qiagen, RNeasy Mini kit)

and yield was determined on a Nanodrop spectrophotometer (Thermo Scientific).

Sample preparation, labeling, and array hybridizations were performed according to

standard protocols from the UCSF Shared Microarray Core Facilities and Agilent

Technologies (http://www.arrays.ucsf.edu and http://www.agilent.com). Total RNA

quality was assessed using a Pico Chip on an Agilent 2100 Bioanalyzer (Agilent

Technologies, Palo Alto, CA). RNA was amplified using the Sigma whole transcriptome

amplification kits following the manufacturer's protocol (Sigma-Aldrich, St Louis, MO),

and subsequent Cy3-CTP labeling was performed using NimbleGen one-color labeling

kits (Roche-NimbleGen Inc, Madison, WI). Labeled Cy3-cDNA was assessed using the

Nandrop ND-8000 (Nanodrop Technologies, Inc., Wilmington DE), and equal amounts

of Cy3 labeled target were hybridized to Agilent whole human genome 4x44K arrays.

Hybridizations were performed for 17 hours, according to the manufacturer's protocol.

Arrays were scanned using the Agilent microarray scanner and raw signal intensities

were extracted with Feature Extraction v10.6 software.

RNA preparation for microarray analysis – IFNγ-stimulated microarrays.

RNA was isolated from FACS-sorted samples using the RNAqueous-Micro kit (Life

Technologies) and subjected to two rounds of linear amplification using the Aminoallyl

MessageAmp II kit (Life Technologies). Cy3-coupled aRNA was fragmented and hybridized overnight to a SurePrint G3 Human Gene Expression 8x60K microarray, which was washed and scanned per manufacturer's instructions (Agilent Technologies).

Statistical analysis of microarrays. For basal gene expression microarrays, the dataset was normalized using the quantile normalization method proposed by Bolstad et al (2003)[20]. No background subtraction was performed, and the median feature pixel intensity was used as the raw signal before normalization. A one-way ANOVA linear model was fit to the comparison to estimate the mean M values and calculated moderated t-statistic, B statistic, false discovery rate and p-value for each gene for the comparison of interest. Adjusted p-values were produced by the method proposed by Holm (1979). All procedures were carried out using functions in the R package *limma* in Bioconductor[21,22].

For the IFNγ-stimulated arrays, raw intensities were extracted using Feature Extraction software (Agilent) and quantile normalized using Limma[21]. Differentially expressed genes were identified using Significance Analysis for Microarrays[23] and data visualized as heat maps using custom Perl scripts. Genes subsets demarcated as different between fetus and adult were determined by stratifying significantly differentially expressed genes such that they were not differentially expressed at baseline (based on relative expression and FDR ≤ 1%), were differentially expressed after stimulation with IFNγ (based on relative expression and FDR ≤ 1%), and were differentially expressed between ABM and FBM IFNγ treated samples (based on relative expression and FDR ≤

5%)(Table S3). All data are available in the NCBI Gene Expression Omnibus under accession GSE54818.

qPCR validation of microarray targets. Classical monocytes were isolated from ABM and FBM by FACS directly into RLT Buffer (Qiagen). RNA was isolated using the RNeasy Mini Kit (Qiagen). 275ng of RNA was used according to the manufacturer's protocol with JAK/STAT qPCR arrays (SABiosciences). Genes of interest were normalized to GAPDH.

Cytokine stimulation and STAT staining. Approximately 1×10^6 mononuclear cells from FBM or ABM were stained with CD14 Qdot605 and CD16 Pacific Blue for 30 minutes, prior to incubation in polystyrene tissue culture treated 96-well plates with appropriate amounts of cytokine in sterile serum free cell culture media (SF X-VIVO 20, Lonza Group Ltd.) at 37°C for 5, 15 or 30 minutes (100 μL total volume). The cells were then fixed with Cytofix Buffer (BD Biosciences), permeabilized with Permeabilization Buffer III (BD Biosciences) and stained with HLA-DR, STAT1, STAT3, STAT5 and STAT6, according to the manufacturer's instructions. Cytokines used were recombinant human IFNγ, IL-4, IL-6 (all from Biolegend), and IL-10 (BD Biosciences).

Bioinformatic promoter analysis. Putative STAT1 and STAT5 promoter sites in genes enriched after IFNγ stimulation in ABM or FBM were determined using the SABiosciences DECODE database. Genes identified with a STAT1 binding site were identified using STAT1 as the transcription factor. Genes identified with a STAT5

binding site were identified using STAT5a and STAT5b. A gene was considered to have a STAT5 binding site if it had either STAT5a or STAT5b binding sites in the promoter.

Statistics. All error bars represented are standard error of the mean (S.E.M.). P values displayed in phenotypic characterizations were determined by non-parametric t test (Mann-Whitney). Sample size for statistical calculations was determined by use of the maximum number of unique biological replicates available. All experiments were performed two or more times with distinct biological samples (total of 8-12). Each individual experiment contained a minimum of four ABM and four FBM samples. No samples were excluded. See previous sections for microarray specific statistics.

Results: To determine whether human fetal monocytes are functionally distinct from those of the adult, we isolated mononuclear cells from human fetal (18-22 gestational weeks) and adult bone marrow. Since the bone marrow becomes the primary site of myelopoiesis during the late second trimester of fetal development[24,25], we reasoned that differences that might exist between fetal and adult monocytes could be explored by directly comparing mononuclear cells obtained from this organ with cells from its adult counterpart. To determine whether human fetal monocytes could be readily identified using known myeloid and monocyte surface markers, bone marrow mononuclear cells were isolated from 18-22 week human fetal and adult bone marrow specimens for phenotypic characterization. Since classical monocytes (HLA-DR$^+$CD14$^+$CD16$^-$) are thought to differentiate into non-classical monocytes (HLA-DR$^+$CD14$^+$CD16$^+$) upon stimulation and activation[26], we chose to examine the classical population as the earliest member of the mature monocyte lineage. Common monocyte markers (Fig. 1a-c, Fig. S1, Fig. S2) were present on classical monocytes and absent on non-monocyte antigen presenting cells (HLA-DR$^+$CD14$^-$CD16$^-$). The classical monocyte population identified as HLA-DR$^+$CD14$^+$CD16$^-$ is a relatively pure monocyte population and is not contaminated by CD3$^+$ T cells, NK T cells, or CD20$^+$B cells (Fig. S2). Compared to the non-monocyte antigen presenting cells, both the fetal and adult CD14$^+$CD16$^-$ populations had uniformly higher expression of the myeloid and monocyte surface markers CD11b, CD11c, CCR2 and CX3CR1. Adult CD14$^+$CD16$^-$ cells, on the other hand, had higher expression of the integrins CD11c and CD11b than fetal CD14$^+$CD16$^-$ cells. CX3CR1 and CCR2 are commonly used to define classical and non-classical monocyte populations and govern properties of cell migration and

Figure 1
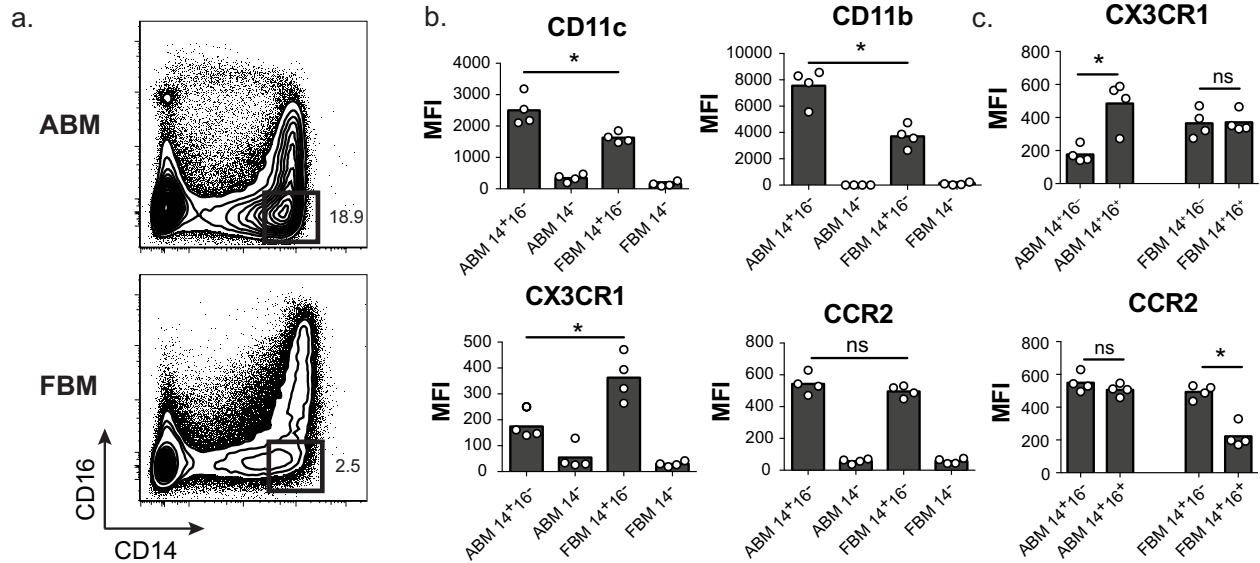
Figure 1: Phenotypic characterization of human bone marrow monocytes. (**A**) Representative plot of bone marrow monocytes in ABM and FBM. CD14$^+$CD16$^-$ classical monocytes are gated as shown. (**B**) Mean fluorescence intensity (MFI) of CD11c, CD11b, CX3CR1 and CCR2 as expressed on classical monocytes or on the CD14$^-$ non-monocyte population in FBM and ABM. (**C**) MFI of CX3CR1 and CCR2 in classical (CD14$^+$CD16$^-$) and non-classical (CD14$^+$CD16$^+$) monocyte populations in ABM and FBM. Representative of three or more experiments, n=12 (total from all experiments)

function[27]. CX3CR1 was expressed only on the non-classical population of adult monocytes but was expressed by both classical and non-classical populations of fetal monocytes (Fig. 1c, upper panel), suggesting that each of these cell populations might have an enhanced ability to enter and to establish resident macrophage and/or dendritic cell populations in tissues from which they would otherwise be restricted such as the brain or skin[28,29]. Conversely, both fetal and adult classical monocytes had similarly high expression of CCR2, while fetal non-classical monocytes expressed half as much CCR2 as their adult counterpart (Fig. 1c, lower panel). These observations of CCR2 expression on both monocyte subsets are contrary to what is seen in peripheral blood non-classical monocytes that express little CCR2 [30]. Although not demonstrated in humans, CCR2 in mice is required for egress from the bone marrow[31]; we speculate that its expression on human adult non-classical monocytes may reflect a similar role in bone marrow egress.

Given the observed differences in surface markers associated with migration and inflammation (*e.g.*, CX3CR1, CD11b, and CD11c), we wondered whether basal gene expression programs were different in fetal and adult monocytes. HLA-DR$^+$CD14$^+$CD16$^-$ classical monocytes were isolated from fetal and adult bone marrow (n=4 each) by fluorescence activated cell sorting (FACS), and subjected to whole genome gene expression analysis (Fig. 2). Fetal and adult classical monocytes were found to have 2,069 significantly differentially expressed genes (FDR ≤ 0.05, fold change ≥ 2), many of which are known to contribute to key immunological pathways associated with monocyte function, including pathogen recognition and sensitivity to cytokines. These

Figure 2
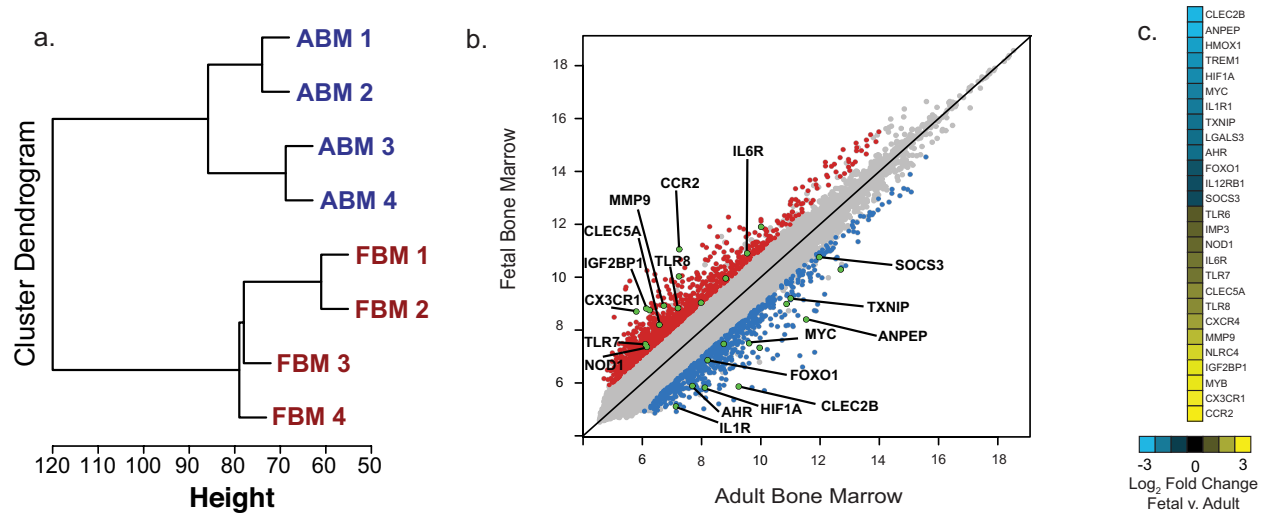
Figure 2: Transcriptional characterization of human bone marrow monocytes. (A) Unbiased cluster analysis of gene expression of ABM and FBM classical monocytes. **(B)** Scatterplot of pairwise global gene expression comparing ABM and FBM classical monocytes (log$_2$ signal intensity). Genes that were differentially expressed between groups are indicated in red and blue. Genes of interest in green are also significantly differentially expressed (FDR ≤ 0.05, fold change ≥ 2). **(C)** log$_2$ fold change of genes in green, fetal vs. adult.

genes include *IL1R1*, *IL6R*, *IL10RA*, and *IL12RB1*, as well as *TLR7*, *TLR8*, *NOD1*, and *NLRC4* (Fig. 2b,c, Table S1).

Spontaneous abortion and the onset of preterm labor are strongly associated with FIRS, which is characterized by robust fetal production of the pro-inflammatory cytokine IL-6[4,8]. Given the observation that the IL-6 receptor (*IL6R*) is expressed at higher levels in fetal as compared to adult monocytes, we tested the possibility that the fetal monocyte response to IL-6 is distinct from that found in the adult. Phosphorylation of canonical (pSTAT3)[32] and non-canonical (pSTAT1 and pSTAT5) STATs was assessed in ABM and FBM mononuclear cells after stimulation with IL-6 for varying amounts of time (Fig. 3, Fig. S3) and at varying concentrations (Fig. S4). IL-6 induced phosphorylation of STAT3 in most fetal and adult monocytes, but a higher frequency of fetal cells phosphorylated STAT3 and did so more rapidly than adult cells (Fig. 3b). Interestingly, the non-canonical mediators, STAT1 and STAT5, were phosphorylated in fetal but not in adult monocytes, suggesting a tendency of the fetus to activate signaling pathways that are not normally activated in the adult (Fig. 3a,c). These differences were observed even at very low IL-6 concentrations (Fig. S4), demonstrating an exquisite sensitivity of fetal monocytes to IL-6. These findings show that fetal monocytes are highly attuned to the presence of IL-6 and are able to mount a strong canonical pSTAT3 response. We also found that even very low concentrations of IL-6 enhanced non-canonical STAT1 and STAT5 phosphorylation at low concentrations (Fig. S4a,c), which has the potential to trigger unique gene expression pathways and monocyte maturation[33,34]. The consequences of activating these pathways in fetal monocytes are unknown, but since

Figure 3

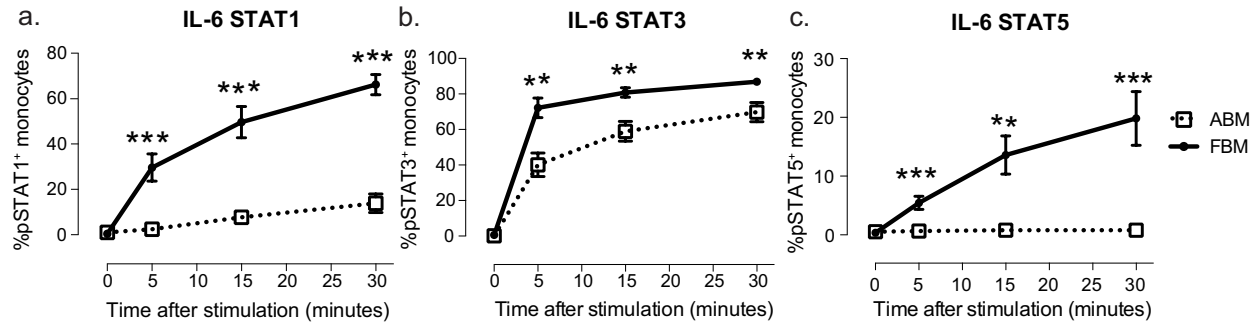**Figure 3: STAT phosphorylation in response to IL-6 stimulation. (A)** Percentage of classical monocytes in FBM and ABM expressing pSTAT1 after IL-6 stimulation. **(B)** Percentage of pSTAT3$^+$ classical monocytes in FBM and ABM. **(C)** Percentage of pSTAT5$^+$ in classical monocytes in FBM and ABM. Cells were stimulated with 70 ng/mL IL-6. All data are from two or more experiments, n=8 (total from all experiments).

JAK/STAT pathways have been characterized as potent mediators of cytokine signaling transduction, it may be that these variant pathways alter the functional response of fetal monocytes to IL-6.

JAK/STAT signaling mediates various aspects of monocyte migration, cytokine responses, and differentiation[2,35-37]. Given the above observation of unique IL-6 mediated pSTAT responses in fetal monocytes, we wondered whether these cells might also respond to other physiologically relevant immunological stimuli via non-canonical JAK/STAT phosphorylation. Of particular interest were the responses to IFNγ, IL-4, and IL-10 due to their involvement in Th1/Th2 polarization and FIRS[4,8,38-40]. As the response of the fetus to these cytokines is unknown, we stimulated ABM and FBM mononuclear cells with IFNγ, IL-10, or IL-4 for varying periods of time (Fig. 4, Fig. S3) or varying concentrations (Fig. S5), after which monocyte phosphorylation of STAT1, 3, 5, and 6 was assessed. Elevated circulating levels of IFNγ in the fetus have been associated with complications of preterm birth, including injury to brain white matter[9]. Just as both fetal and adult monocytes phosphorylate the canonical signaling intermediate STAT3 upon IL-6 stimulation, IFNγ stimulation results in robust phosphorylation of the canonical intermediate STAT1 in both cell types (Fig. 4a). Fetal monocytes were, however, even more sensitive to IFNγ, as demonstrated by higher STAT1 phosphorylation at lower cytokine concentrations (Fig. S5a). As we hypothesized, phosphorylation of a non-canonical intermediate (STAT5) was detected in fetal but not adult monocytes (Fig. 4b).

Figure 4
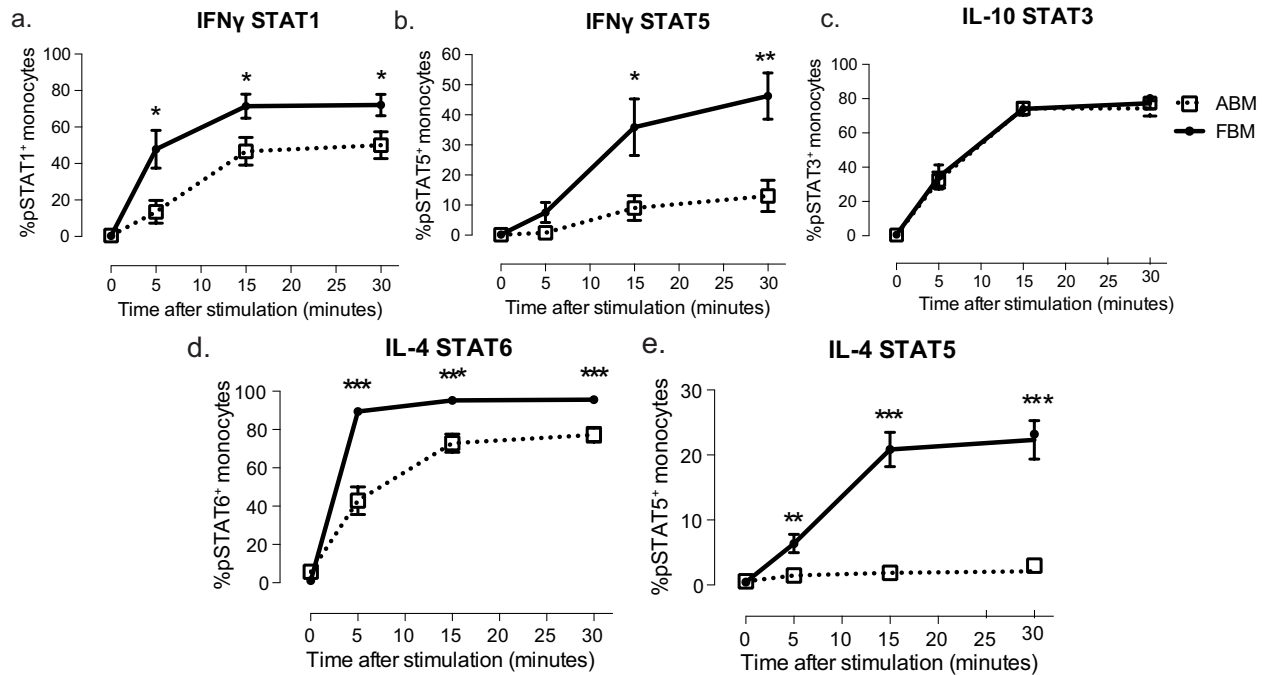
Figure 4: STAT phosphorylation in response to IL-10, IFNγ, and IL-4. (A)
Percentage of pSTAT1$^+$ classical monocytes in FBM and ABM after IFNγ stimulation.
(B) Percentage of pSTAT5$^+$ classical monocytes in FBM and ABM after IFNγ stimulation.
Cells were stimulated with 40 ng/mL IFNγ. **(C)** Percentage of pSTAT3$^+$ classical
monocytes in FBM and ABM after IL-10 stimulation. Cells were stimulated with 70
ng/mL IL-10. **(D)** Percentage of pSTAT6$^+$ classical monocytes in FBM and ABM after IL-
4 stimulation. **(E)** Percentage of pSTAT5 in classical monocytes in FBM and ABM after
IL-4 stimulation. Cells were stimulated with 30 ng/mL IL-4. All data are from two or more
experiments, n=8 (total from all experiments).

Fetal and neonatal immune responses have been previously described to preferentially

activate Th2 responses rather than Th1, though most of the evidence for this skew has

been shown mice[41,42]. Given that unexpected STAT phosphorylation responses were

seen in response to a classical Th1 cytokine (IFNγ), we sought to determine whether

fetal monocyte responses to a keystone Th2 cytokine (IL-4) were also different from

responses described in adults. As in the case of IFNγ, stimulation with IL-4 prompted

both fetal and adult monocytes to phosphorylate the canonical intermediate STAT6. The

fetal STAT6 response was amplified compared to that of the adult (Fig. 4d) and was

triggered at a much lower concentration (Fig. S5d). IL-4 also triggered a strong and

unexpected pSTAT5 response in fetal classical monocytes, similar to that which was

observed after stimulation with IL-6 and IFNγ (Fig. 4e, Fig. S5e), implicating STAT5 as a

common mediator of fetal cytokine responses. Finally, IL-10 is critical for maintenance

of pregnancy in experimental models of spontaneous abortion[43]. After IL-10 stimulation,

both the fetal and adult monocytes displayed an equivalent phosphorylation of the

canonical signaling mediator, STAT3 (Fig. 4c), but no phosphorylation of any other

STATs.

Taken together, these data indicate that fetal monocytes are more sensitive to activation

of canonical signaling pathways in response to IL-6, IFNγ, and IL-4, but also trigger

unexpected non-canonical signaling pathways that are distinct from those observed in

adult monocytes. In contrast, the fetal and adult responses to the anti-inflammatory

cytokine, IL-10, are virtually identical. A unifying and distinctive feature of fetal

monocytes is their robust phosphorylation of STAT5 upon exposure to cytokines that

have diverse effects in adults (*e.g.*, IL-6, IFNγ, and IL-4). STAT5 has been implicated as

a mediator of monocyte maturation[33], suggesting that fetal monocytes may be poised to

respond to cytokines through rapid and sensitive induction of canonical STAT pathways

and through accelerated maturation via activation of non-canonical STAT5-mediated

signaling pathways.

These observations led us to two questions: First, how does differential STAT

phosphorylation affect downstream functional programs; and second, which factors

regulate differential STAT phosphorylation after stimulation with IL-6, IFNγ, and IL-4, but

not IL-10? To assess the potential impact of differential STAT activation on functional

programs, we investigated the response to IFNγ stimulation in more depth. Having

observed differential activation of STAT1 and STAT5 in fetal and adult monocytes after

IFNγ stimulation (Fig. 4a,b), we sought to determine whether inflammatory cytokine

stimulation might lead to activation of different gene-expression programs in fetal and

adult monocytes. To address this question, FBM and ABM cells were stimulated with

IFNγ for 4 hours and subjected to whole genome gene expression analysis. We

identified genes that were not differentially expressed in fetal and adult monocytes at

baseline, but that did become differentially expressed in these two populations after

IFNγ stimulation (Fig. 5, Fig. S6, Table S2, Table S3). Notably, many of the genes up-

regulated by adult monocytes after IFNγ stimulation are associated with antigen

presentation and co-stimulation, including *CIITA* (transports MHCII to the surface of

antigen presenting cells), *CD40* (a co-stimulatory molecule that activates T cells by

binding to CD40L on T cells), *CD74* (MHCII invariant chain), and *CD80* (B7-1, a co-
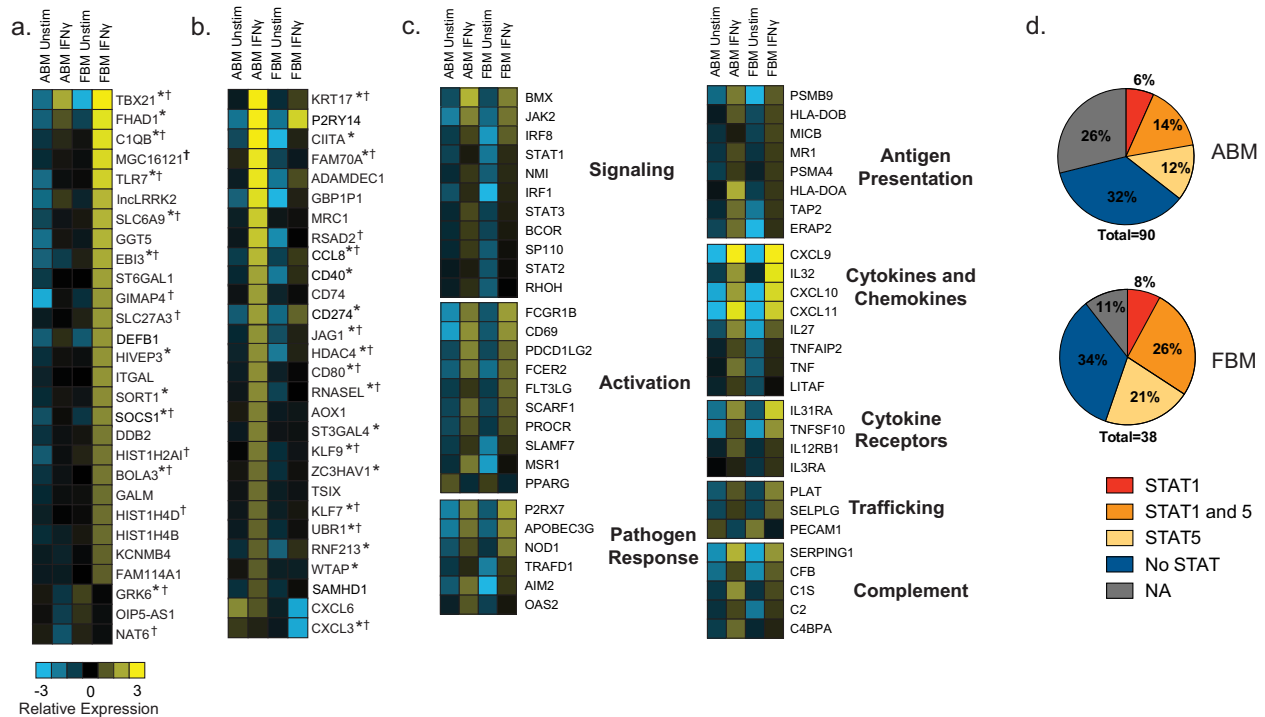
Figure 5

Figure 5: IFNγ-stimulated genes in FBM and ABM classical bone marrow monocytes. (A) Cells were stimulated with 40 ng/mL IFNγ for 4 hours and the sorted to greater than 99% purity for whole genome gene microarray analysis. Figures **A-C** depict a representative subset of the differentially expressed genes. **(A)** A subset of genes is not differentially expressed at baseline between ABM and FBM, but is significantly more highly expressed in FBM than ABM after stimulation with IFNγ (based on relative expression and an FDR ≤ 5%). Relative expression is the $\log_2$ representation of gene expression compared to median normalized array values. All genes marked with a * have bioinformatically identified putative STAT1 binding sites in their promoters; all those marked with a † have bioinformatically identified putative STAT5 binding site in their promoter. **(B)** A subset of genes is not differentially expressed at baseline between ABM and FBM, but is significantly more highly expressed in ABM than FBM after stimulation with IFNγ (based on relative expression and FDR ≤ 5%). **(C)** A subset of genes that is not differentially expressed at baseline between ABM and FBM, and is not significantly differentially expressed between ABM and FBM, and are induced in both subsets after stimulation with IFNγ (based on relative expression and an FDR ≤ 5%). **(D)** Pie chart of putative STAT1 and STAT5 binding sites in the promoters of significantly differentially expressed genes. NA indicates that there is no bioinformatic information (on any transcription factor) available on the gene of interest.

stimulatory molecule that activates T cells by binding to CD28). In contrast, many genes that were up-regulated by fetal monocytes after IFNγ stimulation can trigger and mediate innate pathogen responses, including: *TBX21* (T-bet; expression in dendritic cells instructs them to promote Th1 differentiation in T cells)[44,45], *C1QB* (a critical component of the first step in the complement deposition pathway), *TLR7* (crucial for recognition of intracellular pathogens), and *DEFB1* (a directly toxic antimicrobial peptide). Many genes that were expressed equivalently in IFNγ-stimulated fetal and adult monocytes have been previously defined as canonical interferon-stimulated genes (ISGs) such as *CXCL10*, *STAT1*, *TAP2,* and *FCGR1B* (Fig. 5c), consistent with our finding that canonical JAK/STAT signaling pathways that lead to induction of these genes are activated in both fetal and adult cells after cytokine stimulation (Fig. 4a,b). Analysis of putative STAT1 and STAT5 binding sites in differentially expressed genes (Fig. 5d) revealed an enrichment in STAT1 and STAT5 binding sites in those genes that are more highly expressed in fetal cells, supporting the hypothesis that differential STAT phosphorylation is responsible for activation of distinct gene programs.

These data suggest distinct functional outcomes can arise after STAT phosphorylation in fetal versus adult monocytes. To delineate mechanisms that might control the differential phosphorylation of STATs, we focused on potential inhibitors of STAT phosphorylation that were identified by microarray analysis and validated by qPCR (Tables S1, S4). Of the common inhibitors, the most strikingly differentially expressed was SOCS3 (23 fold higher in the adult; Fig. 2c, Fig. S7, Table S4), a member of the suppressor of cytokine signaling family that can directly inhibit JAK-mediated STAT

phosphorylation via a KIR domain[46]. SOCS3 was of particular interest because it selectively inhibits STAT1 and STAT3 phosphorylation downstream of the IL-6 but not the IL-10 receptor [46-48]. Since SOCS3 mRNA is more abundant in adult monocytes compared to fetal monocytes, we wondered if SOCS3 could be responsible for the relatively attenuated pSTAT3 and absent pSTAT1 responses observed in adult monocytes. To address this question, relative protein expression levels of IL-6R and SOCS3 were assayed by flow cytometry. Surprisingly, SOCS3 protein was not differentially expressed between fetal and adult cells (Fig. 6a). Since intracellular signaling from the IL-6R is directly inhibited by SOCS3, we wondered if IL-6 signaling in fetal cells might be enhanced compared to adult cells due to the relative abundance of IL-6R and SOCS3. As hypothesized, the IL-6R was more highly expressed in the fetal monocytes (Fig. 6b) and the ratio of SOCS3/IL-6R was lower in fetal monocytes compared to adult monocytes (Fig. 6c). This suggests that there are more repressive SOCS3 molecules available per IL-6R in adult monocytes. These data support a putative mechanism in which a higher proportion of SOCS3 to IL-6R in the adult monocytes results in attenuated STAT1 and STAT3 phosphorylation, consistent with our findings above (Fig 3a,b, Fig. S8).

Figure 6
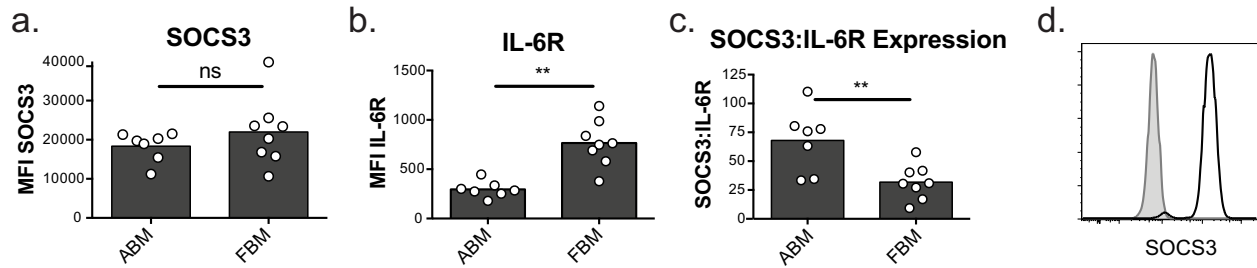
Figure 6: SOCS3 and IL-6R expression in fetal and adult bone marrow monocytes. **(A)** Mean fluorescence intensity of SOCS3 in classical ABM and FBM monocytes. **(B)** Mean fluorescence intensity of IL-6R in classical ABM and FBM monocytes. **(C)** The relative ratio of SOCS3 to IL-6R expression based on mean fluorescence intensity. All SOCS3/IL-6R characterizations represent 2 or more independent experiments with ABM n=7 and FBM n=8. **(D)** Representative histogram of SOCS3 staining in FBM classical monocytes. The grey histogram is stained with secondary alone and the white with anti-SOCS3 primary antibody plus secondary antibody.

Discussion: In aggregate, our findings indicate that fetal and adult monocytes are phenotypically and transcriptionally different from one another at baseline. In particular, we also demonstrate that fetal monocytes generate distinct JAK/STAT signaling responses after stimulation with IFNγ, IL-6, or IL-4. In response to the key pro-inflammatory cytokine, IL-6, fetal monocytes phosphorylate non-canonical STATs (*e.g.*, STAT1 and STAT5), suggesting that IL-6 induced STAT5-mediated signaling may lead to maturation of monocytes into functional phagocytes, whereas concurrent phosphorylation of STAT1 may lead to activation of classical pro-inflammatory genes. Together, these signaling responses that are associated with maturation and immune activation may then also optimize the fetus and newborn's chance of successfully combating a microbial invader.

Our data suggest a mechanism wherein high levels of canonical (STAT3) and non-canonical (STAT1) STAT phosphorylation are found in fetal monocytes due to their lower ratio of SOCS3 to IL-6R and, hence, lower levels of STAT inhibition (Fig. S8). We show that fetal monocytes have stronger JAK/STAT responses to stimulation by multiple cytokines as compared to adult monocytes. It may be that these differential responses are also due to relatively decreased influence of signaling inhibitors. If so, fetal innate immune responses could potentially be modulated using small-molecule JAK/STAT inhibitors.

Differences in oxygen tension and overall cellular composition in fetal versus adult bone marrow may contribute to the observed differences in STAT signaling. In addition, and

as an unavoidable condition of these experiments, observations made on cells in vitro are not necessarily reflective of those that occur in vivo (even though cells from all tissues were cryopreserved immediately after isolation).

Overall STAT levels may also contribute to the differences observed in STAT phosphorylation. Results of transcript analysis by qRT-PCR at baseline and protein analysis in unstimulated phosphoflow samples suggest that there are no major differences in basal STAT levels, however we also acknowledge that, due to cell number constraints, we are unable to determine the absolute protein levels of the various STATs by immunoblotting.

Upon stimulation with IFNγ, we show that fetal monocytes fail to up-regulate co-stimulatory and antigen presentation genes, but instead up-regulate genes involved in primitive anti-microbial responses in response to IFNγ. We propose that failure to generate antigen-presentation and co-stimulation responses in fetal monocytes is a strategy to prevent activation of adaptive (i.e., T cell mediated) immune responses (Fig. S9). While such adaptive responses are crucial for clearance of pathogens in the post-natal period, they may trigger potentially harmful responses in the fetus (such as anti-self or anti-maternal rejection), resulting in preterm labor and delivery. Thus, rather than promoting a strong adaptive and potentially inflammatory response that could trigger labor and expulsion of the fetus, fetal monocytes mount a more primitive, but potentially protective, innate, antimicrobial response. Our findings provide a foundation for

understanding the myeloid immune response to inflammatory cytokines implicated in the pathogenesis of FIRS, spontaneous abortion, and preterm labor.

References:

1. *CDC - Preterm Birth-Prematurity - Maternal Infant Health - Reproductive Health.*

http://www.cdc.gov/reproductivehealth/MaternalInfantHealth/PretermBirth.htm

(accessed August 2, 2013, updated March 21, 2013)

2. Murphy SP, Tayade C, Ashkar AA, Hatta K, Zhang J, Croy BA. Interferon gamma in

successful pregnancies. Biol Reprod. 2009;80:848-859.

3. Erlebacher A. Immunology of the maternal-fetal interface. Annu Rev Immunol.

2013;31:387-411.

4. Gotsch F, Romero R, Kusanovic JP, Mazaki-Tovi S, Pineles BL, et al. The fetal

inflammatory response syndrome. Clinical obstetrics and gynecology. 2007;50:652-683.

5. Mold JE, Michaelsson J, Burt TD, Muench MO, Beckerman KP, et al. Maternal

Alloantigens Promote the Development of Tolerogenic Fetal Regulatory T Cells in

Utero. Science. 2008;322:1562-1565.

6. Stevens A, Nelson JL. Maternal and fetal microchimerism: implications for human

diseases. NeoReviews. 2002;3:e11-e19.

7. Burt TD. Fetal Regulatory T Cells and Peripheral Immune Tolerance In Utero:

Implications for Development and Disease. Am J Reprod Immunol. 2013.

8. Romero R, Savasan ZA, Chaiworapongsa T, Berry SM, Kusanovic JP, et al.

Hematologic profile of the fetus with systemic inflammatory response syndrome. J

Perinat Med. 2011;40:19-32.

9. Hansen-Pupp I, Harling S, Berg AC, Cilio C, Hellström-Westas L, Ley D. Circulating

interferon-gamma and white matter brain damage in preterm infants. Pediatr Res.

2005;58:946-952.

10. Kallapur G, Presicce P, Senthamaraikannan P, Alvarez M, Tarantal F, et al. Intra-Amniotic IL-1 Induces Fetal Inflammation in Rhesus Monkeys and Alters the Regulatory T Cell/IL-17 Balance. The Journal of Immunology. 2013.

11. De Dooy J, Colpaert C, Schuerwegh A, Bridts C, Van Der Planken M, et al. Relationship between histologic chorioamnionitis and early inflammatory variables in blood, tracheal aspirates, and endotracheal colonization in preterm infants. Pediatr Res. 2003;54:113-119.

12. Robertson SA, Care AS, Skinner RJ. Interleukin 10 regulates inflammatory cytokine synthesis to protect against lipopolysaccharide-induced abortion and fetal growth restriction in mice. Biol Reprod. 2007;76:738-748.

13. Mold JE, Venkatasubrahmanyam S, Burt TD, Michaëlsson J, Rivera JM, et al. Fetal and adult hematopoietic stem cells give rise to distinct T cell lineages in humans. Science. 2010;330:1695-1699.

14. Kim I, Saunders TL, Morrison SJ. Sox17 dependence distinguishes the transcriptional regulation of fetal from adult hematopoietic stem cells. Cell. 2007;130:470-483.

15. He S, Kim I, Lim MS, Morrison SJ. Sox17 expression confers self-renewal potential and fetal stem cell characteristics upon adult hematopoietic progenitors. Genes Dev. 2011;25:1613-1627.

16. Montecino-Rodriguez E, Dorshkind K. B-1 B cell development in the fetus and adult. Immunity. 2012;36:13-21.

17. Herzenberg LA, Stall AM. Conventional and Ly-1 B-cell lineages in normal and mu transgenic mice. Cold Spring Harb Symp Quant Biol. 1989;54 Pt 1:219-225.

18. Ikuta K, Kina T, MacNeil I, Uchida N, Peault B, et al. A developmental switch in thymic lymphocyte maturation potential occurs at the level of hematopoietic stem cells. Cell. 1990;62:863-874.

19. Wilber A, Tschulena U, Hargrove PW, Kim YS, Persons DA, et al. A zinc-finger transcriptional activator designed to interact with the gamma-globin gene promoters enhances fetal hemoglobin production in primary human adult erythroblasts. Blood. 2010;115:3033-3041.

20. Bolstad BM, Irizarry RA, Åstrand M, Speed TP. A comparison of normalization methods for high density oligonucleotide array data based on variance and bias. Bioinformatics. 2003;19:185-193.

21. Smyth GK. Linear models and empirical bayes methods for assessing differential expression in microarray experiments. Stat Appl Genet Mol Biol. 2004;3:Article3.

22. Gentleman RC, Carey VJ, Bates DM, Bolstad B, Dettling M, et al. Bioconductor: open software development for computational biology and bioinformatics. Genome biology. 2004;5:R80.

23. Tusher VG, Tibshirani R, Chu G. Significance analysis of microarrays applied to the ionizing radiation response. Proceedings of the National Academy of Sciences. 2001;98:5116-5121.

24. Moore MA, Metcalf D. Ontogeny of the Haemopoietic System: Yolk Sac Origin of In Vivo and In Vitro Colony Forming Cells in the Developing Mouse Embryo*. British journal of haematology. 1970;18:279-296.

25. Tavian M, Péault B. Embryonic development of the human hematopoietic system. Int J Dev Biol. 2005;49:243-250.

26. Ziegler-Heitbrock L, Ancuta P, Crowe S, Dalod M, Grau V, et al. Nomenclature of monocytes and dendritic cells in blood. Blood. 2010;116:e74-e80.

27. Gordon S, Taylor PR. Monocyte and macrophage heterogeneity. Nat Rev Immunol. 2005;5:953-964.

28. Hoeffel G, Wang Y, Greter M, See P, Teo P, et al. Adult Langerhans cells derive predominantly from embryonic fetal liver monocytes with a minor contribution of yolk sac-derived macrophages. J Exp Med. 2012;209:1167-1181.

29. Ginhoux F, Greter M, Leboeuf M, Nandi S, See P, et al. Fate mapping analysis reveals that adult microglia derive from primitive macrophages. Science. 2010;330:841-845.

30. Wong KL, Tai JJ, Wong WC, Han H, Sem X, et al. Gene expression profiling reveals the defining features of the classical, intermediate, and nonclassical human monocyte subsets. Blood. 2011;118:e16-e31.

31. Tsou CL, Peters W, Si Y, Slaymaker S, Aslanian AM, et al. Critical roles for CCR2 and MCP-3 in monocyte mobilization from bone marrow and recruitment to inflammatory sites. J Clin Invest. 2007;117:902-909.

32. Shuai K, Liu B. Regulation of JAK-STAT signalling in the immune system. Nat Rev Immunol. 2003;3:900-911.

33. Woldman I, Mellitzer G, Kieslinger M, Buchhart D, Meinke A, et al. STAT5 involvement in the differentiation response of primary chicken myeloid progenitor cells to chicken myelomonocytic growth factor. The Journal of Immunology. 1997;159:877-886.

34. Chomarat P, Banchereau J, Davoust J, Palucka AK. IL-6 switches the differentiation of monocytes from dendritic cells to macrophages. Nature immunology. 2000;1:510-514.

35. Hu Y, Hu X, Boumsell L, Ivashkiv LB. IFN-γ and STAT1 arrest monocyte migration and modulate RAC/CDC42 pathways. The Journal of Immunology. 2008;180:8057-8065.

36. Lehtonen A, Matikainen S, Miettinen M, Julkunen I. Granulocyte-macrophage colony-stimulating factor (GM-CSF)-induced STAT5 activation and target-gene expression during human monocyte/macrophage differentiation. Journal of leukocyte biology. 2002;71:511-519.

37. Coccia EM, Russo ND, Stellacci E, Testa U, Marziali G, Battistini A. STAT1 activation during monocyte to macrophage maturation: role of adhesion molecules. International Immunology. 1999;11:1075-1083.

38. Makhseed M, Raghupathy R, Azizieh F, Omu A, Al-Shamali E, Ashkanani L. Th1 and Th2 cytokine profiles in recurrent aborters with successful pregnancy and with subsequent abortions. Human Reproduction. 2001;16:2219-2226.

39. Saito S, Sakai M, Sasaki Y, Tanebe K, Tsuda H, Michimata T. Quantitative analysis of peripheral blood Th0, Th1, Th2 and the Th1: Th2 cell ratio during normal human pregnancy and preeclampsia. Clinical and experimental immunology. 1999;117:550.

40. Ansel KM, Djuretic I, Tanasa B, Rao A. Regulation of Th2 differentiation and Il4 locus accessibility. Annu Rev Immunol. 2006;24:607-656.

41. Rose S, Lichtenheld M, Foote MR, Adkins B. Murine neonatal CD4+ cells are poised for rapid Th2 effector-like function. The Journal of Immunology. 2007;178:2667-2678.

42. Adkins B, Bu Y, Vincek V, Guevara P. The Primary Responses of Murine Neonatal Lymph Node CD4+ Cells are Th2-skewed and are Sufficient for the Development of Th2-biased Memory. Clinical and Developmental Immunology. 2003;10:43-51.

43. Murphy SP, Fast LD, Hanna NN, Sharma S. Uterine NK cells mediate inflammation-induced fetal demise in IL-10-null mice. The Journal of Immunology. 2005;175:4084-4090.

44. Lugo-Villarino G, Maldonado-López R, Possemato R, Peñaranda C, Glimcher LH. T-bet is required for optimal production of IFN-γ and antigen-specific T cell activation by dendritic cells. Proceedings of the National Academy of Sciences. 2003;100:7749-7754.

45. Lipscomb MW, Chen L, Taylor JL, Goldbach C, Watkins SC, et al. Ectopic T-bet expression licenses dendritic cells for IL-12-independent priming of type 1 T cells in vitro. J Immunol. 2009;183:7250-7258.

46. Yoshimura A, Naka T, Kubo M. SOCS proteins, cytokine signalling and immune regulation. Nat Rev Immunol. 2007;7:454-465.

47. Croker BA, Krebs DL, Zhang J-G, Wormald S, et al. SOCS3 negatively regulates IL-6 signaling in vivo. Nature Immunology. 2003;4:540.

48. Babon JJ, Kershaw NJ, Murphy JM, Varghese LN, Laktyushin A, et al. Suppression of cytokine signaling by SOCS3: characterization of the mode of inhibition and the basis of its specificity. Immunity. 2012;36:239-250.

Supplemental figure 1

a. **Fetal Bone Marrow**
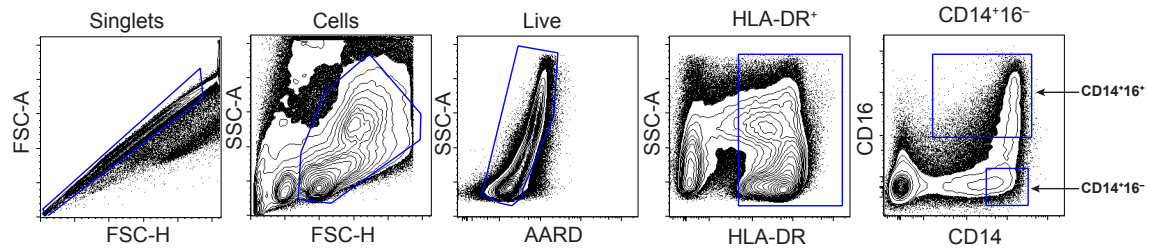
b. **Adult Bone Marrow**
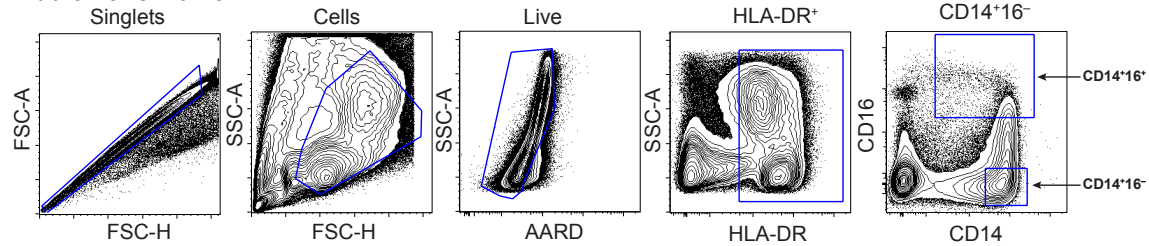
Supplemental figure 1: Gating strategy for identification of CD14$^+$CD16$^-$ classical monocytes. Mononuclear cells were isolated from fetal **(A)** and adult bone marrow **(B)** and stained with HLA-DR, CD14, CD16, and a live-dead marker. Classical monocytes (CD14$^+$CD16$^-$) were sorted using the gating strategy presented for whole genome array analysis. Populations were demarcated as shown.

Supplemental figure 2
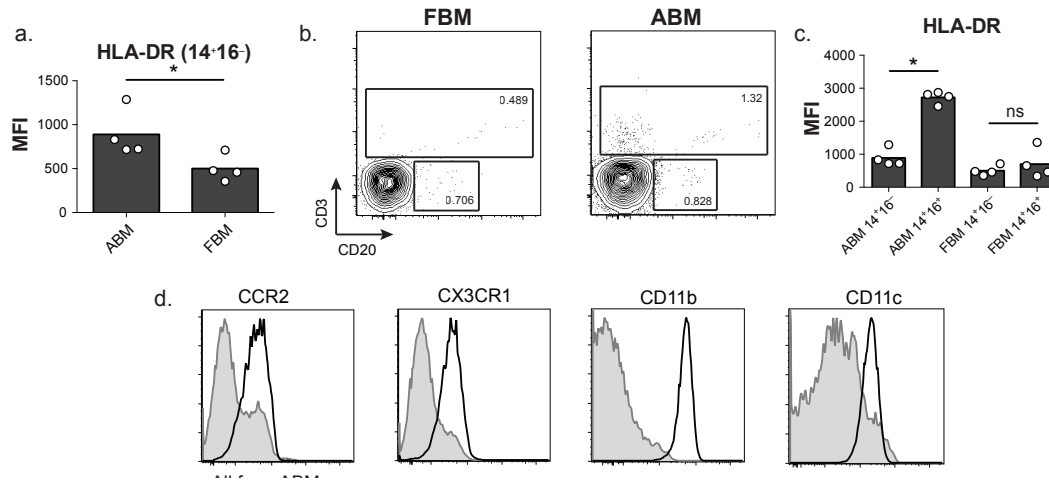
Supplemental figure 2: Expression of phenotypic surface markers. Cells were identified as classical or non-classical monocytes by the gating strategy described previously in Supplemental Figure 1. **(A)** MFI of HLA-DR in FBM and ABM classical monocytes. **(B)** Representative plots of $CD3^+$ and $CD20^+$ cells found in classical monocyte gate. **(C)** MFI of HLA-DR in FBM and ABM classical and non-classical monocytes. **(D)** Representative histograms of CCR2, CX3CR1, CD11c, and CD11b in classical monocytes (white histograms) and HLA-DR^+CD14^- cells (grey histograms). Both classical monocytes and HLA-DR^+CD14^- cells were further gated using an identical FSC vs. SSC gate to account for potential size and granularity differences in the cell populations. All histograms are from ABM.

Supplemental figure 3
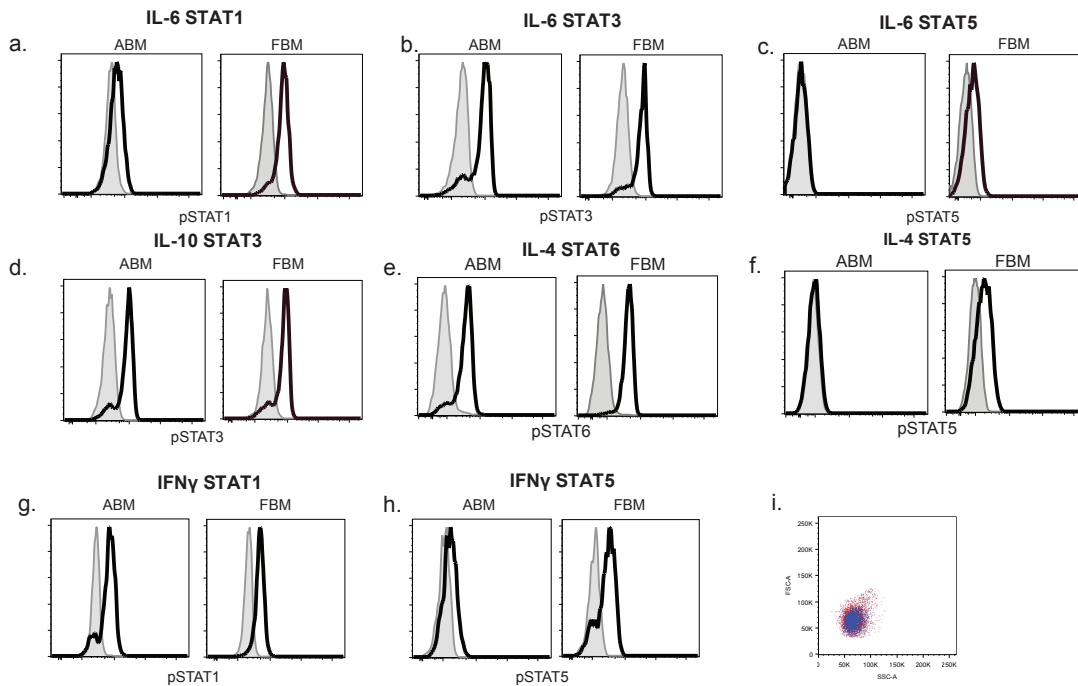
Supplemental figure 3: Representative histograms of STAT phosphorylation after IL-6, IL-10, IFNγ and IL-4 stimulation. (A) Representative histogram of pSTAT1 expression in ABM and FBM classical monocytes, before (shaded areas) and after stimulation with IL-6. **(B)** Representative histogram of pSTAT3 expression in ABM and FBM classical monocytes, before (shaded areas) and after stimulation with IL-6. **(C)** Representative histogram of pSTAT5 expression in ABM and FBM classical monocytes, before (shaded areas) and after stimulation with IL-6. **(D)** Representative histogram of pSTAT3 expression in ABM and FBM classical monocytes, before (shaded areas) and after stimulation with IL-10. **(E)** Representative histogram of pSTAT6 expression in ABM and FBM classical monocytes, before (shaded areas) and after stimulation with IL-4. **(F)** Representative histogram of pSTAT5 expression in ABM and FBM classical monocytes, before (shaded areas) and after stimulation with IL-4. **(G)** Representative histogram of pSTAT1 expression in ABM and FBM classical monocytes before (shaded areas) and after stimulation with IFNγ. **(H)** Representative histogram of pSTAT5 expression in ABM and FBM classical monocytes, before (shaded areas) and after stimulation with IFNγ. Representative histograms are of 30 minutes after stimulation. **(I)** Representative overlay plot of FSC vs. SSC to demonstrate equivalent size and granularity of stimulated (red) and unstimulated (blue) classical monocytes.

Supplemental figure 4
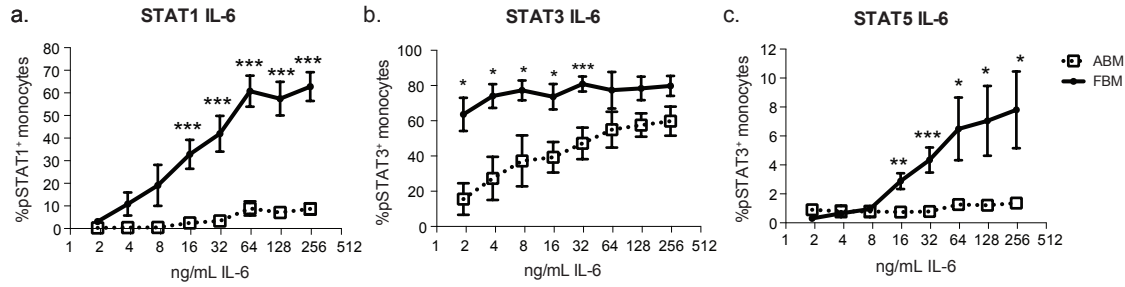
Supplemental figure 4: Differential STAT phosphorylation is maintained at low concentrations of IL-6. (A) Percentage of pSTAT1⁺ classical monocytes in FBM and ABM after IL-6 stimulation. Cells were stimulated with 125, 62.5, 31.25, 16, 8, 4, or 2 ng/mL IL-6. **(B)** Percentage of pSTAT3⁺ classical monocytes in FBM and ABM after IL-6 stimulation. Cells were stimulated with 125, 62.5, 31.25, 16, 8, 4, or 2 ng/mL IL-6. **(C)** Percentage of pSTAT5⁺ classical monocytes in FBM and ABM after IL-6 stimulation. Cells were stimulated with 125, 62.5, 31.25, 16, 8, 4, or 2 ng/mL IL-6. Figure is representative of two or more independent experiments, total n=4 at each concentration.

Supplemental figure 5
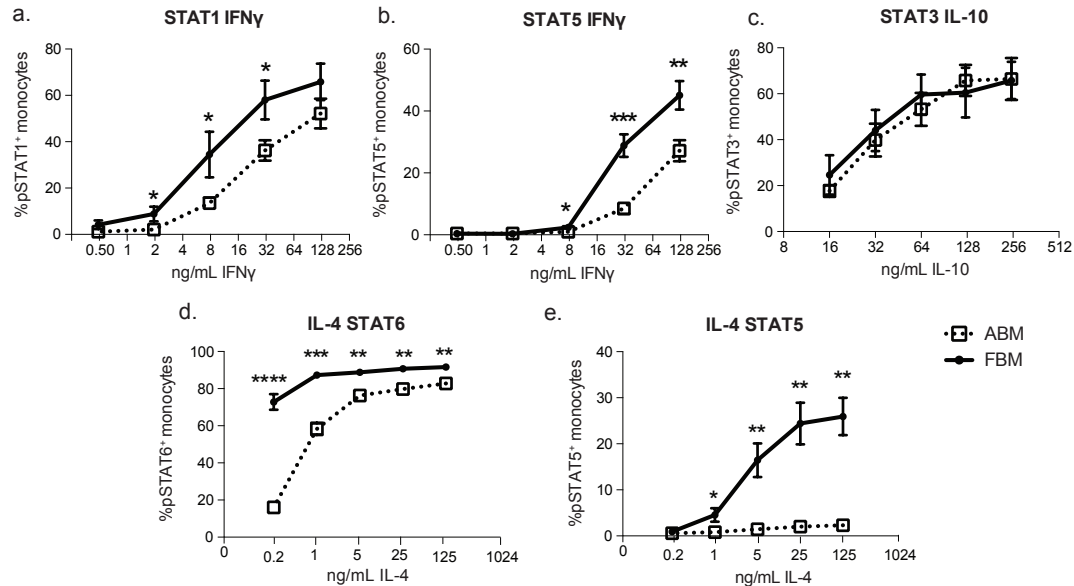
Supplemental figure 5: Differential STAT phosphorylation is maintained at low concentrations of IFNγ, IL-10, and IL-4. (A) Percentage of pSTAT1$^+$ classical monocytes in FBM and ABM after IFNγ stimulation. Cells were stimulated with 125, 31.25, 7.81, 1.95, or 0.5 ng/mL IFNγ for 30 min. **(B)** Percentage of pSTAT5$^+$ classical monocytes in FBM and ABM after IFNγ stimulation. Cells were stimulated with 125, 31.25, 7.81, 1.95, or 0.5 ng/mL IFNγ for 30 min. **(C)** Percentage of pSTAT3$^+$ classical monocytes in FBM and ABM after IL-10 stimulation. Cells were stimulated with 125, 62.5, 31.25, 15.626 ng/mL IL-10 for 30 min. **(D)** Percentage of pSTAT6$^+$ classical monocytes in FBM and ABM after IL-4 stimulation. Cells were stimulated with 125, 25, 5, 1, or 0.2 ng/mL IL-4 for 30 min. **(E)** Percentage of pSTAT5$^+$ classical monocytes in FBM and ABM after IL-4 stimulation. Cells were stimulated with 125, 25, 5, 1, or 0.2 ng/mL IL-4 for 30 min. All data are representative of two or more experiments, n=4 (total from all experiments) for IL-4, IL-6, IL-10 stimulations; n=12 (total from all experiments) for IFNγ stimulation.

Supplemental figure 6
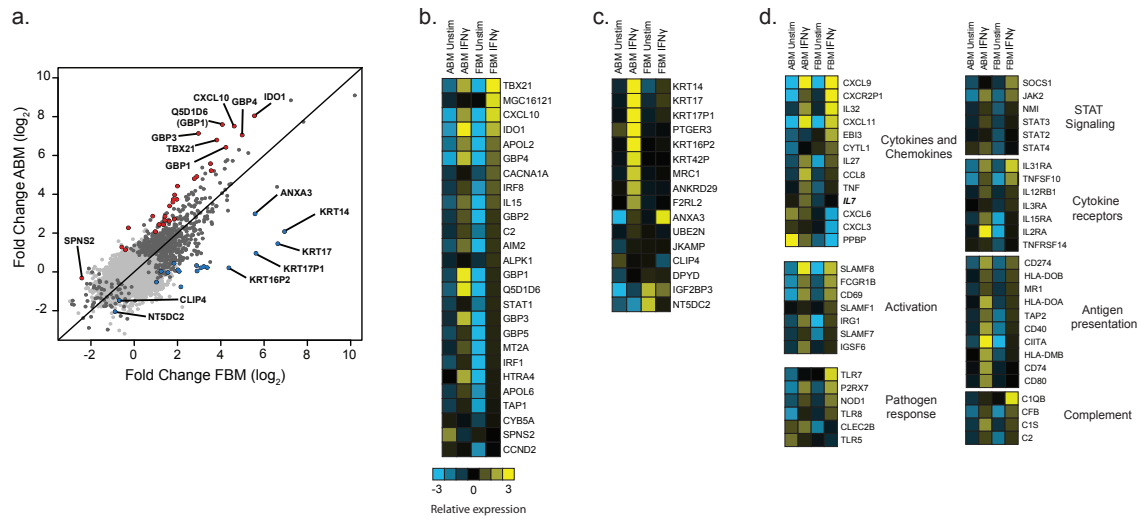
Supplemental figure 6: Fold induction of IFNγ stimulated in FBM and ABM classical monocytes. (A) Scatterplot of pairwise fold change between stimulated and unstimulated FBM and ABM. Dark grey dots represent all genes that are significantly (FDR ≤ 1%) differentially induced or repressed after IFNγ stimulation. Red dots are significantly more highly induced in the fetus than the adult (FDR ≤ 1%, fold change ≥ 2). Blue dots are significantly more highly induced in the adult than the fetus (FDR ≤ 1%, fold change ≥ 2). **(B)** A subset of genes that are more highly differentially induced (fold change) in FBM classical monocytes after stimulation with IFNγ than ABM. **(C)** A subset of genes that are more highly differentially induced (fold change) in ABM classical monocytes after stimulation with IFNγ than FBM. **(D)** A subset of genes that are similarly induced (fold change) in FBM and ABM classical monocytes after stimulation with IFNγ. Relative expression is the $\log_2$ representation of gene expression compared to median normalized array values.

Supplemental figure 7
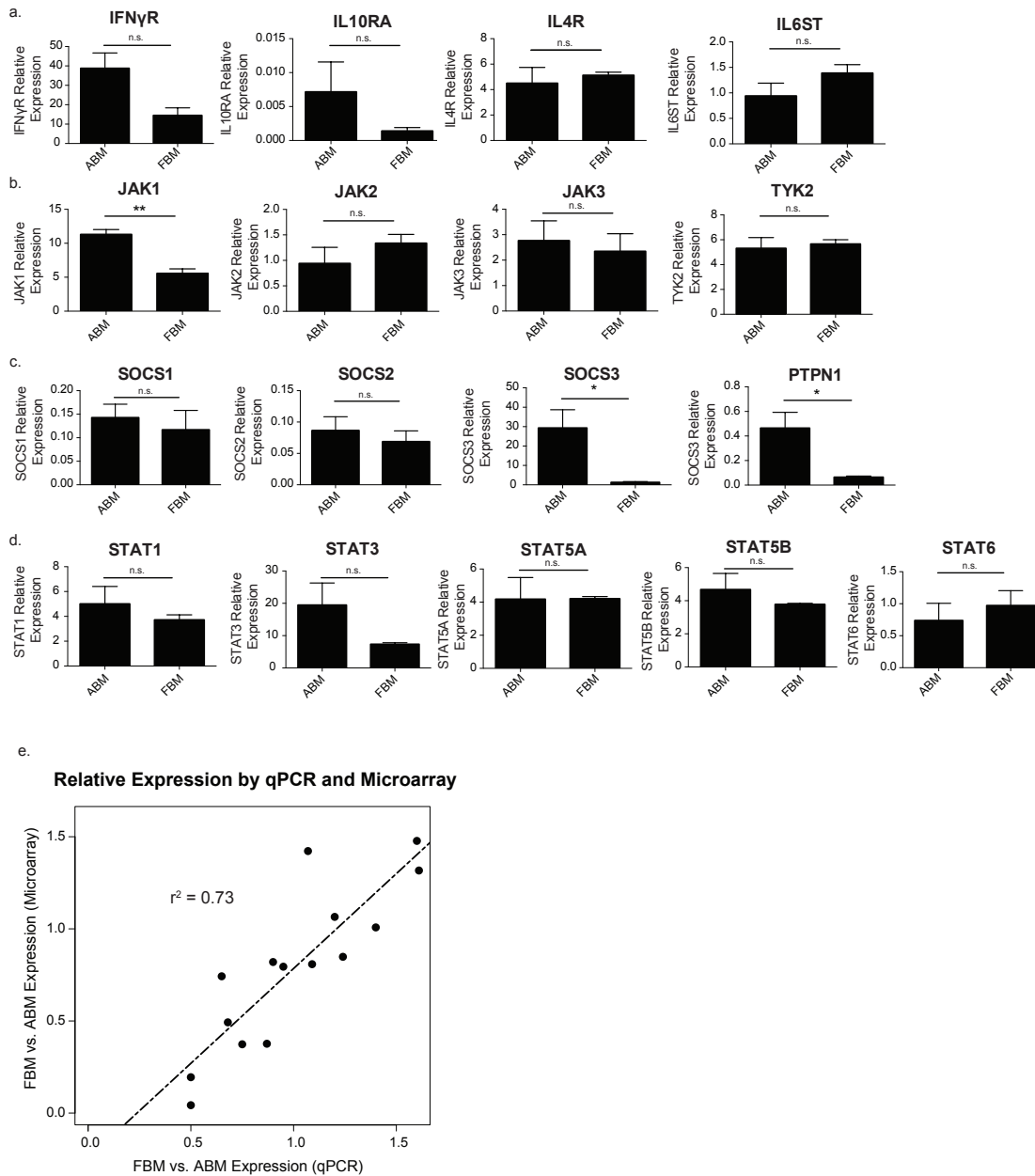
Supplemental figure 7: qPCR validation of JAK/STAT pathway components.
Classical monocytes from FBM and ABM were isolated by FACS and probed using a JAK/STAT qPCR array. All genes in both FBM and ABM are normalized to GAPDH.**(A)** Relative expression of cytokine receptors involved in JAK/STAT signaling. **(B)** Relative expression of kinases involved in JAK/STAT signaling. **(C)** Relative expression of inhibitors of JAK/STAT signaling. **(D)** Relative expression of STATs. **(E)** Fold change of FBM versus ABM classical monocytes as determined by qPCR and by microarray. Each graph represents an n=3 for ABM and FBM.

Supplemental figure 8

| Adult bone marrow | Fetal bone marrow |
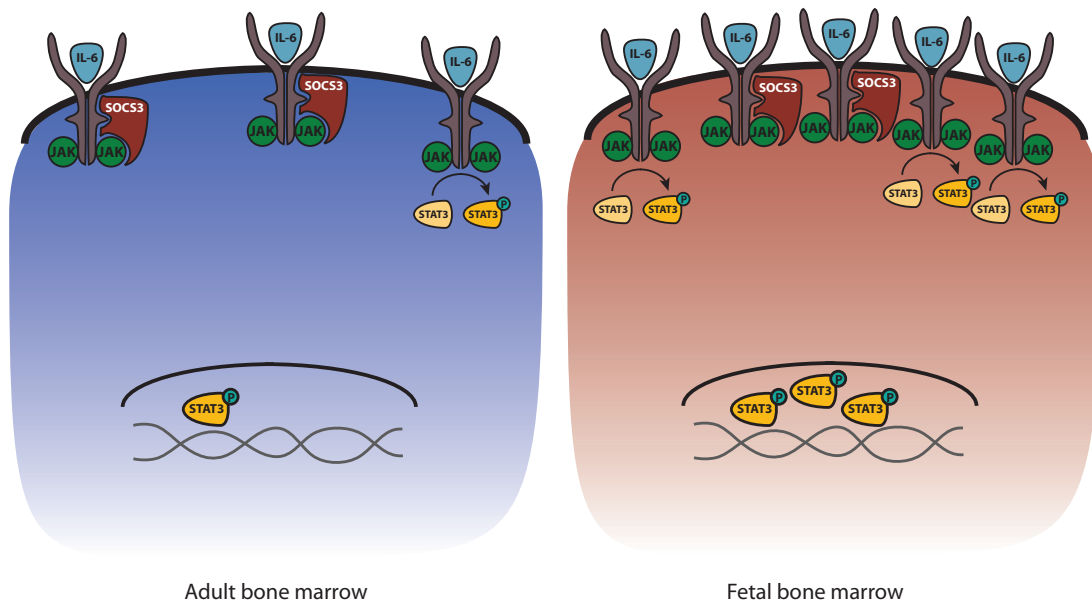
Supplemental figure 8: Model for SOCS3-mediated control of STAT3 phosphorylation. Our data demonstrates that the absolute levels of SOCS3 in fetal and adult bone marrow monocytes are the same, but that fetal monocytes express relatively more IL-6R than adult monocytes. SOCS3 interacts with the IL-6R as well as with the JAK family to mediate inhibition of STAT3 phosphorylation. We suggest a model in which the inhibitory effect of SOCS3 is insufficient to block signaling in fetal monocytes because they have a relatively higher number of IL-6Rs compared to the adult. Thus, signaling can proceed normally from the uninhibited IL-6Rs. Conversely, the higher relative ratio of SOCS3 to IL-6R found in adult monocytes allows for a relatively higher number of IL-6Rs to be inhibited by SOCS3, leading to attenuated STAT signaling.

Supplemental figure 9
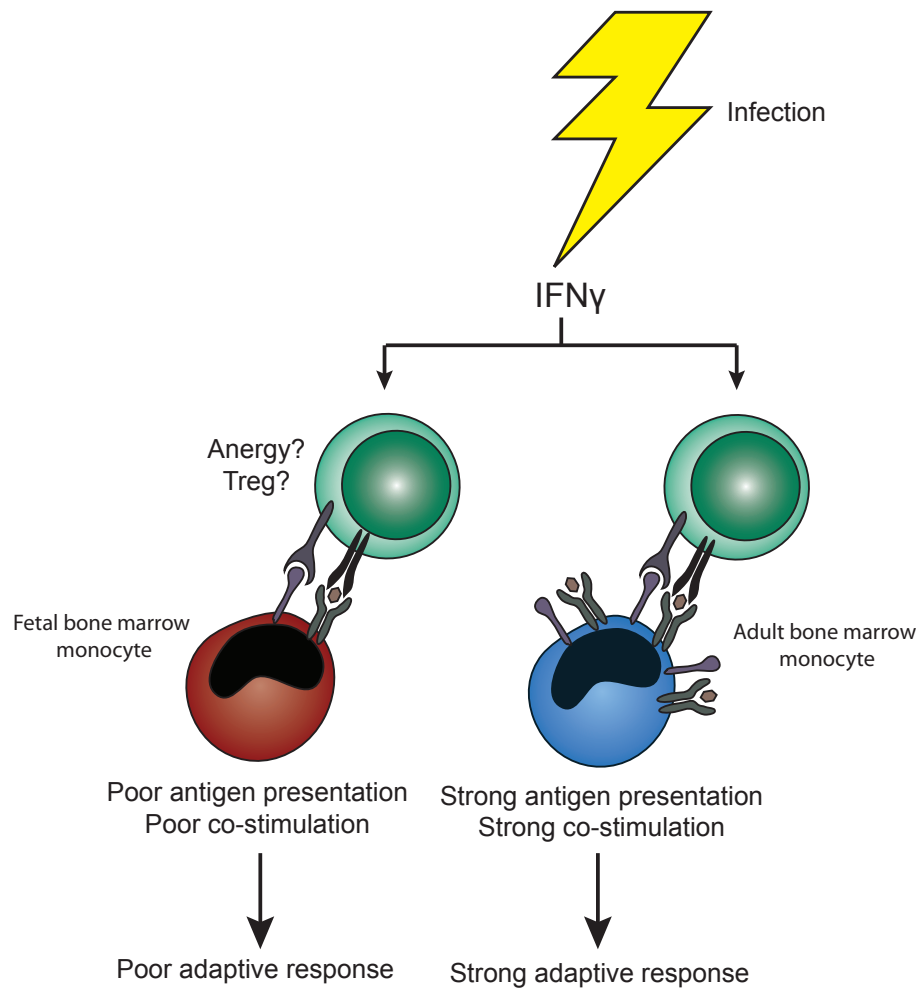
Supplemental figure 9: Model for response to IFNγ.
Stimulation of fetal monocytes with IFNγ results in a failure to up-regulate co-stimulatory and antigen presentation machinery. In contrast, adult monocytes highly up-regulate these molecules. As such, fetal monocytes are hypothesized to stimulate a poor T cell response, perhaps even inducing anergy or generation of Tregs, whereas adult monocytes can effectively prime an immunoreactive adaptive response.

For Supplemental Tables, please see publication.

Addendum to figure 5
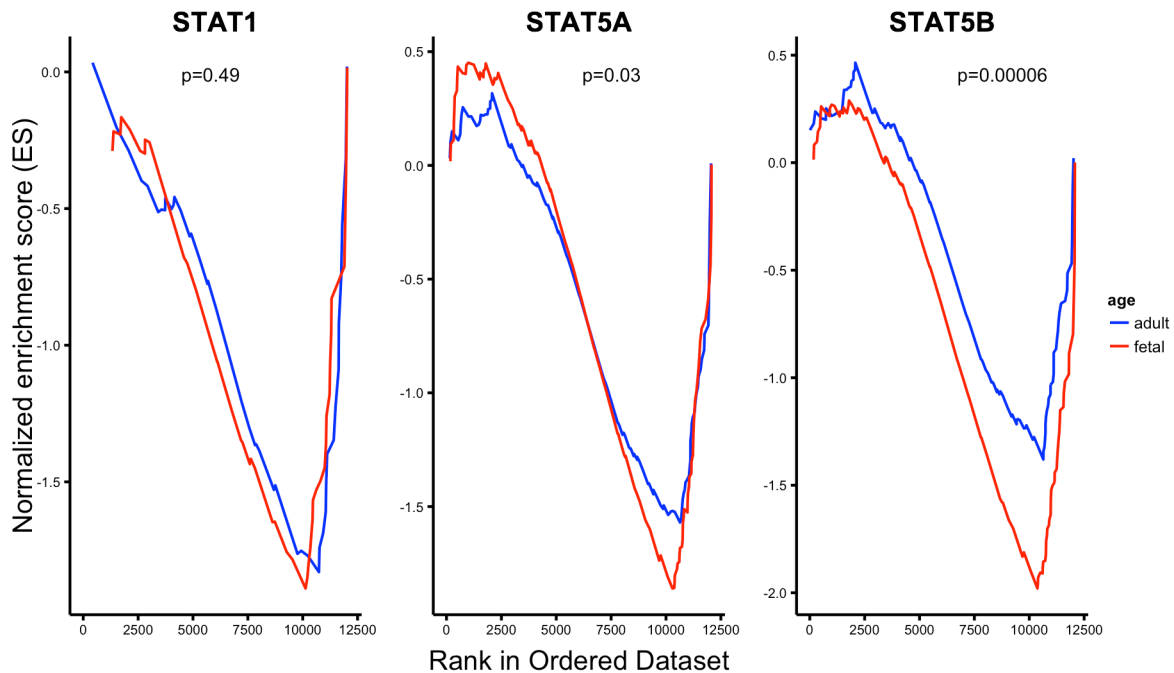
Transcription factor enrichment in IFNγ-stimulated fetal and adult monocytes.
Gene set enrichment analysis of FBM and ABM classical monocytes after stimulation
with IFNγ. Whole genome gene expression data was queried for enrichment before and
after stimulation for enrichment of STAT1, STAT5A, and STAT5B promoter elements.

Results Addendum: In order to ascertain whether differential STAT phosphorylation

after IFNγ stimulation is related to differential gene expression, the whole genome gene

expression analysis before and after IFNγ stimulation was queried using Gene Set

Enrichment Analysis (GSEA). These results indicate that there is a significant

enrichment after stimulation between fetal and adult samples in genes which are

potentially regulated by STAT5A and STAT5B, while there is similar induction of genes

potentially regulated by STAT1. Similar to what is seen in the phosphoflow data (Fig. 4),

these results indicate that the differences in functional gene expression program may be

controlled by differential STAT5 phosphorylation after stimulation with IFNγ.

Materials and methods:

Gene Set Enrichment Analysis (GSEA). Fetal and adult bone marrow monocyte stimulated with IFNγ or unstimulated whole genome gene expression arrays were probed with a gene sets from GSEA (Broad Institute) demarcating genes with STAT1, STAT5A, or STAT5B binding sites in their promoters. Enrichment was determined using GSEA software. Statistical analysis between fetal and adult curves was determined using a Kolmogorov-Smirnov test.

Chapter 3

Development of the human immune system in the

lymphoid and myeloid compartments

Abstract:

The immune system early in life contributes to a variety of susceptibilities including response to vaccination and development of asthma. However, understanding of how the human immune system develops and how the unique mechanisms present in utero[1,2] affect neonatal health has never been fully studied. Here we demonstrate that we can identify a genetic signature potentially capable of discriminating between fetal-like and adult-like cells present at birth. With this capability, we can address the basic developmental questions about how the immune system matures; either as a layered fetal and adult admixed population, or as a maturational gradient. We can also then address the question of persistence of the fetal phenotype as fetal-like cells in umbilical cord blood and whether this persistence affects downstream immune responses.

Introduction:

The identification of a fetal HSPC[2] suggests that immune maturation in humans may proceed in a layered fashion[3], with a fetal system that predominates *in utero* and an adult system that predominates later in life, as opposed to a linear model of maturation (Fig 1a). In this scenario, birth represents an admixture of fetal and adult-like cells. Developmentally this could represent itself either as an admixture of fetal and adult cells, independently and irrevocably derived from fetal and adult HSPCs (Fig 1b), or it could represent a gradient of fetal cells maturing into adult cells, such that there are some purely fetal and some purely adult cells and some that are neither fetal nor adult but some transitional stage in between (Fig 1c).

The immune system of neonates is often characterized as immature when compared to the adult[4]. Some of these "deficiencies" of monocytes in particular include low baseline expression of co-stimulatory molecules, lack of up-regulation of these co-stimulatory molecules after IFNγ stimulation, decreased inflammatory cytokine production, and decreased responsiveness to TLRs[4-9]. It has also been shown that there are more Tregs present in cord blood than in adult peripheral blood[4]. Interestingly, there are also more Tregs present in the cord blood from premature babies as compared to full-term babies[10]. Many of these phenotypes, in particular the low co-stimulatory molecules even after IFNγ stimulation as well as the expanded Treg population very closely mirror the situation found *in utero*.

Figure 1
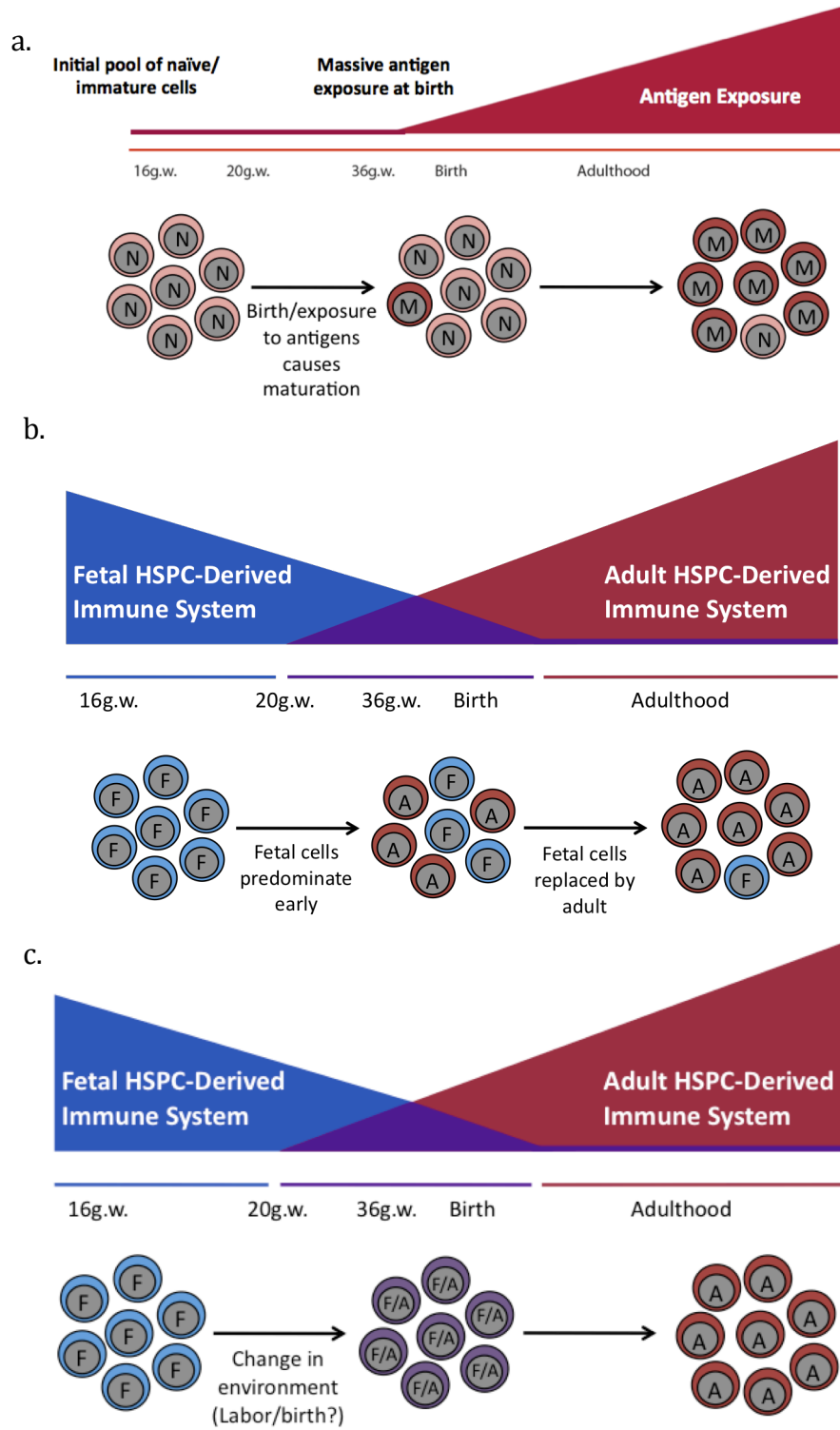
Figure 1. Models of immune maturation. (A) The linear model of maturation. The fetal immune system is completely naïve. After birth it is exposed to massive antigenic doses and matures into the adult immune system. **(B)** The layered model of maturation. Several types of HSPC appear sequentially and function at specific times during development in a cell autonomous manner, creating unique layers of HSPC derived cells with different functional outcomes. During gestation cells are derived from a fetal HSPC and have a specific functional outcome while in the adult the vast majority of the cells come from an adult HSPC which has an adult functional outcome. This model suggests that there is a period between 20 gw and 6 months to a year after birth where there is an admixture of fetal and adult derived cells and that it is this admixture of functionally different cell populations that gives rise to the differences observed in the neonatal immune system. **(C)** The maturation model. Fetal cells mature into adult cells such that at birth there are cells with a mixture of both fetal and adult characteristics.

61

Thus, perhaps the "deficiencies" found in the neonatal immune system are actually the result of the persistence (appropriate or inappropriate) of the fetal phenotype.

Differences in environmental factors, including *in utero* infection, preterm labor, stochastic developmental events, etc. could then potentially alter the relative frequency of fetal-like cells present at birth. These differences at birth, resulting in either in a skewing towards an excessively adult or fetal phenotype, could then affect the neonatal response to such immunological insults as vaccination, infection, and/or development of atopic disease.

Materials and Methods:

Isolation of fetal monocytes and naïve T cells. Fetal bone marrow, mesenteric lymph node, and peripheral blood were obtained from 18-22 gestational week specimens obtained under the auspices of CHR-approved protocols from the Department of Obstetrics, Gynecology and Reproductive Science, San Francisco General Hospital. Fetal samples were obtained after elective termination of pregnancy. Samples were excluded in the case of (1) known maternal infection, (2) intrauterine fetal demise, and/or (3) known or suspected chromosomal abnormality. Fetal monocytes were isolated from femurs by bisection and mechanical dispersion of marrow in RPMI-1640 (Sigma Aldrich). Fetal peripheral blood was obtained by cordocentesis prior to abortion. Mesenteric lymph node was isolated from the mesentery by mechanical dispersion and collagenase treatment. Adult bone marrow samples were obtained from healthy donors (AllCells, LLC. and Lonza Group Ltd.). Adult peripheral blood samples were obtained from healthy donors. Cord bloods were obtained in a de-identified manner under the

auspices of CHR approval (exempt protocol 98014889). Both adult and fetal mononuclear cells were isolated by density centrifugation of a Ficoll-Hypaque gradient (Amersham Biosciences). All samples, both fetal and adult, were viably cryopreserved prior to use.

Flow cytometry. Mononuclear cell preparations were incubated in FACS staining buffer (PBS with 2% FBS and 2 mM EDTA) with fluorochrome-conjugated, anti-human surface antibodies. Antibodies used included: CD3 Alexa-700 (OKT3, eBiosciences), CD14 qDot605 (Tuk4, Invitrogen), CD16 FITC (3G8, BD Pharmingen), HLA-DR PE-Cy7 (G46-6, BD Biosciences), CD4 qDot655 (S3.5, Life Technologies), CD45RA ECD (3P, Beckman Coulter), CD27 APC-eFluor780 (O323, eBiosciences), CD25 PE(PC61, BD Biosciences), and CD8 PE(SK1, BD Biosciences). All cells were stained with a live/dead marker (Amine-Aqua/AmCyan; Invitrogen) to exclude dead cells from the analysis.

Fluorescence activated cell sorting (FACS). Mononuclear cells were stained with the appropriate antibodies and were subsequently sorted by FACS (FACS Aria, BD Biosciences) into PBS. These cells were then re-sorted to a purity of greater than 99% directly into RNAqueous Micro lysis buffer (Ambion – Life Technologies).

RNA preparation for microarray analysis. RNA was isolated from FACS-sorted samples using the RNAqueous-Micro kit (Life Technologies) and subjected to two rounds of linear amplification using the Aminoallyl MessageAmp II kit (Life Technologies). Cy3-coupled aRNA was fragmented and hybridized overnight to a

SurePrint G3 Human Gene Expression 8x60K microarray, which was washed and scanned per manufacturer's instructions (Agilent Technologies).

Statistical analysis of microarrays. Raw intensities were extracted using Feature Extraction software (Agilent) and quantile normalized using Limma[11]. Differentially expressed genes were identified using Significance Analysis for Microarrays[12] and data visualized as heat maps using custom Perl scripts.

Fluidigm qPCR validation of microarray targets. Classical monocytes and naïve T cells were isolated by FACS from healthy umbilical cord blood as described previously. The cells were sorted directly into RLT buffer (Qiagen) and RNA was isolated according to the manufacturer's protocol (Qiagen, RNeasy Micro kit) and yield was determined on a Nanodrop spectrophotometer (Thermo Scientific). Reverse transcription was done using the Qiagen Omniscript kit according to the manufacturer's instructions. 50ng of RNA was reverse transcribed and 2-fold serial dilutions were tested with the primers enumerated in Tables S2 and S3 and Supplemental figures 4 and 5. Efficiency was calculated as 2^(-1/slope).

Results: In order to identify a fetal and adult signature present in peripheral blood, we isolated mononuclear cells from human fetal (18-22 gestational weeks) and adult peripheral blood. Because umbilical cord blood represents the fetal peripheral blood compartment at birth, we reasoned that differences seen in the peripheral blood monocytes and T cells would be applicable to a cord blood source. Classical monocytes (HLA-DR$^+$CD14$^+$CD16$^-$) and naïve T cells (as HLA-DR$^-$CD3$^+$CD4$^+$CD45RA$^+$CD27$^+$) were isolated by fluorescence activated cell sorting (FACS)and gene expression levels determined by whole genome gene expression array (Fig. 1, Fig. S1). Both fetal and adult peripheral blood had phenotypically similar classical monocyte and naïve T cell populations. The relative proportions of other populations, however, including higher CD16 expression on non-classical monocytes and an absence of CD14dimCD16hi monocytes, as well as the absence of memory T cells in the fetus, suggests that there are differences in the composition of fetal versus adult peripheral blood. Unbiased clustering of the classical monocytes population (Fig. 2) demonstrated that two of the adult peripheral blood samples unexpectedly clustered with fetal samples. In order to understand why this might be, a heatmap of the genes most highly associated with generation of the cluster (Fig. 3) was generated and the genes contributing to the inappropriate clustering were identified (Fig. 3 Box C). These genes were then queried using Ingenuity Pathway Analysis software to better elucidate the pathways contributing to the clustering. The genes identified were genes that were upregulated in APB1 and APB5 as well as in the fetal samples, but not in the other adult samples. Interestingly, these genes fell primarily into the category of response to viral infection – particularly influenza (Table 1). These data suggest two possibilities: (1) The two adult subjects
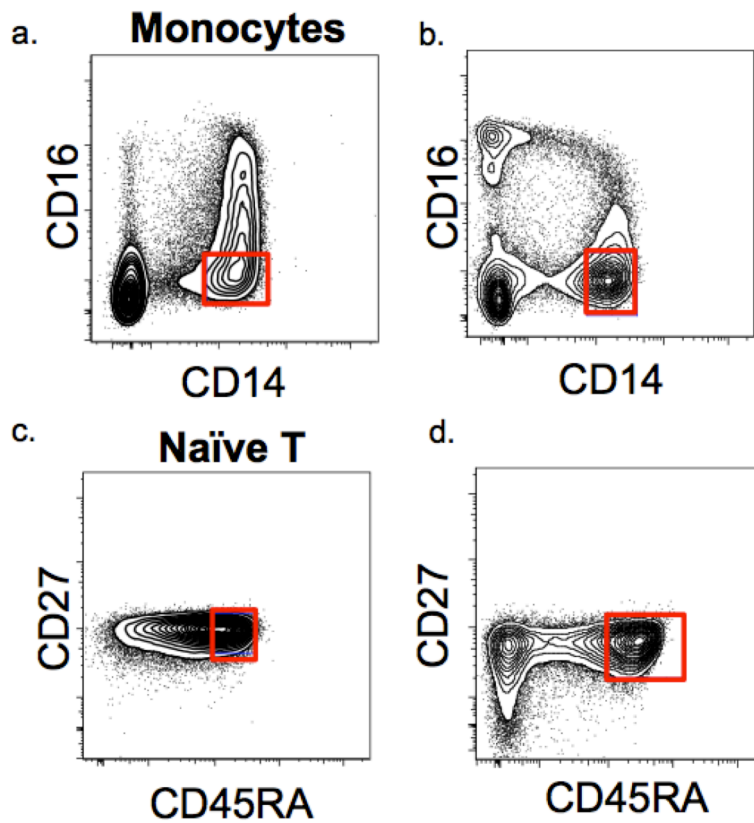
Figure 1: Phenotypic characterization of fetal and adult peripheral blood classical monocytes and naïve T cells. (A) Fetal peripheral blood classical monocytes defined as HLA-DR$^+$CD14$^+$CD16$^-$.**(B)** Adult peripheral blood classical monocytes defined as HLA-DR$^+$CD14$^+$CD16$^-$. **(C)** Fetal peripheral blood naïve T cells defined as HLA-DR$^-$ CD3$^+$CD4$^+$CD45RA$^+$CD27$^+$. **(D)** Adult peripheral blood naïve T cells defined as HLA-DR$^-$CD3$^+$CD4$^+$CD45RA$^+$CD27$^+$.

Cluster Dendrogram

Figure 2: Transcriptional characterization of human adult and fetal peripheral blood monocytes. Unbiased cluster analysis of gene expression of APB and FPB classical monocytes.
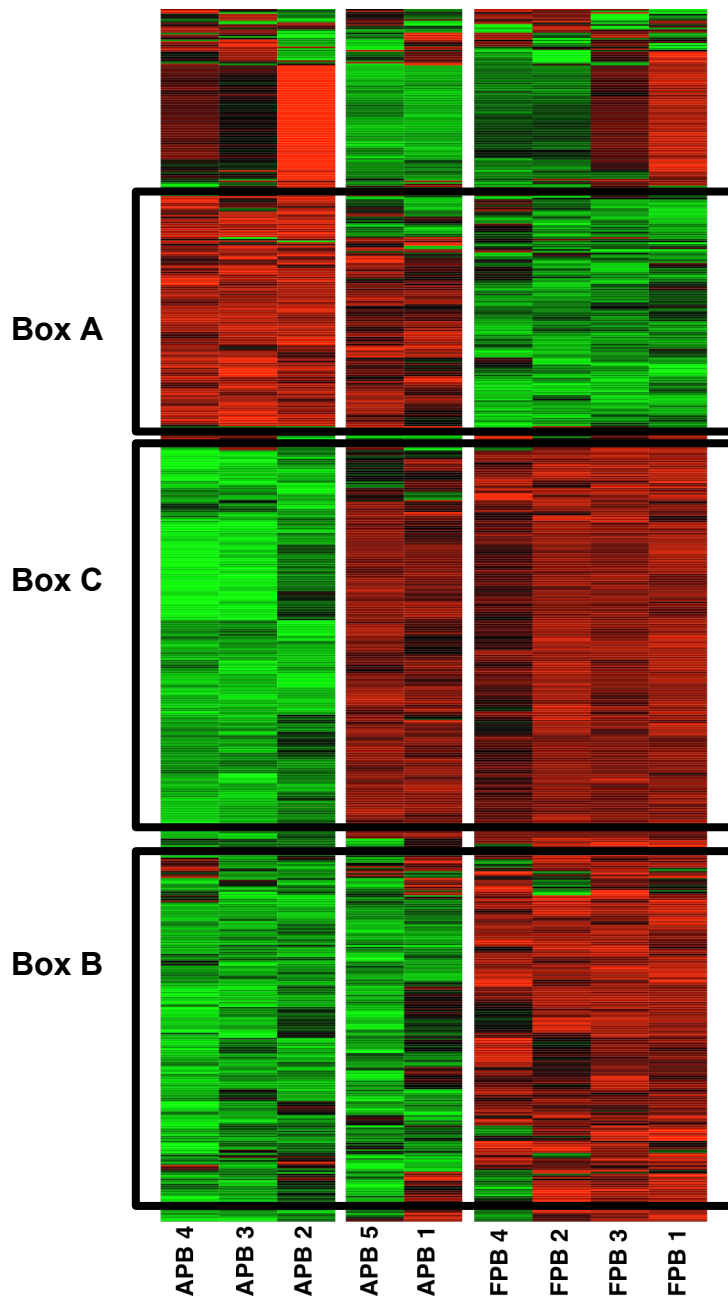
Figure 3: Heatmap of differentially expressed genes in monocytes. The genes most responsible for driving clustering in monocytes were isolated and represented as a heatmap. Boxes A and B represent genes conserved between all APB and FPB samples. Box C represents the subset of genes responsible for APB1 and 5 clustering with FPB samples

Major pathways driving APB clustering with FPB
Apoptosis Signaling
Integrin Signaling
Lymphotoxin β Receptor Signaling
PI3K/AKT Signaling
IL-8 Signaling
NF-κB Activation by Viruses
IL-6 Signaling

Table 1: Canonical pathways driving APB samples to cluster with FPB. These pathways were identified using Ingenuity Pathway Analysis (IPA) software. The pathways described fell into the viral infection, particularly influenza, categories as defined by IPA.

were infected with or recovering from a viral infection or (2) these individuals might exhibit persistence of fetal like cells not seen in the other individuals tested.

Because these genes are potentially inducible by outside factors, the two samples were removed from subsequent pathway analysis in the monocyte compartment. The remaining samples were then queried via pathway analysis to better understand the distinct pathways present in fetal versus adult peripheral blood (Fig. 4). Many of these pathways are involved in production of and response to cytokines. Many of the cytokines, including IL-10, IL-6, and IL-1, are known to play important roles in the maintenance of pregnancy and the onset of preterm labor respectively[13]. Overall, the differentially expressed pathways suggest that fetal peripheral blood monocytes are highly active and may have highly potent responses to potential inflammatory stimuli; this observation has been previously described in human fetal bone marrow monocytes[1], suggesting that perhaps the fetal myeloid compartment is poised to respond very rapidly to potential immunological threats.

Because differences have also been described in the fetal T cell compartment[2,14], we also assayed naïve T cells (Fig. 1, Sup Fig. 1). Unlike the monocytes, all of the T cell samples cluster with the appropriate age range (Fig. 5). Subsequent pathway analysis showed that the differences in T cells appear to be in metabolic and proliferative pathways (Fig. 6). These differences in metabolism may underlie the predisposition of fetal T cells to become T regulatory cells as it has been shown that effector and Treg cells preferentially use and require different metabolic pathways[15,16].

Figure 4: Canonical pathways most highly differentially expressed between FPB and APB in classical monocytes. Pathway analysis of FPB versus APB classical monocytes excluding APB1 and APB5.
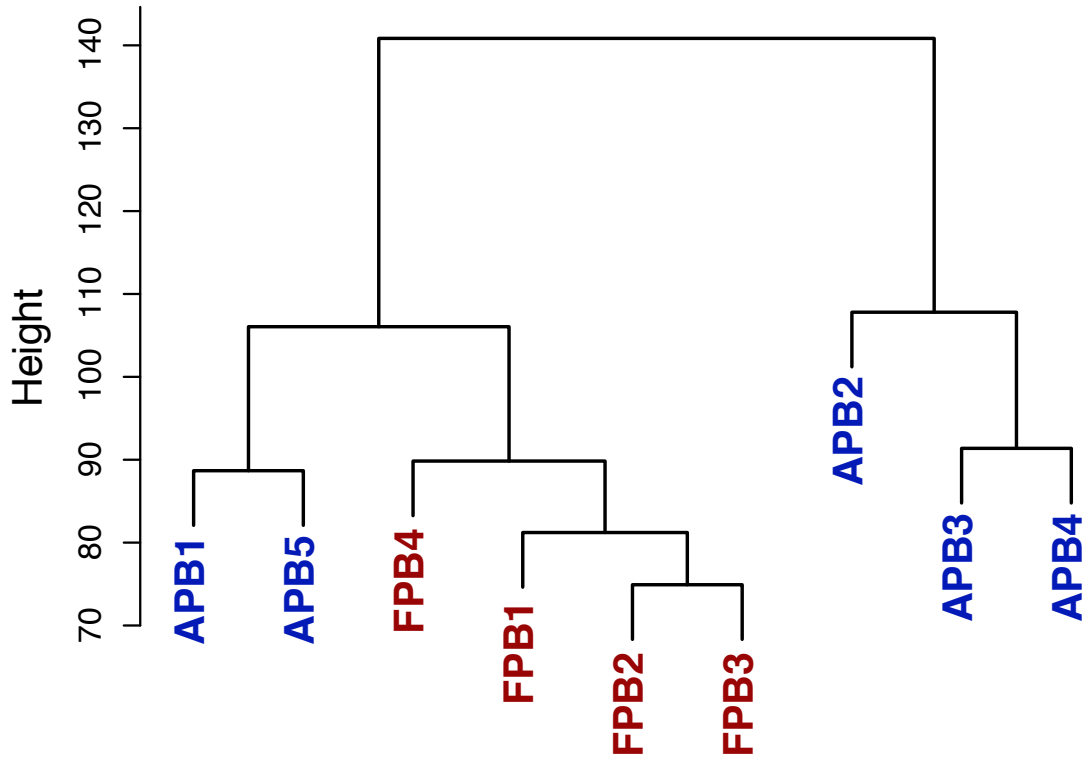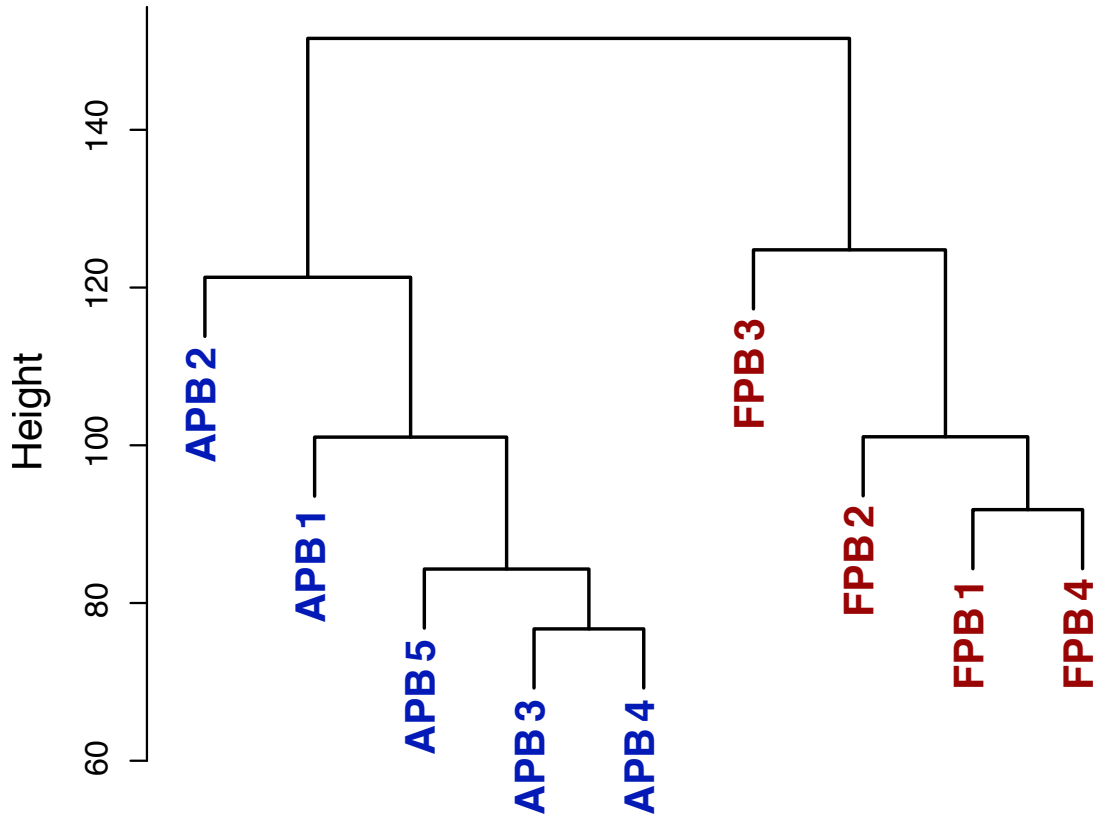
Figure 5: Transcriptional characterization of human adult and fetal peripheral blood naïve T cells. Unbiased cluster analysis of gene expression of APB and FPB naïve T cells.
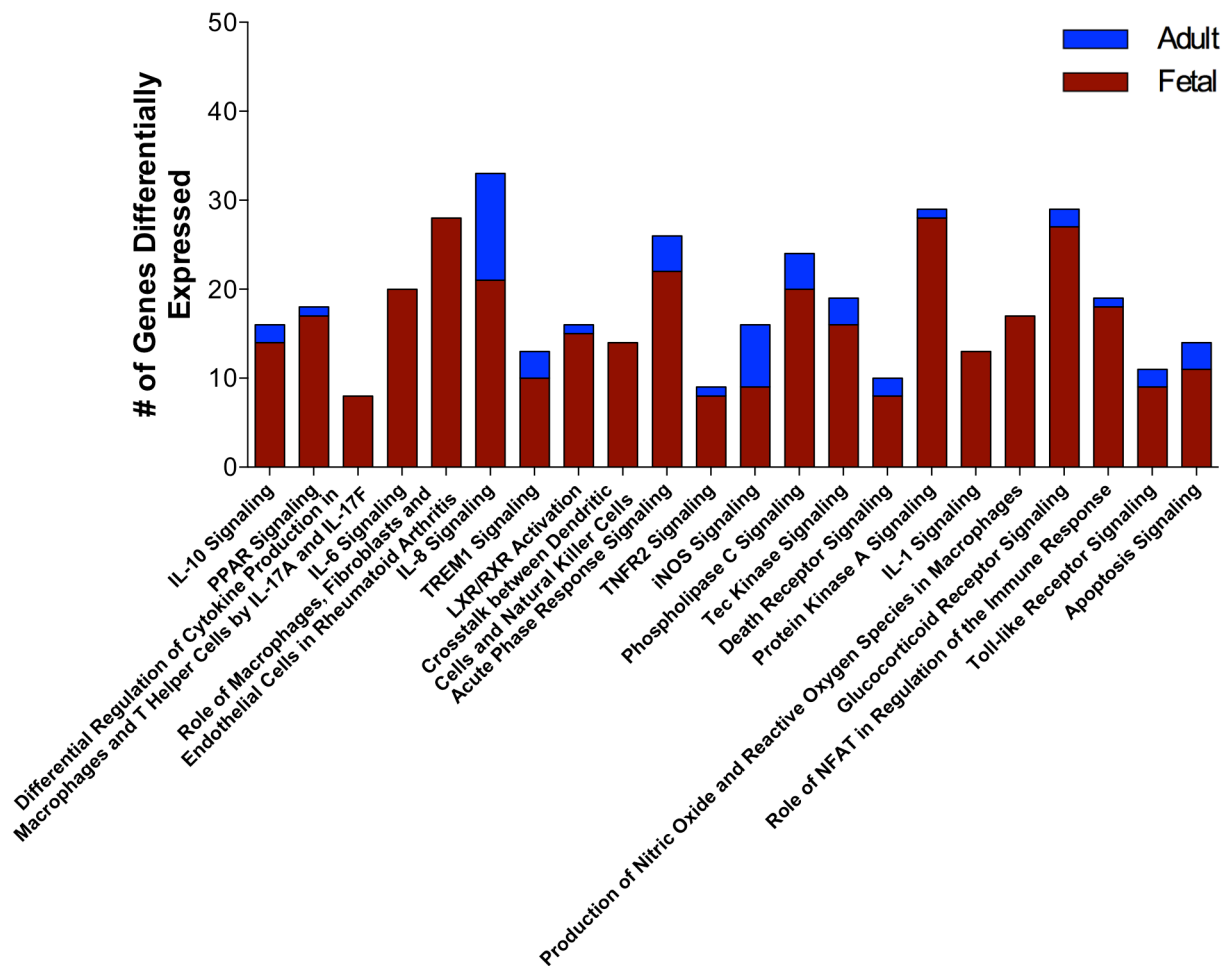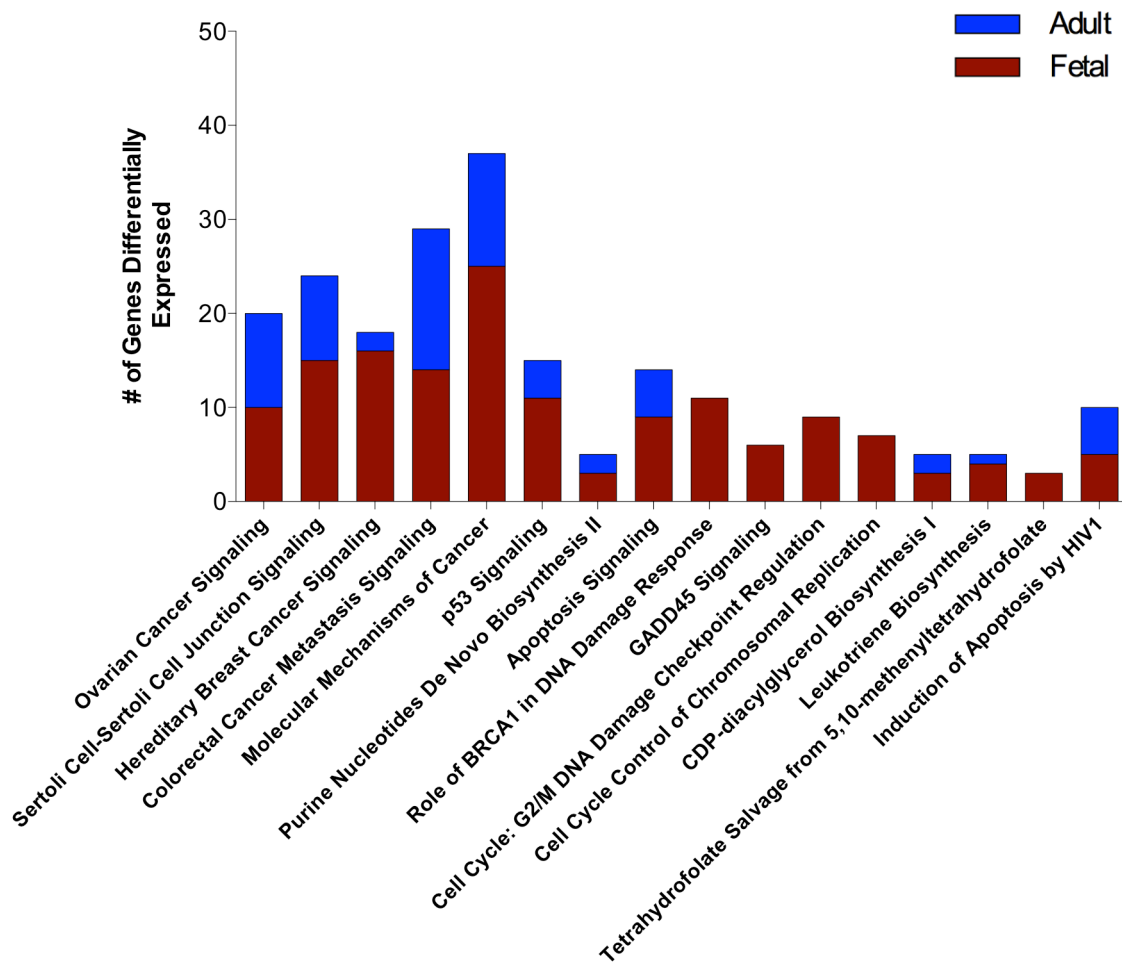
Figure 6: Canonical pathways most highly differentially expressed between FPB and APB naïve T cells. Pathway analysis of FPB versus APB naïve T cells.

Based on these expression arrays, we sought to determine if we could isolate a fetal-specific and adult-specific gene signature. Because all of the lineages downstream of the HSPC are different between fetus and adult, we wondered if there were developmental programs conserved between fetal lymphoid and myeloid cells. To that end we used gene expression data to identify genes that were significantly differentially expressed ($p<0.05$) and greater than 1.5 fold differentially expressed in both the monocytes and the naïve T cells in the same direction (Fig. 7, Table S1). Monocyte and T cell specific genes were also added to this list in order to create a robust genetic signature (Table S1). To assay the presence of these genes in umbilical cord blood, we used the Fluidigm nanofluidic qpCR platform. Primers were validated on normal full term umbilical cord blood (Fig. S2, Fig. S3, Table S2, Table S3), in preparation for bulk testing.

Discussion and Future Directions: In these studies, we have identified major pathway differences between fetal and adult peripheral blood monocytes and naïve T cells. These differences indicate that the myeloid compartment in the fetus is poised to respond to bacterial, viral, or inflammatory cues, while the lymphoid compartment is primarily tolerogenic. These data suggest that there are multiple mechanisms at play in the maintenance of a successful pregnancy and call into question the idea of a purely inert or tolerogenic fetal immune system. Further, we have identified a potential signature to analyze presence of fetal and adult associated transcripts in umbilical cord blood and validated this signature using a high throughput technology.
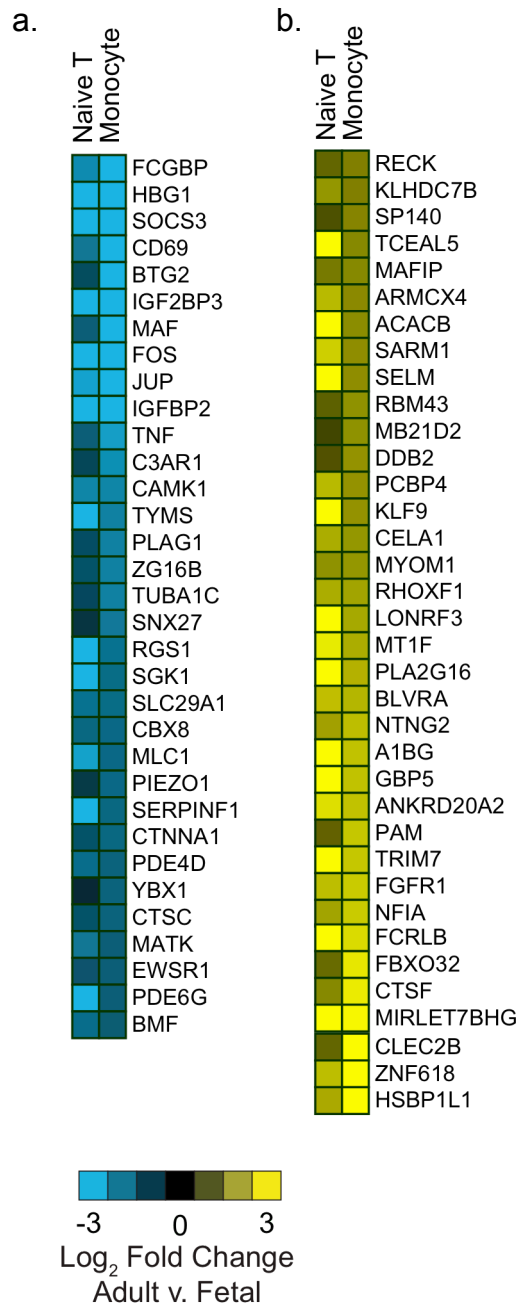
Figure 7: Identification of a genetic signature conserved in monocyte and T cells in APB and FPB. Genes to be used in the signature were identified as being significantly differentially expressed (p<0.05), greater than 1.5 fold differentially expressed in monocytes, and greater than 1.5 fold differentially expressed in T cells in the same direction as in monocytes. **(A)** A subset of differentially expressed genes more highly expressed in fetal monocytes and T cells. **(B)** A subset of differentially expressed genes more highly expressed in adult monocytes and T cells.

In future work, this signature can and will be used to answer two questions: (1) Is there a persistence of fetal genes in umbilical cord blood and (2) are fetal transcripts exclusively expressed on a single cell basis when compared to the adult? The first of these questions can be addressed by assaying bulk monocyte and naïve T cells from umbilical cord blood and determining the relative expression of fetal and adult transcripts. This assay could then be further used to ask the question of whether or not the persistence of this fetal phenotype affects neonatal health, in particular, response to vaccination and development of asthma.

The second question can be addressed using single cell technology to ask if the expression of fetal and adult genes are exclusive at the single cell level or whether cells can express both fetal and adult transcripts. This will address and answer the question of immune maturation and elucidate whether the layered model or maturation model is present during human immune development.

References:

1. Krow-Lucal E.R., Kim C.C., Burt T.D., McCune J.M. Distinct functional programming of human fetal and adult monocytes. Blood. 2014.

2. Mold JE, Venkatasubrahmanyam S, Burt TD, Michaëlsson J, Rivera JM, et al. Fetal and adult hematopoietic stem cells give rise to distinct T cell lineages in humans. Science. 2010;330:1695-1699.

3. Herzenberg LA, Herzenberg LA. Toward a layered immune system. Cell. 1989;59:953-954.

4. Velilla PA, Rugeles MT, Chougnet CA. Defective antigen-presenting cell function in human neonates. Clin Immunol. 2006;121:251-259.

5. Levy O, Zarember KA, Roy RM, Cywes C, Godowski PJ, Wessels MR. Selective impairment of TLR-mediated innate immunity in human newborns: neonatal blood plasma reduces monocyte TNF-alpha induction by bacterial lipopeptides, lipopolysaccharide, and imiquimod, but preserves the response to R-848. J Immunol. 2004;173:4627-4634.

6. Chelvarajan RL, Collins SM, Doubinskaia IE, Goes S, Van Willigen J, et al. Defective macrophage function in neonates and its impact on unresponsiveness of neonates to polysaccharide antigens. J Leukoc Biol. 2004;75:982-994.

7. Upham JW, Lee PT, Holt BJ, Heaton T, Prescott SL, et al. Development of interleukin-12-producing capacity throughout childhood. Infection and immunity. 2002;70:6583.

8. Han P, McDonald T, Hodge G. Potential immaturity of the T-cell and antigen-presenting cell interaction in cord blood with particular emphasis on the CD40-CD40 ligand costimulatory pathway. Immunology. 2004;113:26-34.

9. Hodge S, Hodge G, Flower R, Han P. Cord blood leucocyte expression of functionally significant molecules involved in the regulation of cellular immunity. Scand J Immunol. 2001;53:72-78.

10. Takahata Y, Nomura A, Takada H, Ohga S, Furuno K, et al. CD25+CD4+ T cells in human cord blood: an immunoregulatory subset with naive phenotype and specific expression of forkhead box p3 (Foxp3) gene. Exp Hematol. 2004;32:622-629.

11. Smyth GK. Linear models and empirical bayes methods for assessing differential expression in microarray experiments. Stat Appl Genet Mol Biol. 2004;3:Article3.

12. Tusher VG, Tibshirani R, Chu G. Significance analysis of microarrays applied to the ionizing radiation response. Proceedings of the National Academy of Sciences. 2001;98:5116-5121.

13. Erlebacher A. Immunology of the maternal-fetal interface. Annu Rev Immunol. 2013;31:387-411.

14. Mold JE, Michaelsson J, Burt TD, Muench MO, Beckerman KP, et al. Maternal Alloantigens Promote the Development of Tolerogenic Fetal Regulatory T Cells in Utero. Science. 2008;322:1562-1565.

15. Gerriets VA, Rathmell JC. Metabolic pathways in T cell fate and function. Trends Immunol. 2012;33:168-173.

16. Michalek RD, Gerriets VA, Jacobs SR, Macintyre AN, MacIver NJ, et al. Cutting edge: distinct glycolytic and lipid oxidative metabolic programs are essential for effector and regulatory CD4+ T cell subsets. J Immunol. 2011;186:3299-3303.
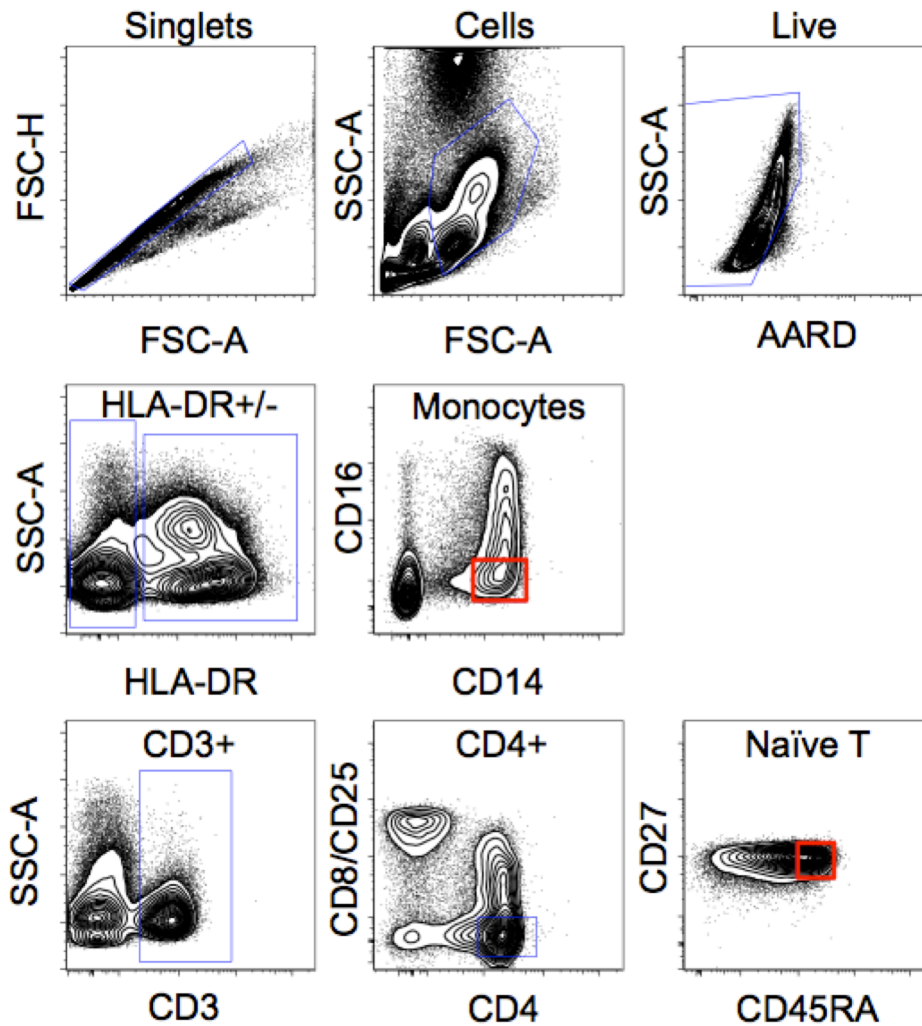
Supplemental Figure 1: Gating strategy for identification of classical monocytes and naïve T cells in fetal peripheral blood. Mononuclear cells were isolated from fetal peripheral blood and stained with HLA-DR, CD14, CD16, CD3, CD4, CD8, CD25, CD27, CD45RA and a live-dead marker. Classical monocytes (CD14$^+$CD16$^-$) and naïve T cells (CD3$^+$CD4$^+$CD8$^-$CD25$^-$CD27$^+$CD45RA$^+$) were sorted using the gating strategy presented for whole genome array analysis. Populations were demarcated as shown.
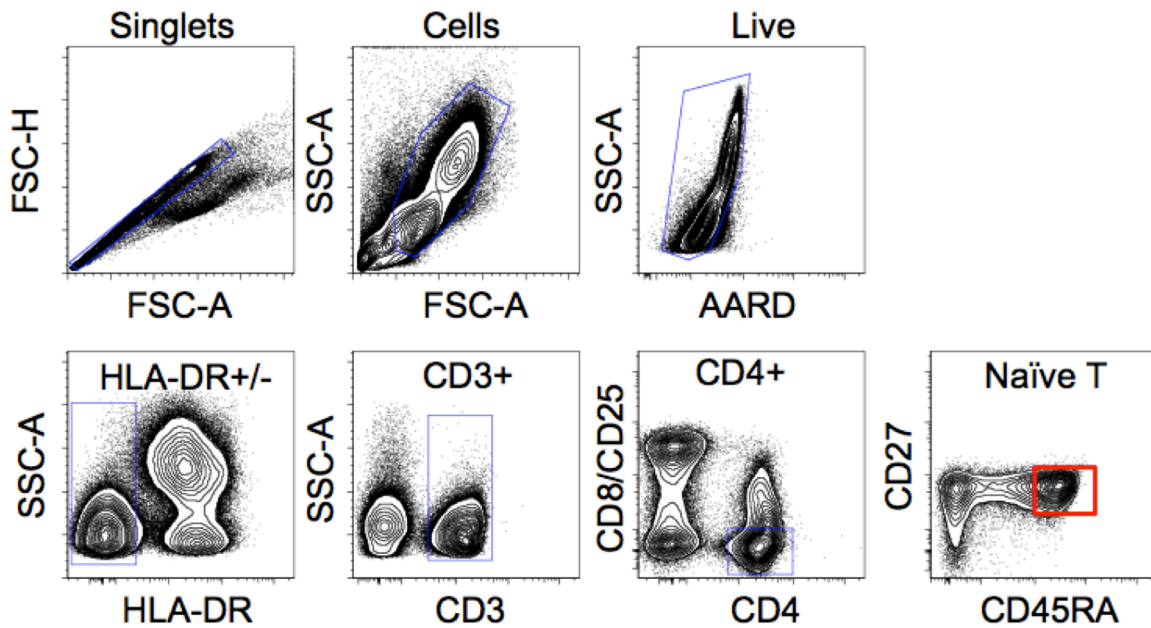
Supplemental Figure 2: Gating strategy for identification of naïve T cells in adult peripheral blood. Mononuclear cells were isolated from adult peripheral blood and stained with HLA-DR, CD14, CD16, CD3, CD4, CD8, CD25, CD27, CD45RA and a live-dead marker. Naïve T cells ($CD3^+CD4^+CD8^-CD25^-CD27^+CD45RA^+$) were sorted using the gating strategy presented for whole genome array analysis. Populations were demarcated as shown.
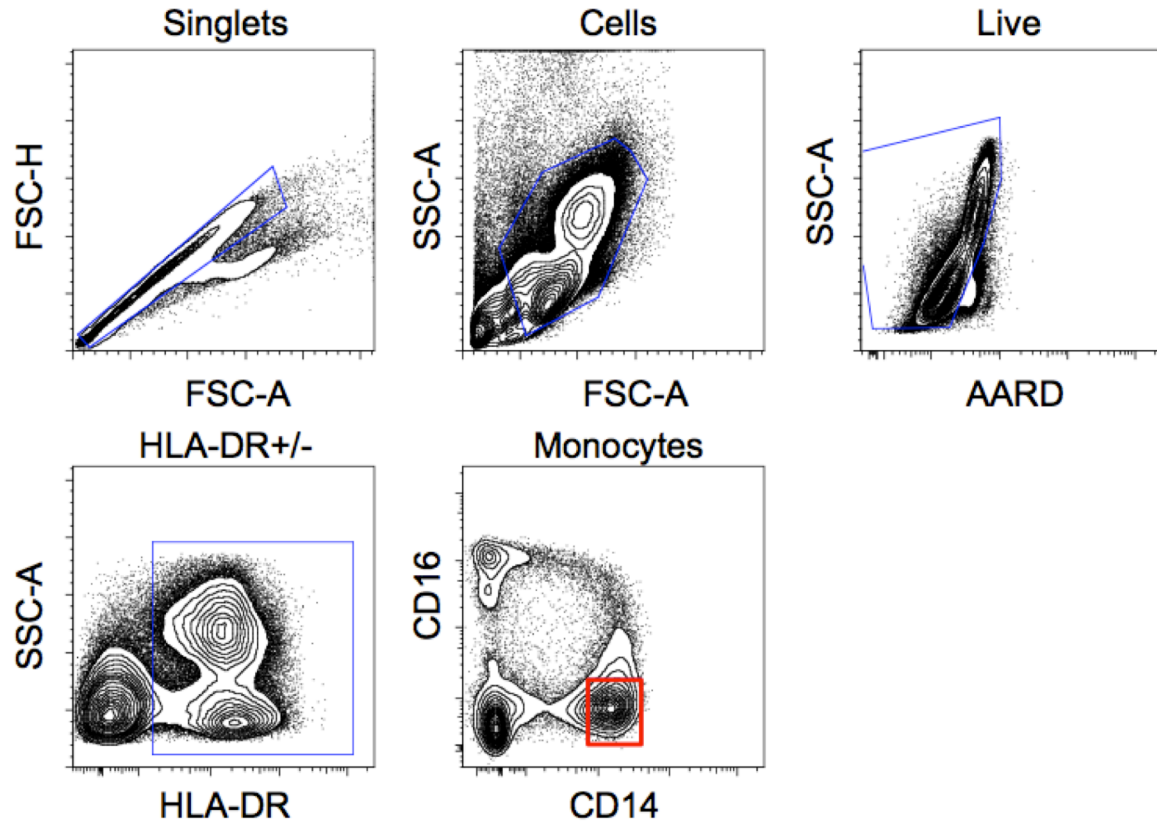
Supplemental Figure 3: Gating strategy for identification of classical monocytes in adult peripheral blood. Classical monocytes (CD14$^+$CD16$^-$) were sorted using the gating strategy presented for whole genome array analysis. Populations were demarcated as shown.
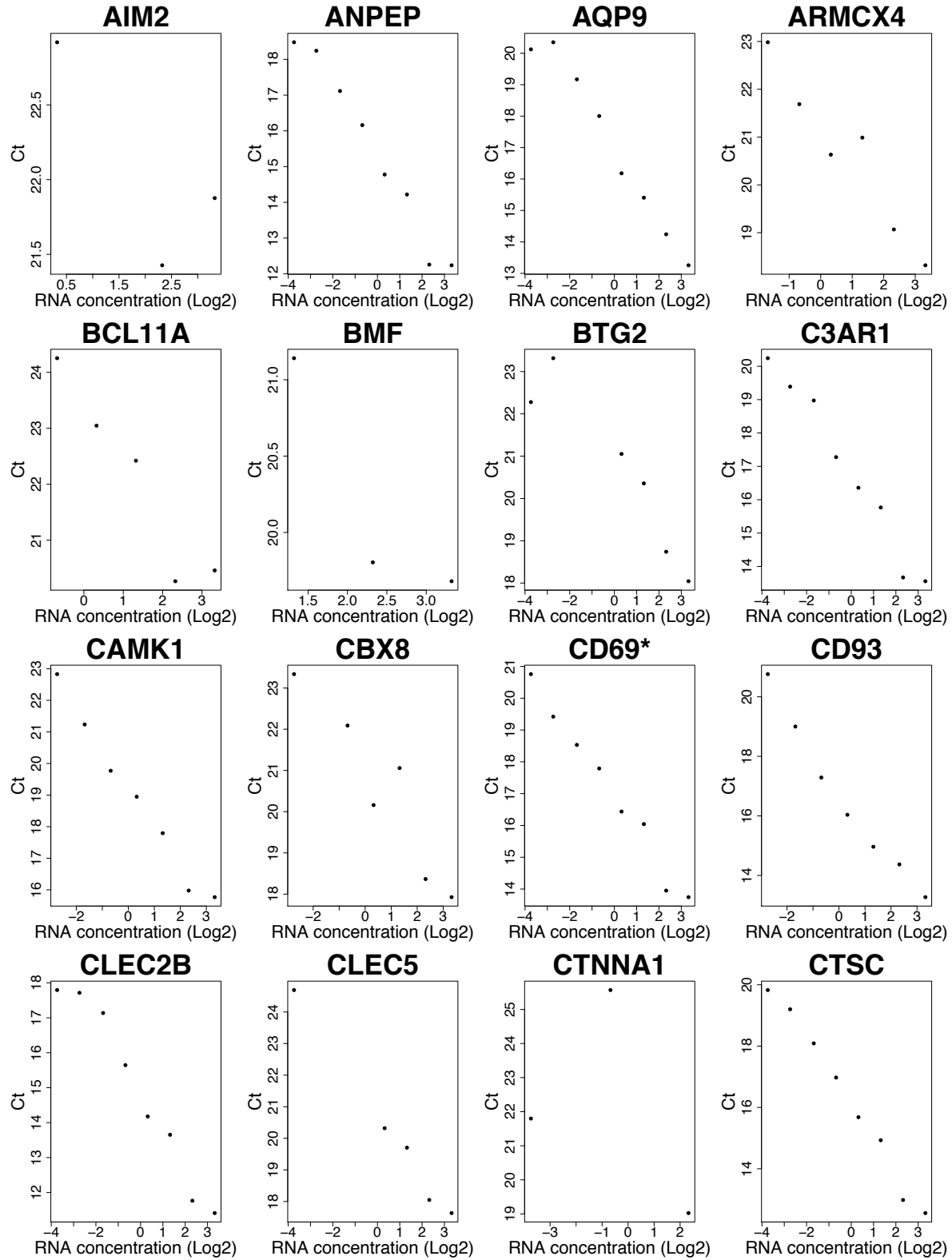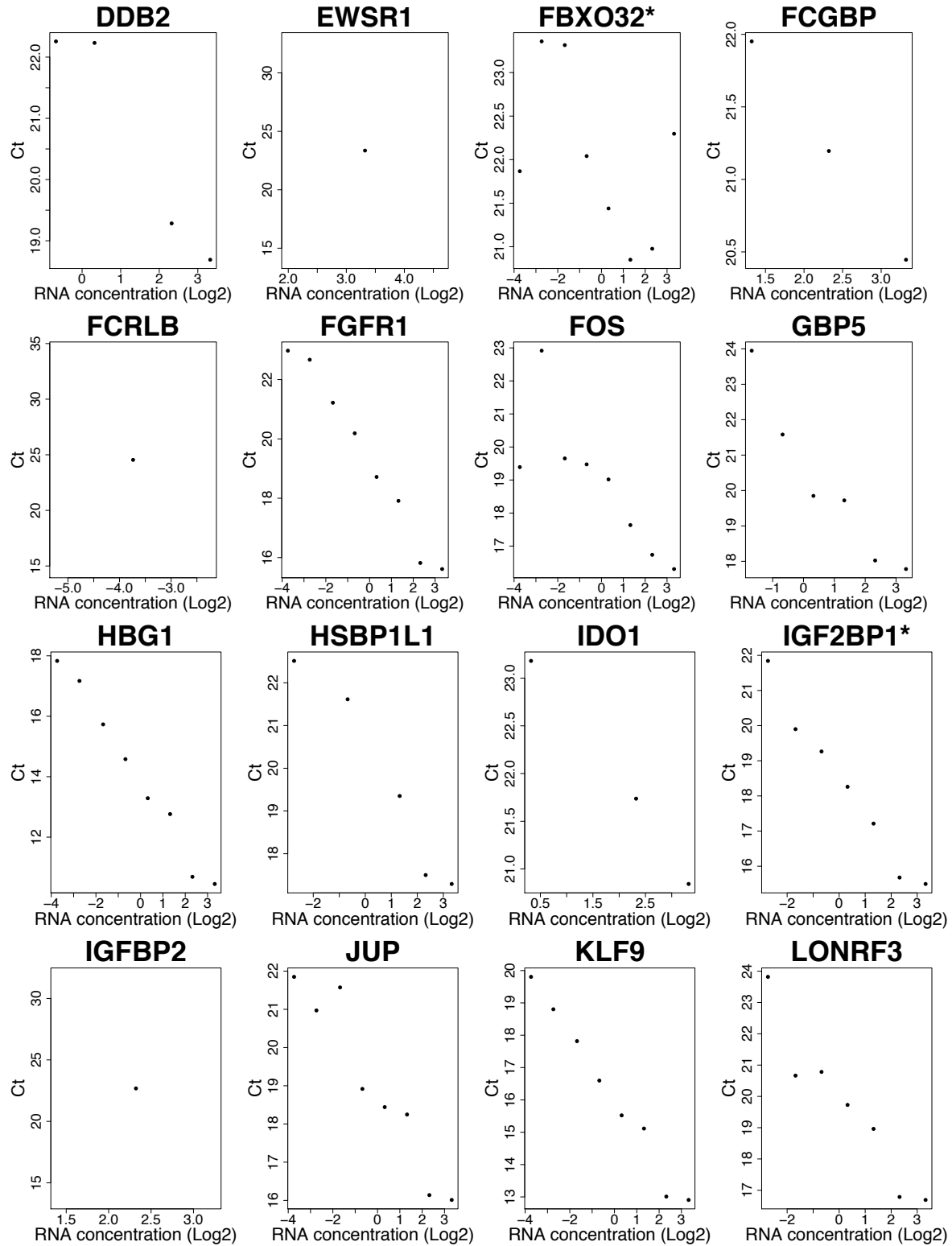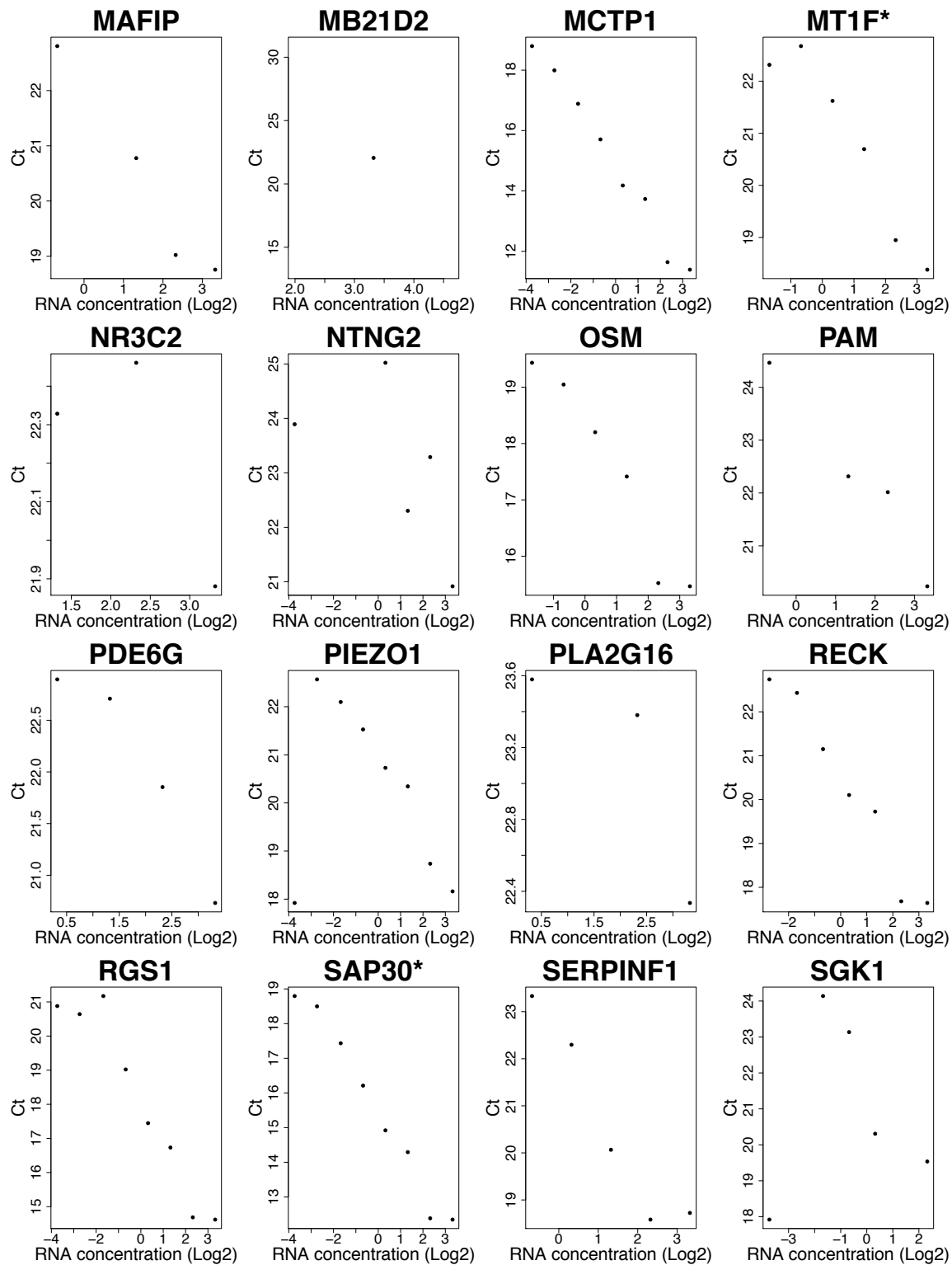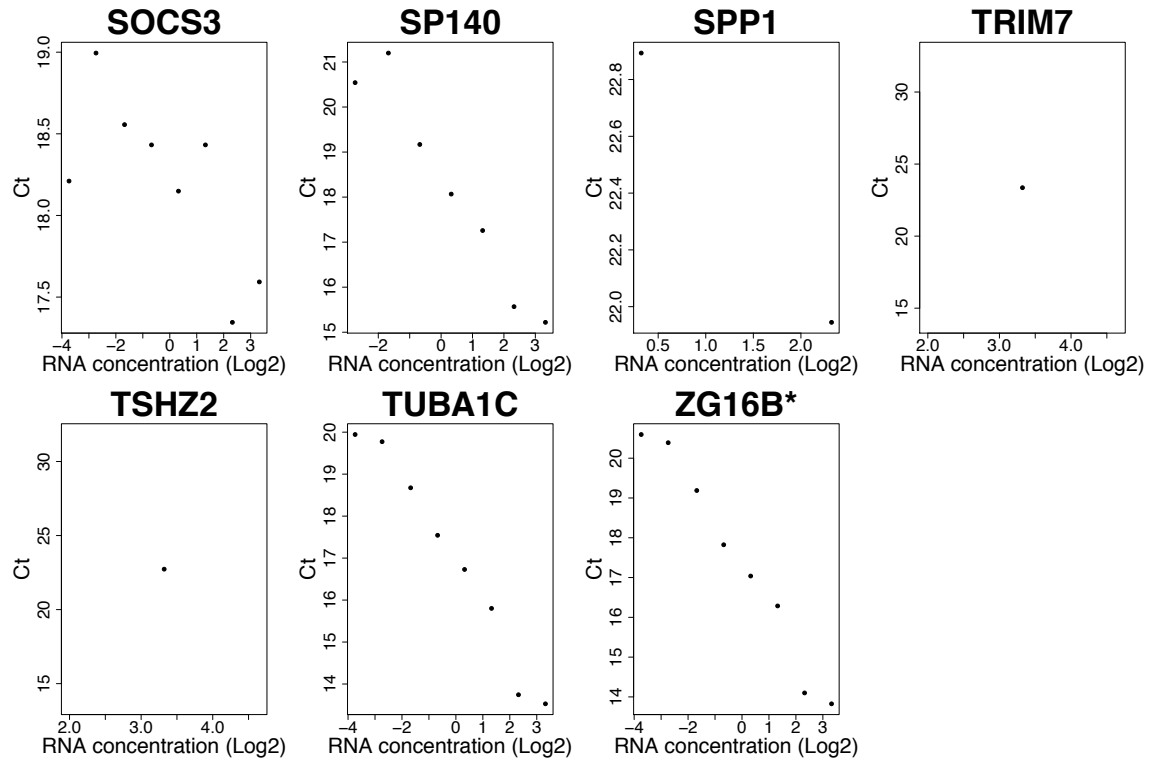
Supplemental figure 4. Monocyte fluidigm primer validation. CD14$^+$16$^-$ classical monocytes cDNA was diluted in a two-fold dilution and primer efficiency was tested. Samples were run in technical triplicate. Values were averaged if the range of the triplicates was less than 2 cycles different.
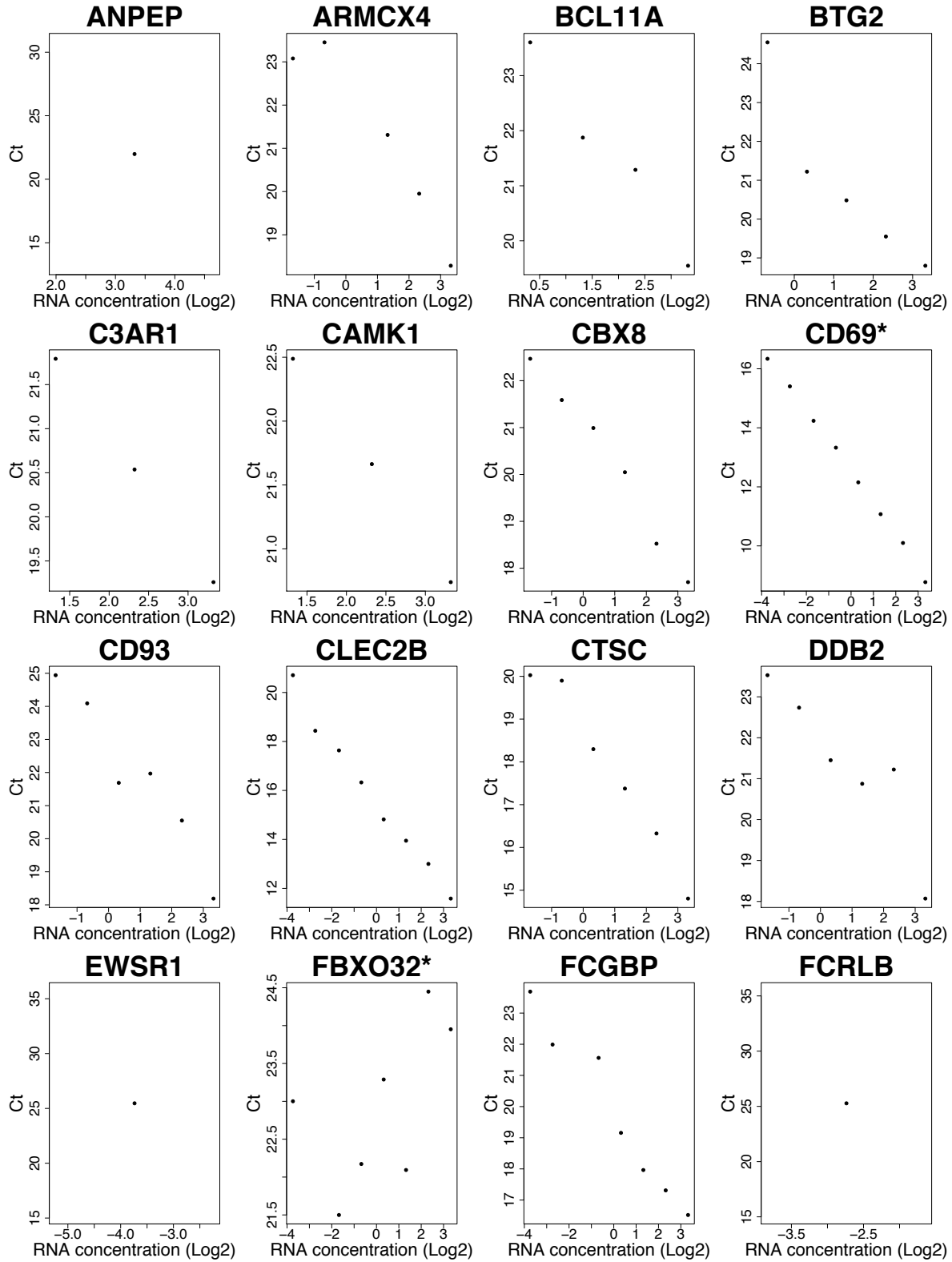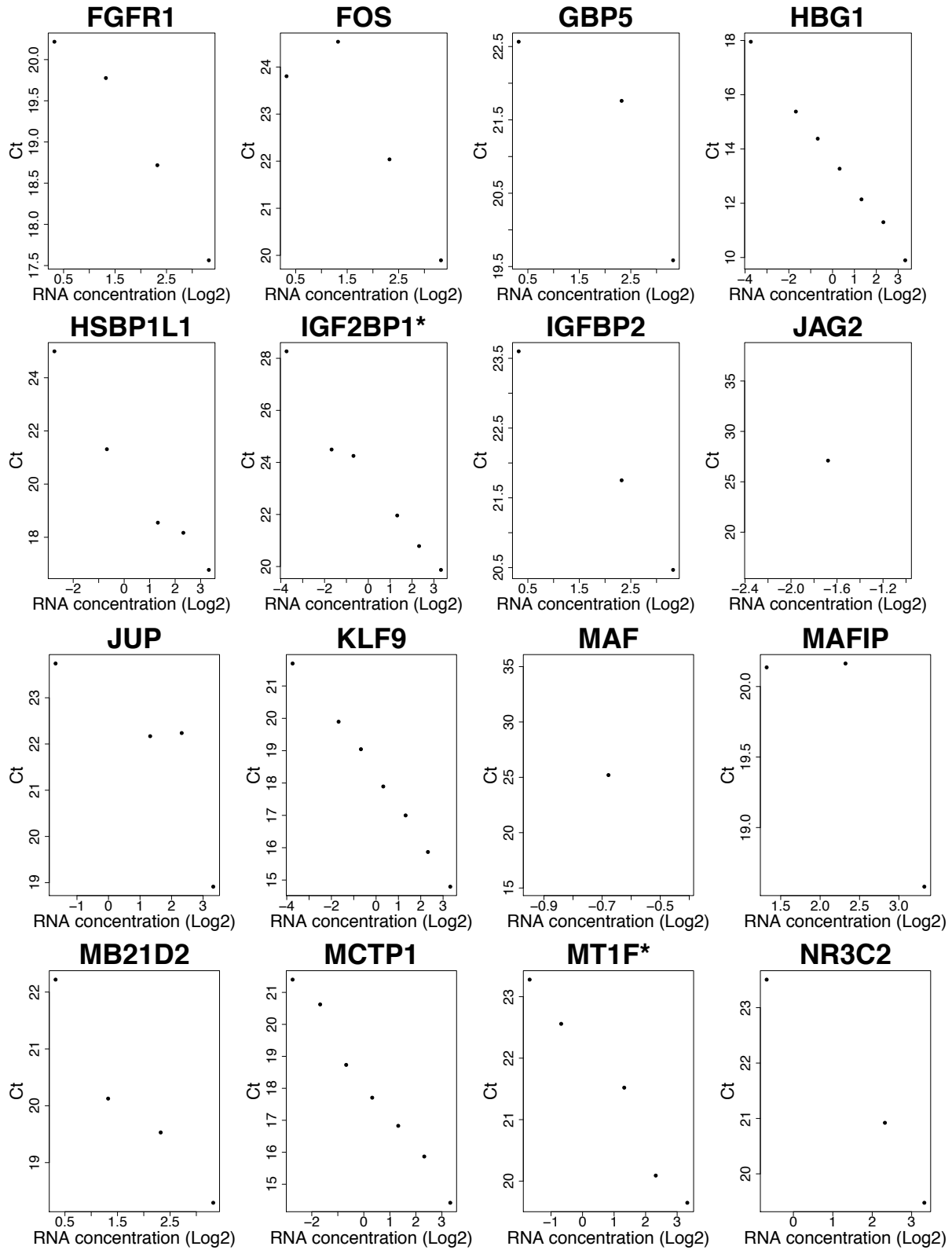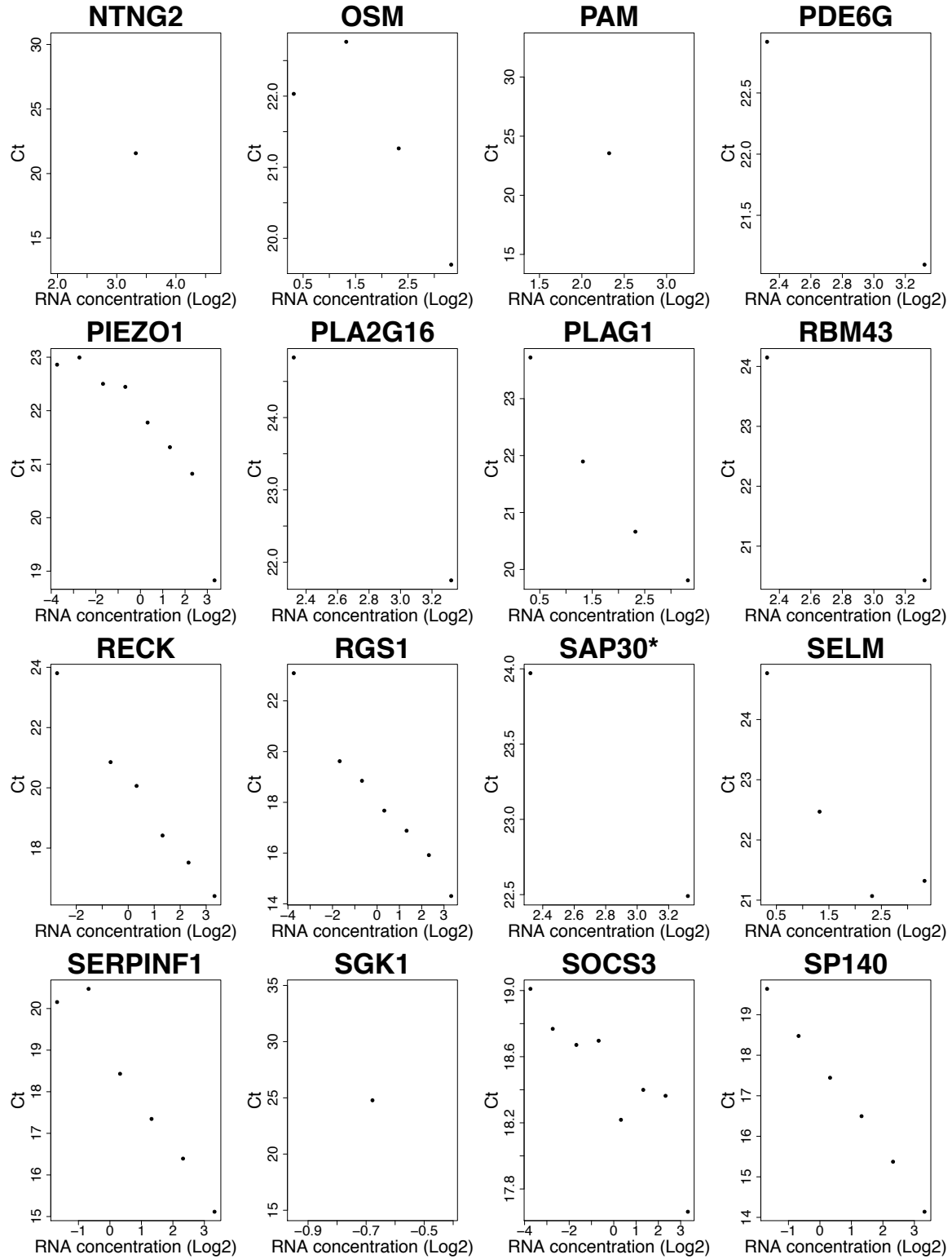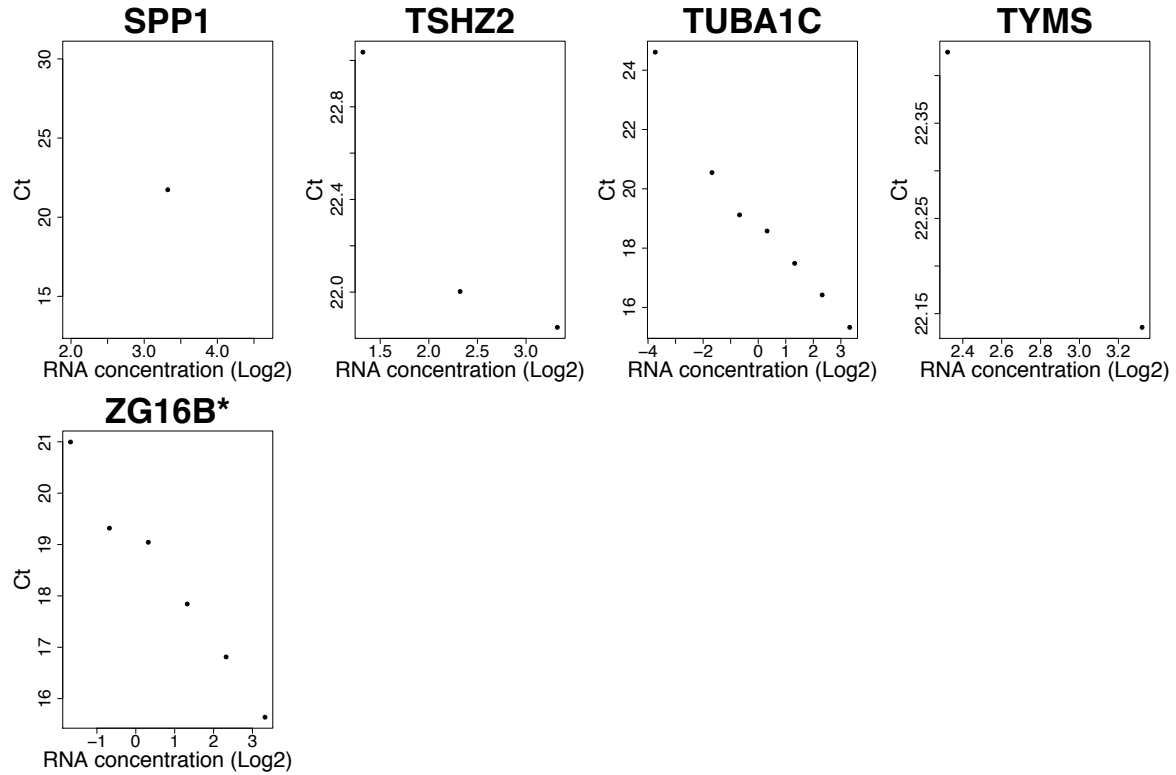
Supplemental Figure 5. Naïve T fluidigm primer validation. Naïve T cell cDNA was diluted in a two-fold dilution and primer efficiency was tested. Samples were run in technical triplicate. Values were averaged if the range of the triplicates was less than 2 cycles different.

For supplemental tables, please see appendix 1 (pg. 120)

Chapter 4:

HIV restriction factors in fetal and adult classical monocytes

Abstract:

The factors controlling mother-to-child transmission of HIV *in utero* are not well understood. While the mother and fetus share a blood supply, the rate of transmission *in utero* remains low [1,2], suggesting that perhaps the fetus is more resistant to HIV infection than the adult. In these studies, we demonstrate that fetal bone marrow monocytes have a stronger induction of HIV restriction factors after stimulation with IFNγ. We also show that the fetal response to IFNα/β is characterized by very high levels of canonical STAT1 and non-canonical STAT3 and STAT5 phosphorylation. Taken together, these data suggest that the fetus may be protected from HIV infection due to non-canonically mediated up-regulation of HIV restriction factors.

Introduction:

Many chronic blood-borne pathogens have surprisingly low *in utero* transmission including HCV, malaria, and HIV[1-4]. In the case of HIV in particular, T cell activation has been linked to viral entry and spread [5], as such the predominance of Tregs which would prevent T cell activation in the fetus may serve as a direct mechanism of inhibiting infection *in utero.* However, the myeloid compartment would still then be vulnerable.

HIV infection in myeloid cells can be inhibited by HIV restriction factors[6]. Restriction factors decrease HIV infectivity in cells and have recently been described as one of the primary reasons that myeloid cells are less susceptible to HIV infection than T cells[6]. These factors maybe expressed basally, but many are also highly inducible by both type I and type II interferon[6]. To this end, we wondered if fetal myeloid cells might be less susceptible to HIV infection due to increased expression of restriction factors. In these studies, we demonstrate that a subset of restriction factors are more enriched after IFNγ stimulation in fetal monocytes than in adult. Further, we demonstrate that the fetal response to type I IFN results in higher levels of canonical STAT1 phosphorylation, as well as high levels of less well-characterized STAT phosphorylation, including STAT3 and STAT5. Taken together, these data suggest that there are potential differences in the response to interferons that may assist the fetus in being resistant to viral infections, HIV in particular.

Materials and methods:

Isolation of bone marrow monocytes. Fetal bone marrow was obtained from 18-22 gestational week specimens obtained under the auspices of CHR-approved protocols from the Department of Obstetrics, Gynecology and Reproductive Science, San Francisco General Hospital. Fetal samples were obtained after elective termination of pregnancy. Samples were excluded in the case of (1) known maternal infection, (2) intrauterine fetal demise, and/or (3) known or suspected chromosomal abnormality. Fetal monocytes were isolated from femurs by bisection and mechanical dispersion of marrow in RPMI-1640 (Sigma Aldrich). Adult bone marrow samples were obtained from healthy donors (AllCells, LLC. and Lonza Group Ltd.). Both adult and fetal mononuclear cells were isolated by density centrifugation of a Ficoll-Hypaque gradient (Amersham Biosciences). All samples, both fetal and adult, were viably cryopreserved prior to use.

Flow cytometry. Mononuclear cell preparations were incubated in FACS staining buffer (PBS with 2% FBS and 2 mM EDTA) with fluorochrome-conjugated, anti-human surface antibodies. Antibodies used for phenotyping included: CD14 qDot605 (Tuk4, Invitrogen), CD16 Pacific Blue (3G8, BD Biosciences), and HLA-DR PE-Cy7 (G46-6, BD Biosciences). All cells were stained with a live/dead marker (Amine-Aqua/AmCyan; Invitrogen) to exclude dead cells from the analysis. For intracellular STAT staining, cells were first stained with CD14 and CD16, prior to fixation/permeabilization and subsequent STAT staining according to the manufacturer's protocol (BD Biosciences, Cytofix Buffer and Permeabilization Buffer III). Intracellular antibodies used included: STAT1 (pY701) Alexa488 (4a, BD Biosciences), STAT3 (pY705) PE-CF594 (4/P-

STAT3, BD Biosciences), and STAT5 (pY694) AlexaFluor 647 (47/STAT5(pY694), BD Biosciences).

Cytokine stimulation and STAT staining. Approximately 1x10^6 mononuclear cells from FBM or ABM were stained with CD14 Qdot605 and CD16 Pacific Blue for 30 minutes, prior to incubation in polystyrene tissue culture treated 96-well plates with appropriate amounts of type I IFN (Universal Type I IFN, Fisher Scientific) in sterile serum free cell culture media (SF X-VIVO 20, Lonza Group Ltd.) at 37°C for 30 minutes (100 μL total volume). The cells were then fixed with Cytofix Buffer (BD Biosciences), permeabilized with Permeabilization Buffer III (BD Biosciences) and stained with HLA-DR, STAT1, STAT3, and STAT5 according to the manufacturer's instructions.

Gene Set Enrichment Analysis (GSEA). Fetal and adult bone marrow monocyte stimulated with IFNγ or unstimulated whole genome gene expression arrays were probed with a subset of HIV restriction factors described in the literature[7]. Enrichment was determined using GSEA software (Broad Institute).

Results: Restriction factors can be lowly expressed at baseline, but are also inducible by interferons. In order to determine whether fetal samples had an enrichment in HIV restriction factors, we utilized GSEA to query IFNγ-stimulated and unstimulated fetal and adult classical monocyte whole genome arrays [8] with a subset of HIV restriction factors previously described in the literature[7](Fig. 1). These data, while not significant (due to low sample number and small size of the enrichment group), suggest that fetal monocytes may more strongly induce restriction factors following stimulation with IFNγ than adult monocytes.

While IFNγ can be a potent inducer of restriction factors, type I IFN is an even stronger driver. To assess the effects of IFNα/β stimulation on fetal monocytes, we stimulated FBM and ABM monocytes with varying concentrations of universal type I IFN and assayed for STAT phosphorylation downstream (Fig. 2). After type I IFN stimulation, the fetus had stronger canonical STAT1 phosphorylation than the adult. The fetal cells also had very strong pSTAT3 and pSTAT5 signal which were virtually absent in the adult. These responses were maintained at very low concentrations.
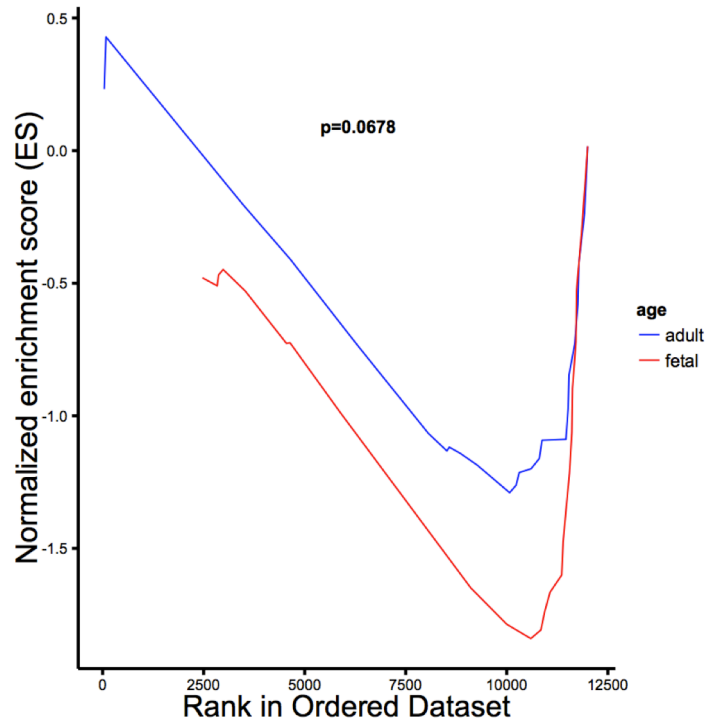
Figure 1: Enrichment of HIV restriction factors after IFNγ stimulation. Fetal and adult bone marrow monocyte stimulated with IFNγ or unstimulated whole genome gene expression arrays were probed with a subset of HIV restriction factors described in the literature[7].
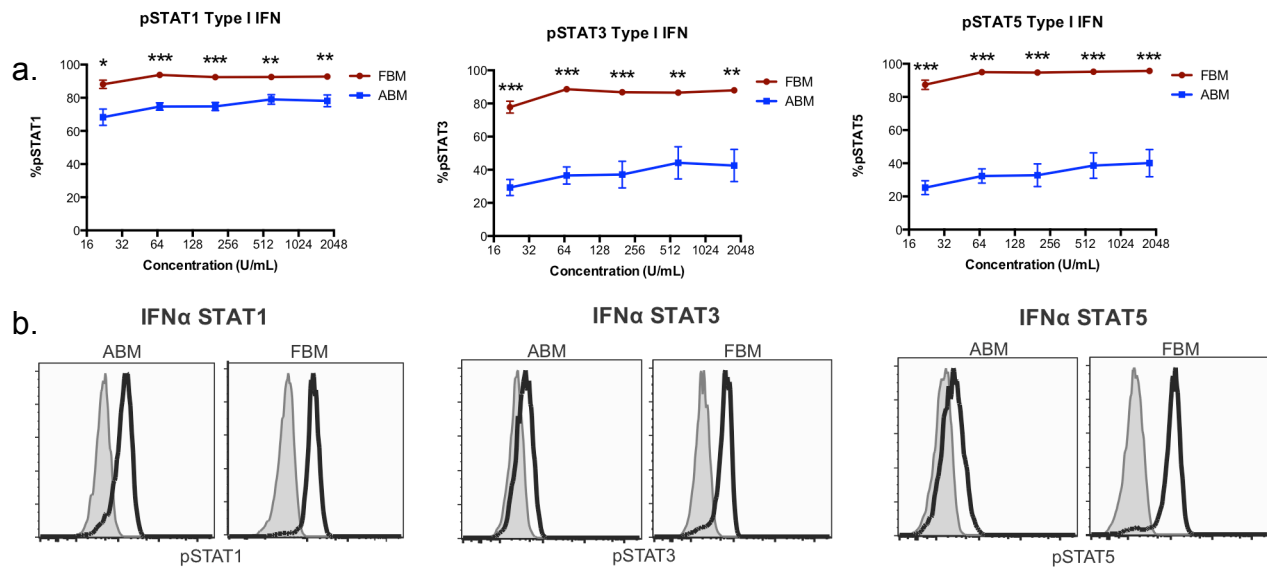
Figure 2. Phospho-STAT responses to type I IFN stimulation. (A) Percentage of pSTAT1[+], pSTAT3[+], and pSTAT5[+], classical monocytes in FBM and ABM after type I IFN stimulation. Cells were stimulated with 1800, 600, 200, 66.7, or 22.2 U/mL IFNα/β for 30 min. **(B)** Representative histograms of pSTAT phosphorylation after stimulation with IFNα/β. Representative histograms are of 1800 U/mL IFNα/β after 30 minutes. Experiments depicted represent an n=4 for both fetal and adult samples.

Discussion and future directions:

These data suggest that fetus may be partially protected from HIV infection due to up-regulation of restriction factors after type I IFN stimulation. In response to type I IFN the fetus mounts a highly robust pSTAT response utilizing both canonical (pSTAT1) and non-canonical (pSTAT3 and pSTAT5) signaling pathways. This raises several potentially interesting questions and future directions.

First, as the fetus appears to be highly sensitive both to type I and type II IFN, is there differential production of these IFNs after exposure to viral antigen? To assay this question, we will stimulate ABM and FBM samples with TLR7/9 agonists and use intracellular flow cytometry to assess production of IFNα and IFNγ. Of note, it has been previously described that there is an enrichment of plasmacytoid dendritic cells, the main producers of interferon, in umbilical cord blood[9]. Similarly, we have observed a robust pDC population in FBM (data not shown). It is possible that the fetus not only responds robustly to IFNα, but may secrete IFNα at a different level than the adult in response to potential viral infection.

Second, it would be of great interest to know if fetal myeloid cells are resistant to HIV infection and whether this resistance is restriction factor mediated. To test this, we would infect classical monocytes from fetal or adult samples with an HIV reporter virus before and after stimulation with IFNα. We would predict a similar level of infectivity at baseline but that after IFNα stimulation, the fetal population would be more resistant to productive viral infection than the adult. This could be further elucidated using knock-down experiments to test which, if any, of the restriction factors mediate these potential differences.

Third and finally, it would be of interest to know if the differential STAT phosphorylation observed after stimulation is affecting restriction factor expression. To date, very little work has been done to link the signaling pathways downstream of type I IFN to restriction factor induction. To this end, we would use a combination of JAK/STAT inhibitors as well as potential knock-down experiments to see if differential STAT phosphorylation, particularly the non-canonical STAT3 and STAT5 phosphorylation could contribute to up-regulation of restriction factors. This then could potentially identify target pathways to generate protection and/or resistance to HIV infection of myeloid cells in the adult.

References:

1. Taha TE, James MM, Hoover DR, Sun J, Laeyendecker O, et al. Association of recent HIV infection and in-utero HIV-1 transmission. AIDS. 2011;25:1357-1364.

2. Magder LS, Mofenson L, Paul ME, Zorrilla CD, Blattner WA, et al. Risk factors for in utero and intrapartum transmission of HIV. JAIDS Journal of Acquired Immune Deficiency Syndromes. 2005;38:87-95.

3. Resti M, Azzari C, Mannelli F, Moriondo M, Novembre E, et al. Mother to child transmission of hepatitis C virus: prospective study of risk factors and timing of infection in children born to women seronegative for HIV-1. Tuscany Study Group on Hepatitis C Virus Infection. BMJ. 1998;317:437-441.

4. Inion I, Mwanyumba F, Gaillard P, Chohan V, Verhofstede C, et al. Placental malaria and perinatal transmission of human immunodeficiency virus type 1. Journal of Infectious Diseases. 2003;188:1675-1678.

5. Biancotto A, Iglehart SJ, Vanpouille C, Condack CE, Lisco A, et al. HIV-1 induced activation of CD4+ T cells creates new targets for HIV-1 infection in human lymphoid tissue ex vivo. Blood. 2008;111:699-704.

6. Harris RS, Hultquist JF, Evans DT. The restriction factors of human immunodeficiency virus. J Biol Chem. 2012;287:40875-40883.

7. Raposo RA, Abdel-Mohsen M, Bilska M, Montefiori DC, Nixon DF, Pillai SK. Effects of cellular activation on anti-HIV-1 restriction factor expression profile in primary cells. J Virol. 2013;87:11924-11929.

8. Krow-Lucal ER, Kim CC, Burt TD, McCune JM. Distinct functional programming of human fetal and adult monocytes. Blood. 2014.

9. Velilla PA, Rugeles MT, Chougnet CA. Defective antigen-presenting cell function in human neonates. Clin Immunol. 2006;121:251-259.

Chapter 5:

Conclusions

Conclusions

Summary

In this thesis, we have shown that there are distinct functional programs in human fetal classical monocytes as compared to adult. These programs are present at baseline and also contribute to differences in JAK/STAT signaling and downstream functional programming after cytokine stimulation. We have also identified and validated a genetic signature capable of identifying fetal-like and adult-like cells in human umbilical cord blood. Finally, we have shown that human fetal monocytes have a stronger induction of HIV restriction factors after IFNγ stimulation and strongly phosphorylate canonical and non-canonical STATs in response to IFNα/β stimulation.

Distinct functional programs in human fetal monocytes

Differences in the basal transcriptional profiles of human fetal monocytes as compared to the adult suggest that the fetal myeloid compartment is intrinsically different than that of the adult. Ontologically, this makes sense, as the challenges faced *in utero* are very different than those face *ex utero*. The downstream differences we have identified here, in particular the differential STAT phosphorylation and downstream differential gene expression may shed some light on the purpose of these differences.

While the purpose of STAT5 phosphorylation remains unclear, there are a variety of possible scenarios as to why this is important to fetal development. First, STAT5 has been associated with Treg function{Burchill 2007} and, similar to the T cell phenotype, may be regulating some tolerogenic program within the myeloid compartment. Second,

STAT5 may be playing a heretofore unknown role inhibiting canonical STATs, either through competition for receptor docking, for DNA binding, or for targeting other STATs for degradation{Ho 2006}. This hypothesis seems less likely as the other STAT signaling pathways appear to be intact and signaling even in the present of pSTAT5. Finally, it may be that, at the protein level, there is an overabundance of STAT5 found in fetal cells. Studies in mice have shown that having excess STAT5 allows it to be phosphorylated by nan-canonical cytokine mediators{Tormo 2012}.

These differences in phosphorylation have been shown to potentially mediate downstream differences in gene function. These differences suggest that the fetus has an impairment in antigen presentation and co-stimulation. Interestingly, this has also been described in trophoblast-derived cells{Choi 2007}, suggesting that this may be an ontologically conserved mechanism throughout the conceptus. This might then be a mechanism for limiting large scale adaptive responses and maintaining *in utero* tolerance and maintaining a viable pregnancy. Also of interest, is the up-regulation in the fetus but not the adult of a subset of innate genes, particularly geared towards monocyte clearance, particularly of viruses. This suggests, as is discussed previously, that the fetus may have mechanism in place that specifically protect it from viral infection.

Models of immune development

We have developed a genetic signature found in both monocytes and T cells that can potentially identify fetal and adult cells in umbilical cord blood. This signature and gene expression data is interesting for many reasons. First, it clearly demonstrates that

fetal peripheral blood monocytes as compared to adult are enriched in anti-viral programs. This calls into question the idea of an innate and tolerogenic myeloid compartment *in utero*. Instead, these results seem to suggest that the innate compartment in the fetus is highly active and geared towards rapid defense and clearance of intracellular pathogens. Second, this signature allows us to address many heretofore unanswered developmental questions. With this signature, we can probe umbilical cord blood and determine whether immune development in the human proceeds in a maturational fashion such that fetal cells mature into their adult counterparts or in a layered fashion where fetal and adult cells remain distinct throughout life. These insights can then help us understand the unique challenges faced during early life and potentially help us design interventions to boost neonatal immunity to particular pathogens.

HIV infection *in utero*

This work began due to a desire to understand the low rates of mother-to-child transmission of HIV *in utero*. We have now shown that after stimulation with IFNγ, fetal monocytes more strongly induce HIV restriction factors than their adult counterparts. Further, we have shown that fetal cells have a much stronger canonical and non-canonical response to IFNα/β, suggesting that this difference could potentially be stronger after type I IFN stimulation. For the first time, these data offer a potential mechanism explaining how it is that there is such low *in utero* transmission. If the fetus is capable of more strongly up-regulating restriction factors in myeloid cells, as well as preventing activation in the T cell compartment through preferential differentiation into

Treg cells, this suggests that both compartments can then effective resist HIV infection. We hope to work further in this field and discover if the non-canonical signaling pathways downstream of type I and type II interferon contribute to the up-regulation of these restriction factors, and, if so, can we mimic these response in adult and either prevent or cure HIV infection.

Appendix 1

Supplemental table 1: Full list of signature genes.

Gene signature		
A1BG	GBP5	PDE6G
ACACB*	HBG1	PIEZO1
ACVR1C	HPGD	PLA2G16
AIM2	HSBP1L1	PLAG1
ANKRD20A2	IDO1	PPARG
ANPEP	IGF2BP1*	RBM43
AQP9	IGF2BP3	RECK
ARMCX4	IGFBP2	RGS1
BCL11A	JAG2	RHOXF1
BLVRA	JUP	SAP30*
BMF	KLF10	SARM1
BTG2	KLF9	SELM
C3AR1	KLHDC7B	SERPINB6
CAMK1	Lin28b	SERPINF1
CBX8	LONRF3	SGK1
CD69*	MAF	SLC18A2
CD93	MAFIP	SLC29A1
CELA1	MATK	SMAD1
CLEC2B	MB21D2	SNX27
CLEC5	MCTP1	SOCS3
CTNNA1	MIRLET7BHG	SP140
CTSC	MLC1	SPIB
CTSF	MMP9	SPP1
DDB2	MT1F*	TCEAL5
DUSP2	MYOM1	TNF
EWSR1	NFIA	TRIM7
FBXO32*	NR3C2	TSHZ2
FCGBP	NTNG2	TUBA1C
FCRLB	OSM	TYMS
FGFBP2	PAM	YBX1*
FGFR1	PCBP4	ZG16B*
FOS	PDE4D	ZNF618

Supplemental table 2: Efficiency of monocytes validated primers. Primers were considered validated if they had a minimum of 70% efficiency.

Primer	Slope	Efficiency
ANPEP	-0.98784158	2.017135594
AQP9	-1.082285835	1.89732961
ARMCX4	-0.880887183	2.196519263
BCL11A	-1.035825252	1.952623511
BMF	-0.730500605	2.582779103
BTG2	-0.674244288	2.795569028
C3AR1	-1.014111654	1.980802051
CAMK1	-1.19579024	1.785424428
CBX8	-0.913444225	2.135771923
CD69*	-1.006267759	1.991383776
CD93	-1.209494477	1.7737365
CLEC2B	-1.018475075	1.975010141
CLEC5	-1.026264527	1.964834291
CTSC	-1.095004234	1.883268208
DDB2	-1.008021981	1.988998046
FCGBP	-0.752786785	2.511235606
FGFR1	-1.146589754	1.830390568
FOS	-0.696831143	2.70394891
GBP5	-1.189396849	1.790996198
HBG1	-1.113092872	1.863994537
HSBP1L1	-0.949124718	2.075706285
IDO1	-0.770917933	2.457437855
IGF2BP1*	-1.049216583	1.936017596
JUP	-0.890073621	2.178752877
KLF9	-1.020175793	1.972770619
LONRF3	-1.100398109	1.877433766
MAFIP	-1.075960177	1.904486982
MCTP1	-1.116176584	1.860790437
MT1F*	-0.907256265	2.146854486
OSM	-0.891614104	2.175823364
PAM	-0.994757451	2.007319379
PDE6G	-0.734461819	2.569595309
RECK	-0.929399077	2.108130322
RGS1	-1.043117972	1.94350974
SAP30*	-1.020040143	1.972948878
SERPINF1	-1.292788561	1.709437523
SP140	-1.0325765	1.956738882
TUBA1C	-0.996945111	2.004252467
ZG16B*	-1.042353821	1.944456737

Supplemental table 3: Efficiency of naïve T cell validated primers. Primers were considered validated if they had a minimum of 70% efficiency.

Primer	Slope	Efficiency
ARMCX4	-0.99923925	2.001055705
BCL11A	-1.27531584	1.722040992
BTG2	-1.317079455	1.692617088
C3AR1	-1.2669026	1.728267653
CAMK1	-0.87426165	2.209656835
CBX8	-0.970088597	2.043204605
CD69*	-1.064306134	1.917968849
CD93	-1.260034664	1.733429257
CLEC2B	-1.223214141	1.762371836
CTSC	-1.078633119	1.901449062
DDB2	-0.925665768	2.114480907
FCGBP	-1.020526978	1.972309422
FGFR1	-0.901630781	2.157112535
FOS	-1.422358156	1.627951594
GBP5	-0.908953861	2.143793362
HBG1	-1.113055374	1.864033642
HSBP1L1	-1.325896249	1.686704009
IGF2BP1*	-1.138971358	1.837806919
IGFBP2	-1.027133726	1.9637116
JUP	-0.797064719	2.386015255
KLF9	-0.982173413	2.02532038
MAFIP	-0.77754123	2.438688402
MB21D2	-1.237205584	1.751114118
MCTP1	-1.148373027	1.828673086
MT1F*	-0.739918863	2.551772185
NR3C2	-0.973540192	2.038035184
OSM	-0.87040397	2.217435005
PDE6G	-1.82117018	1.463170105
PLAG1	-1.297539009	1.706085252
RECK	-1.216337209	1.768027155
RGS1	-1.162657186	1.815162559
SAP30*	-1.48049139	1.597096418
SELM	-1.175076239	1.803761525
SERPINF1	-1.100702625	1.87710662
SP140	-1.078398626	1.901714778
TSHZ2	-0.593909065	3.212640275
TUBA1C	-1.240134197	1.748798835
ZG16B*	-1.014591028	1.980162472

Supplemental table 4: Genes contributing to unbiased cluster analysis of monocytes. Genes most associated with unbiased clustering analysis in monocytes were used to generate a heatmap.

	FPB1	FPB2	FPB3	FPB4	APB1	APB2	APB3	APB4	APB5
PSPHP1	0.92	0.80	1.00	-0.59	-1.10	-0.98	1.03	-1.05	0.94
ITGB2	1.12	-1.07	-1.01	-0.76	1.06	-0.69	-0.20	-0.78	1.01
FOSB	0.84	0.88	0.86	0.61	0.80	-0.67	-1.40	-1.37	-1.09
EGR3	0.93	1.33	1.23	-0.22	0.00	-0.54	-1.24	-1.09	-1.12
DUSP2	1.03	1.16	1.17	0.57	-0.01	-1.04	-1.04	-1.21	-1.05
HTRA1	-0.23	-1.16	-1.28	-0.59	0.81	0.93	0.75	1.55	0.24
ACTB	0.93	0.93	0.98	0.11	0.90	-0.66	-1.30	-0.93	0.53
SIRPB1	-0.67	-0.72	1.55	1.36	-0.54	-0.61	-0.52	-0.59	-0.67
CD83	1.35	1.01	0.87	-0.66	0.41	-0.23	-1.14	-1.11	-1.27
FCGBP	1.01	0.58	0.94	1.37	-0.12	-1.17	-1.20	-1.21	-0.64
EGR2	0.77	1.10	1.12	0.02	-0.11	-0.20	-1.04	-1.14	-1.56
SPP1	1.75	-0.30	1.12	0.28	-0.82	-0.77	-0.70	-0.82	-0.88
XLOC_002643	0.78	-0.38	0.40	-0.17	-1.04	1.75	0.42	0.74	-1.47
LOC728052	-0.57	-0.86	-0.90	-1.23	1.25	0.55	0.98	0.82	1.01
XLOC_008760	1.01	-0.49	0.70	-0.49	-1.00	1.59	0.33	0.70	-1.40
HBG1	0.81	1.04	0.70	0.80	-0.52	-1.19	-1.06	-1.00	-0.85
OSM	0.96	1.45	0.90	-0.06	-0.45	-0.34	-0.87	-1.03	-1.48
XLOC_I2_013031	-1.03	-0.78	-1.04	-1.08	0.12	0.63	1.40	1.23	0.99
XLOC_010238	1.09	-0.63	0.34	-0.85	-1.09	1.88	0.28	0.63	-0.75
PTGS2	1.05	1.27	1.21	-0.43	-0.36	-0.13	-1.10	-1.12	-1.18
G0S2	0.98	1.29	1.00	-1.31	0.89	-0.05	-0.77	-0.98	-1.14
FIGNL2	0.86	0.82	1.07	0.91	-1.12	-1.01	-0.59	-0.95	-1.02
CD69	1.07	1.14	1.13	-0.03	-0.54	-0.38	-1.07	-1.24	-1.07
SOCS3	1.01	1.05	0.77	0.91	-0.29	-0.60	-1.28	-1.17	-1.19
ENST00000477036	-0.68	0.96	-1.81	1.06	-0.76	-0.87	0.93	-0.02	0.22
APOLD1	1.13	-1.04	0.48	-0.89	-1.12	1.80	0.13	0.55	-0.89
HCAR3	0.75	1.05	0.73	0.37	0.28	-1.06	-0.99	-1.68	-0.59
SLC4A3	1.12	0.89	0.63	1.04	-0.76	-1.20	-0.89	-1.02	-0.79
A_33_P3252134	1.03	-0.70	0.54	-0.53	-1.13	1.80	0.46	0.48	-1.11
AB073651	-0.99	-0.97	-1.06	-1.38	1.07	0.22	1.04	0.86	0.99
OSMR	1.11	-0.76	0.72	-0.57	-1.19	1.70	0.25	0.49	-1.20
IGF2BP1	0.71	0.99	0.85	1.01	-0.97	-0.88	-1.00	-0.96	-0.90
EGR1	0.57	0.94	0.83	0.75	0.36	-0.19	-1.49	-1.27	-1.35
XLOC_I2_014048	1.11	-0.84	0.45	-0.76	-0.98	1.80	0.27	0.66	-1.11
CCL3L3	0.84	0.82	1.07	-0.14	0.26	-0.75	-0.70	-1.28	-1.42
A_33_P3212360	0.90	-0.75	0.59	-0.63	-1.01	1.80	0.44	0.60	-1.24
NAMPT	0.99	1.12	0.69	-0.41	0.32	-0.04	-1.56	-1.01	-1.17
ARID5A	0.94	-0.19	0.72	1.45	0.05	-1.16	-0.65	-1.39	-0.82
MAFF	1.14	0.96	1.12	0.44	0.18	-0.83	-1.35	-1.32	-0.87
IL6	1.58	0.27	1.31	0.10	-0.08	-0.84	-1.05	-1.11	-1.00
A_33_P3292126	1.24	-0.56	0.67	-0.69	-1.06	1.70	0.06	0.54	-1.17
PLD4	1.21	0.96	0.85	1.05	-0.48	-1.25	-0.90	-1.20	-0.72
ZYX	0.97	0.87	0.82	0.43	0.56	-0.53	-1.17	-1.34	0.81
NR4A1	0.91	1.27	1.55	-0.62	0.07	-0.76	-0.87	-0.89	-1.18

NR4A2	1.00	1.47	0.87	-0.16	0.83	-0.46	-1.17	-1.30	-1.05
LOC100509100	-0.10	-0.67	-0.13	0.04	0.51	-1.43	1.18	1.25	0.91
EFR3B	0.94	-0.44	0.70	-0.40	-1.07	1.63	0.36	0.66	-1.07
CCL4	1.00	0.46	0.93	0.09	-0.06	-0.36	-0.75	-1.38	-1.43
FRMD3	-0.51	-0.90	-0.65	-0.68	0.91	1.10	0.89	0.83	0.73
LOC100131831	0.72	0.23	1.07	1.08	0.63	-1.34	-0.99	-1.35	-0.78
IGF2BP3	0.77	0.95	0.82	1.02	-1.20	-0.79	-0.62	-0.88	-1.16
A_33_P3324687	1.00	-0.38	0.67	-0.43	-1.20	1.68	0.14	0.72	-1.06
MYBPH	1.44	0.92	0.15	0.82	-0.46	-0.87	-1.07	-0.71	-1.27
JUNB	1.06	1.16	1.21	0.70	0.22	-1.02	-1.07	-1.38	-0.27
DES	1.16	0.85	0.93	0.90	-0.85	-0.37	-1.07	-1.26	-1.05
BEX1	-0.31	-1.00	-0.93	-0.98	-0.12	0.98	1.29	1.56	0.43
A_33_P3301129	0.47	0.14	0.79	1.07	-0.52	-0.65	-1.00	-1.00	-1.07
ENST00000494840	0.81	-0.52	0.25	-0.72	-0.88	2.05	0.26	0.71	-0.99
CDKN2C	-0.41	-0.83	-0.91	-0.91	0.61	0.94	0.94	0.83	1.22
HLA-DQA2	-0.91	0.59	-1.88	0.97	-0.56	-0.59	1.20	0.12	-0.05
CDKN1C	0.48	1.04	1.16	0.85	-0.90	-0.55	-1.02	-1.24	-0.90
LOC388780	1.19	1.29	0.94	-0.93	1.17	-0.72	-0.96	-0.66	-0.76
ATF3	0.86	1.61	0.80	-1.02	0.50	-0.63	-0.96	-0.88	-1.03
ENST00000390361	1.24	-0.56	0.76	-0.47	-1.15	1.45	0.15	0.75	-1.10
CCL3	0.69	0.84	1.00	-0.07	0.34	-0.34	-0.82	-1.36	-1.56
IL1B	0.73	1.24	0.88	-0.10	-0.26	-0.46	-0.89	-1.11	-1.40
CENPN	1.08	-0.44	0.65	-0.26	-1.21	1.76	0.02	0.48	-1.35
LOC284260	1.23	-0.77	0.50	-0.36	-1.35	1.77	0.02	0.54	-0.72
COL23A1	0.99	-0.57	0.55	-0.61	-1.06	1.86	0.20	0.64	-0.90
HBEGF	1.26	1.73	0.94	-0.32	0.18	-0.46	-1.19	-0.78	-1.01
NDRG2	1.20	1.10	0.79	1.01	-0.92	-0.90	-1.10	-0.96	-0.77
NRG1	-0.13	-1.22	-0.35	-0.85	0.83	1.14	0.96	0.78	0.54
MAF	1.07	0.43	0.89	0.85	-0.71	0.10	-1.82	-0.41	-1.21
LRRC45	0.69	-0.79	0.09	-0.71	-1.03	2.13	0.53	0.49	-1.06
CD300E	-1.38	-0.04	-1.10	-1.42	1.09	0.34	0.97	0.89	0.90
IFI44	-0.97	-1.39	-0.81	-0.08	0.34	0.99	0.63	0.60	1.65
GABRE	1.09	1.13	0.93	0.87	-1.18	-0.38	-1.17	-0.75	-1.07
XLOC_l2_006797	0.70	0.30	1.15	0.87	-0.13	-1.05	-0.82	-1.22	-1.13
C1orf138	0.88	0.18	0.64	1.24	0.26	-1.36	-0.86	-1.27	-0.83
LOC100131733	-1.22	-0.87	-0.94	-1.19	0.76	0.89	1.38	0.77	0.71
BTG2	1.00	1.20	0.98	0.24	-0.15	-0.49	-1.27	-1.54	-0.78
AREG	1.18	1.74	0.63	-0.72	0.46	-0.72	-0.54	-0.80	-1.41
LOC150381	-0.91	-1.03	-1.11	-0.41	1.03	1.23	1.00	0.81	0.50
HSBP1L1	-0.93	-1.15	-1.10	-1.17	0.83	0.81	1.52	0.45	0.58
LOC100287437	-0.66	-1.02	-0.67	0.31	-0.16	1.03	1.30	0.84	0.75
XLOC_l2_011120	1.01	-0.33	0.61	-0.22	-1.04	1.66	0.17	0.64	-1.09
KLF6	0.60	0.41	0.90	1.01	0.49	-1.48	-1.43	-1.14	-0.27
XLOC_011171	1.01	-0.38	0.55	-0.58	-1.17	1.81	0.14	0.67	-0.95
HOXB2	-0.42	-1.40	-0.58	-1.09	0.12	1.34	1.40	0.99	0.34
ZNF618	-0.30	-0.63	-1.15	-0.68	1.02	1.25	0.95	0.60	0.54
L1TD1	0.79	0.24	0.75	1.17	-1.07	-1.15	-0.98	-0.01	-1.08
TNFRSF25	1.03	0.85	1.34	-0.62	-0.65	-0.39	-0.86	-1.40	-0.52
CTSG	-0.02	1.32	-0.37	-0.53	1.23	-1.21	-0.75	-0.74	-0.50

IL8	0.92	0.30	1.40	-0.70	0.25	-0.24	-0.28	-1.30	-1.52
XLOC_l2_000423	0.73	-0.11	0.67	1.33	-0.85	-0.91	-0.88	-0.91	-0.68
CHRM4	-1.10	0.54	-0.97	1.23	-0.63	-0.39	-0.12	1.52	1.01
SYTL1	1.09	1.01	0.96	0.99	0.00	-1.12	-1.06	-1.55	0.05
MSRB3	-0.96	-0.90	-0.85	-0.92	1.17	0.80	0.85	1.11	0.76
PTP4A3	0.96	0.96	1.07	0.86	0.05	-0.98	-1.20	-1.04	-1.22
ANXA3	0.91	0.97	0.91	1.49	-0.94	-0.78	-1.04	-0.94	0.23
TRIM71	0.49	0.96	1.10	1.42	-0.89	-0.56	-1.01	-1.24	-0.81
IDO1	-0.61	-1.24	-1.20	-0.99	0.41	0.68	1.15	1.11	1.14
C1orf151-NBL1	1.34	-0.98	0.37	-0.90	-0.53	2.03	-0.19	0.11	-0.80
LOC100507043	0.96	-0.17	0.52	-0.20	-0.99	1.54	0.28	0.72	-0.98
CXCL9	0.02	-1.25	-1.20	-0.05	0.02	0.36	1.38	1.20	0.85
PGLYRP1	1.18	1.01	1.27	1.12	-0.88	-0.83	-1.00	-0.86	-0.64
GLB1L2	0.92	-0.69	0.39	-0.74	-1.04	1.97	0.39	0.50	-1.13
XLOC_010257	1.32	-0.74	0.40	-0.73	-0.89	1.98	-0.14	0.30	-0.98
LOC285181	-0.89	-0.89	-0.24	-1.75	-0.01	1.11	1.13	0.89	0.94
SESN2	1.21	-0.34	0.47	-0.44	-1.02	1.82	0.11	0.40	-0.95
XLOC_014107	1.11	-0.71	0.39	-0.74	-1.12	2.01	0.15	0.33	-0.98
IL17RE	1.25	-0.65	0.63	-0.72	-1.04	1.68	0.24	0.44	-1.29
TMEM45A	0.06	1.36	0.76	1.37	-1.20	-1.08	0.57	-0.21	-0.38
HLA-DQA1	-0.08	0.83	-2.25	0.81	-0.39	-0.78	0.96	-0.20	0.20
A_33_P3382887	1.01	-1.70	0.28	-0.54	0.79	-1.59	0.94	0.23	-0.18
XLOC_007909	1.09	-0.48	0.59	-0.26	-1.06	1.79	0.05	0.54	-1.06
S100P	-0.48	0.93	0.77	0.90	-0.12	-0.47	0.00	-2.34	-0.07
IGFBP2	0.89	0.16	1.06	1.21	-1.19	-0.62	-1.26	-1.29	0.52
FONG	0.45	-1.79	0.34	0.75	0.57	-0.98	1.01	1.04	-1.22
LOC100132207	0.86	-0.38	0.58	-0.86	-0.97	2.01	0.04	0.52	-0.62
XLOC_007098	1.00	-0.76	0.52	-0.79	-0.69	2.06	0.01	0.41	-1.07
RAP1GAP2	-0.96	-0.84	0.66	1.05	1.78	-1.16	0.72	-0.85	-0.24
ICAM4	1.09	-0.29	0.71	0.68	-1.33	0.52	0.45	-1.09	-1.61
ANKMY1	1.24	-0.63	0.57	-0.53	-0.98	1.77	0.08	0.51	-0.83
INO80D	0.92	-0.19	0.67	-0.42	-1.13	1.79	0.10	0.56	-0.98
LINC00458	1.18	-0.22	0.40	-1.13	-0.96	1.84	-0.02	0.55	-0.56
GRASP	1.35	1.45	0.68	0.07	0.48	-0.79	-1.17	-1.16	-1.01
DACH1	-1.02	-1.03	-0.67	-1.43	0.42	0.84	1.11	1.17	0.91
A_33_P3301876	0.84	0.23	0.61	1.31	-0.50	-0.84	-0.30	-1.11	-1.50
PPP1R15A	1.20	0.81	0.89	-0.02	1.12	-0.68	-1.32	-1.59	-0.18
FOS	0.97	1.01	0.94	0.66	0.43	-1.14	-1.15	-1.52	-0.64
PRKCH	-0.52	-0.97	-0.71	-0.99	0.72	0.95	0.86	1.18	0.88
GPR20	0.32	0.23	0.59	0.97	-1.00	-0.36	-0.97	-0.74	-1.01
A_33_P3363305	1.43	-1.53	0.58	-0.83	0.70	-1.17	0.95	0.04	-0.72
SHKBP1	0.88	0.94	0.73	0.34	0.77	-0.73	-1.30	-0.99	0.84
RBM38	0.96	0.98	0.99	0.78	0.15	-1.06	-0.96	-1.03	0.62
RGL4	0.50	1.16	0.78	1.26	-0.58	-0.96	-1.17	-1.31	-0.49
CBX4	1.17	0.97	1.01	0.26	0.25	-0.77	-0.76	-1.10	0.64
WASF2	1.04	0.87	0.74	0.71	0.42	-0.87	-1.48	-1.30	0.74
A_33_P3390226	0.63	-0.06	0.74	1.05	-0.35	-1.43	-0.37	-0.94	-0.95
EMB	-1.05	-0.77	-1.12	-1.18	0.27	0.99	0.97	1.23	1.00
MAP4K1	1.20	1.13	1.00	0.63	0.28	-1.30	-1.15	-1.08	0.07

TMTC1	-0.83	-0.38	-1.35	0.26	0.56	1.10	1.17	0.29	0.82
XLOC_001011	-0.97	-0.61	-1.31	-1.02	1.43	0.84	0.82	1.11	0.19
JUN	0.35	0.20	0.86	1.04	0.05	-1.03	-0.27	-1.16	-1.52
FZD1	-1.11	-0.87	-0.46	-1.01	0.83	1.02	1.02	0.97	0.79
SLC46A2	-0.37	-0.85	-0.72	-1.24	1.04	0.15	0.91	0.82	1.44
LOC100505746	0.67	0.87	0.92	0.88	0.38	-0.69	-0.99	-1.00	0.71
F2RL1	-0.22	-0.70	-0.25	-1.07	0.17	1.15	1.08	0.58	1.08
CAPN1	0.61	0.81	0.89	0.57	0.76	-0.58	-1.67	-0.88	0.80
PRR25	0.94	-0.72	-0.67	-0.71	-0.91	2.28	0.25	0.30	-0.69
XLOC_005711	1.07	-0.27	0.70	-0.39	-0.86	1.59	0.03	0.63	-0.83
A_33_P3399755	1.43	-1.74	0.27	-0.91	0.70	-1.12	0.94	0.06	-0.25
LILRA3	0.65	0.71	0.77	0.94	0.74	-0.70	-1.07	-1.19	0.72
ADRA2B	1.17	0.61	1.63	-0.79	-0.27	-0.89	-0.64	-1.07	-0.75
SPATA20	0.59	0.99	0.42	0.79	0.87	0.35	-1.08	0.12	-1.21
LOC440934	-0.55	-0.79	-0.75	-0.95	-0.09	1.16	1.65	0.89	0.61
COPZ2	-0.65	-0.56	-0.56	-1.04	2.50	0.33	0.46	0.08	-0.04
CLIP4	-0.74	-1.31	-0.38	-1.40	0.40	1.19	1.08	1.20	0.45
RHOB	0.82	1.11	1.10	0.76	-0.20	-0.63	-1.02	-1.49	-1.10
LOC254896	0.59	0.05	0.40	1.81	-0.48	-1.25	-0.40	-1.08	-0.83
CD2	1.33	0.97	0.96	1.04	-1.16	-0.93	-0.39	-0.89	-1.05
OAF	0.45	0.71	0.76	0.67	1.06	-0.46	-1.46	-1.37	0.79
OR8H2	0.97	-0.36	0.59	-0.44	-1.21	1.79	0.25	0.49	-0.73
XLOC_l2_003897	0.79	0.69	0.61	-1.27	-0.92	-1.47	0.86	0.96	-0.89
FKBP1A	0.77	0.85	1.36	0.09	0.64	-0.67	-1.26	-1.20	0.65
PADI6	0.09	-1.29	0.25	0.90	-0.13	0.88	-1.16	0.41	-1.41
UBA1	0.94	0.97	0.77	0.27	0.32	-0.20	-1.49	-1.38	0.95
SEZ6L2	1.03	-0.75	-0.57	-0.77	-0.77	2.27	0.08	0.09	-0.81
H1FX	1.07	0.80	0.96	0.70	0.42	-1.16	-0.87	-1.32	0.60
ADCY9	-0.86	-0.75	-0.69	-1.16	0.56	1.33	1.35	0.95	0.26
CLEC2B	-0.85	-1.21	-1.23	-0.95	1.15	0.57	0.97	1.31	-0.05
SLC22A16	-0.21	0.82	-0.13	-1.08	0.63	-1.16	1.71	-1.29	0.88
AP1M1	1.01	0.79	0.76	0.44	0.77	-0.89	-1.23	-1.39	0.79
ENST00000334363	1.16	-0.28	0.61	-0.35	-1.11	1.66	0.07	0.59	-1.18
C17orf62	0.97	0.06	0.27	1.33	-0.88	-1.07	-0.52	-1.09	-0.62
C17orf87	0.34	0.81	0.21	-1.59	-0.88	-0.66	0.74	0.94	-1.18
CXCL3	2.10	-0.65	0.99	-0.54	0.66	0.22	-0.51	-0.89	-1.16
ARID1A	0.62	0.84	0.96	0.63	0.20	-0.10	-1.35	-1.10	0.93
HS3ST1	0.93	-0.81	0.38	1.56	-1.13	-1.07	0.63	0.71	-1.25
CD37	0.94	0.81	0.89	0.55	0.48	-0.35	-1.40	-1.63	0.68
LILRB3	1.01	0.65	0.75	0.65	0.75	-0.83	-1.16	-1.12	0.77
THBS1	0.60	1.32	1.08	0.87	0.03	-0.65	-0.44	0.11	-1.64
LOC100134317	-0.36	0.51	-1.41	0.15	0.57	-1.55	1.17	-0.78	0.39
GBP1	-0.40	-0.94	-0.58	-1.00	0.83	1.11	0.72	0.64	1.16
CSRNP1	1.23	1.20	0.93	-0.46	0.49	-0.64	-1.16	-1.63	-0.39
IFI44L	-0.46	-0.97	-0.59	0.07	0.43	0.97	0.36	0.09	1.82
ADRB1	0.83	0.49	1.18	0.70	-1.03	-0.27	-0.97	-0.88	-1.31
SIK1	1.01	1.71	0.48	-0.23	0.88	-0.70	-0.95	-0.80	-1.41
HCK	0.94	0.88	0.74	0.41	0.70	-1.11	-1.21	-1.11	0.91
XLOC_007052	1.69	-1.40	0.38	-0.99	0.63	-1.13	0.90	-0.15	-0.50

PLAG1	0.57	0.89	0.66	1.15	-1.38	-0.87	-0.10	-1.05	-1.01
RARRES3	-0.61	-1.18	-1.10	-1.47	0.64	1.06	1.23	0.47	0.75
LEPREL1	0.74	0.59	0.06	1.10	-1.03	-0.95	-0.33	-1.06	-0.85
LOC100129831	1.23	-0.29	0.64	-0.38	-0.95	1.69	-0.18	0.55	-0.97
LOC100302650	0.81	0.98	1.25	0.02	0.02	-0.39	-0.39	-1.98	-1.05
OTUD1	1.17	0.77	0.82	0.36	0.02	-1.03	-1.49	-0.63	-1.13
SNRNP70	0.88	0.99	0.91	0.46	0.39	-1.34	-0.92	-0.85	0.87
GPR183	1.13	1.00	0.64	-0.73	0.78	-0.15	-1.28	-0.45	-1.67
JUND	0.80	1.09	1.23	0.50	0.73	-1.08	-1.21	-1.41	-0.23
POTEM	0.98	0.95	0.79	0.49	0.56	-1.41	-1.09	-1.17	0.79
HPGDS	1.21	0.28	0.47	0.44	-0.83	-1.04	-0.38	-0.97	-0.98
SNED1	-0.93	-1.06	-0.40	-0.50	0.96	1.51	0.83	0.80	0.22
BZRAP1	1.62	0.54	1.27	-0.90	-0.41	-0.42	-0.80	-0.92	-0.95
ARHGEF1	0.72	1.17	0.83	0.46	0.56	-0.78	-1.16	-1.16	0.78
DDIT4L	0.24	0.56	0.74	0.89	-1.27	-1.36	0.17	-1.02	-0.53
ST5	1.28	0.97	1.04	1.13	-1.01	-0.69	-1.21	-0.77	-0.74
LOC100132356	-0.43	0.77	0.98	0.52	0.89	-1.21	-0.57	1.20	-0.51
HDAC5	1.47	-0.71	0.63	-0.76	-0.32	1.77	0.06	-0.15	-1.22
LOC731223	0.78	0.69	1.03	0.35	0.16	-1.26	-1.07	-1.28	-0.74
INHBA	1.53	1.08	0.81	-0.95	-0.52	-0.97	-0.41	-0.87	-0.78
CYP2S1	1.14	1.14	1.26	0.79	-1.11	-1.01	-0.92	-1.01	-0.29
HLX	1.23	1.41	1.06	-0.12	-0.57	-1.14	-0.94	-1.30	0.01
NKIRAS2	0.63	0.65	0.67	0.49	0.82	-0.17	-1.00	-1.03	0.91
POTEE	0.97	0.93	0.79	0.55	0.57	-1.35	-1.04	-1.18	0.78
TMEM176B	0.64	-1.44	1.58	0.82	0.94	-0.80	-1.23	-0.52	-0.15
COL9A2	1.15	1.10	0.78	0.84	-0.01	-1.00	-1.43	-1.45	0.09
ZFP36L1	0.71	-0.13	0.96	0.94	-0.28	-0.97	-0.70	-1.21	-0.98
AAK1	1.18	-0.67	0.66	-0.33	-0.91	1.90	-0.09	0.29	-1.08
OPN3	1.21	-0.51	0.44	-0.62	-1.10	1.93	-0.22	0.53	-0.73
EGFL8	-0.94	-0.34	-0.44	-1.10	0.72	1.11	1.17	1.12	0.19
AKR1C3	-0.23	-1.15	-0.95	-1.22	0.67	0.16	0.96	1.28	1.26
CXCL2	1.96	0.25	0.74	-0.51	0.98	-0.29	-0.79	-1.38	-0.84
XLOC_002080	-1.27	-0.96	-0.97	-0.51	-0.87	0.67	1.15	1.21	0.97
DDX3Y	-0.72	-0.22	1.22	0.86	1.48	-1.56	-1.06	0.49	-0.47
RIN3	0.78	0.75	0.58	0.33	0.93	-0.55	-1.47	-1.34	1.06
OBFC2A	0.14	1.27	1.23	0.08	-0.93	-0.94	-0.89	-0.96	-0.48
A_33_P3407235	-1.08	-0.55	1.03	0.85	1.25	-1.61	-0.10	0.86	-0.89
PLD3	1.08	0.69	0.61	0.37	0.86	-0.32	-1.39	-1.57	0.71
DDX39B	0.82	0.82	0.82	0.36	0.44	-0.35	-0.71	-0.94	0.83
PPM1M	1.08	0.84	0.43	0.34	0.82	-1.13	-1.08	-1.19	1.02
AFF3	0.75	0.45	0.68	1.29	-0.68	-1.27	-0.97	-1.10	-0.45
ORM2	0.67	0.77	0.65	0.04	-0.97	-1.12	0.23	-0.72	-1.30
UNC93B1	0.51	0.71	0.73	0.57	0.75	-0.54	-1.04	-1.16	1.14
APCDD1	-0.60	-1.10	-0.89	-1.29	0.29	1.31	0.67	1.09	1.09
ENST00000412019	-0.72	1.19	0.22	-1.05	1.50	-0.93	-0.49	-0.68	1.38
BPI	1.09	0.74	0.92	1.14	0.06	-1.26	-0.88	-0.75	0.39
TRNT1	1.25	-0.31	0.49	-0.34	-0.92	1.76	-0.02	0.40	-0.84
A_33_P3325336	0.89	0.81	0.66	0.47	0.42	-1.48	-0.69	-0.16	0.87
HLA-F	-1.46	-0.09	-1.80	0.44	0.84	0.31	0.88	0.59	0.99

ZBTB22	0.59	0.80	0.80	0.32	1.10	-0.19	-1.36	-1.45	0.66
KLHL30	1.35	-0.12	0.89	0.81	-1.40	-0.59	0.69	0.62	-1.24
LILRA4	1.05	0.57	0.73	0.70	0.71	-1.03	-1.02	-1.06	0.81
KRTAP19-2	1.73	-1.51	0.51	-0.93	0.49	-0.99	0.93	-0.07	-0.58
NFIA	-0.40	-0.69	-0.88	-0.65	0.94	0.97	0.70	1.03	0.77
FERMT3	0.90	0.85	0.72	0.42	0.79	-0.72	-1.27	-1.59	0.82
KANK1	-0.51	-0.29	-0.86	-0.79	0.42	0.79	0.99	1.37	0.65
DKFZp434L192	1.05	-0.33	0.56	-0.44	-1.00	1.80	0.09	0.56	-0.95
PKM2	0.76	0.77	0.75	0.22	0.74	0.02	-1.54	-1.30	0.90
RETN	0.57	0.43	0.45	0.98	-1.15	1.40	-0.92	-1.19	-1.19
TRIM7	-0.51	-0.89	-1.27	-1.04	1.19	1.07	0.95	0.49	0.88
MIRLET7BHG	-0.86	-1.21	-0.93	-0.81	0.70	1.48	1.09	0.49	0.79
LOC399900	0.61	0.53	1.21	0.55	0.21	-1.02	-1.08	-1.23	-1.07
COL5A1	1.24	-0.68	-0.03	-0.76	-1.22	1.95	0.38	0.25	-0.94
POTEKP	0.94	0.95	0.83	0.52	0.57	-1.48	-1.00	-1.16	0.74
ARC	1.54	0.21	0.59	1.42	-1.05	-0.64	-1.16	-0.90	-0.54
ENST00000409310	-1.15	-1.03	-1.24	1.34	-0.88	0.96	0.00	0.26	0.82
CYB5R2	0.24	-0.90	-0.84	-1.07	0.75	0.65	0.30	0.79	1.56
HOXA9	0.37	-1.13	-0.44	0.03	-1.15	0.56	1.25	0.75	1.22
TRIB2	0.56	0.98	0.99	1.52	-0.77	-1.21	-0.44	-0.82	0.36
TGFB1	0.66	0.74	0.64	0.57	0.96	-0.38	-1.28	-1.47	0.86
LOC100216545	0.14	-0.81	0.52	0.93	0.87	-1.02	0.39	-1.24	-1.24
LOC100293962	0.29	0.21	0.74	1.40	-0.01	-0.93	-0.43	-1.52	-1.09
PHACTR1	0.87	1.08	0.68	-0.43	1.05	-0.34	-0.92	-1.56	-1.18
ENST00000378350	0.25	0.40	1.33	0.42	0.05	-0.83	-0.77	-1.06	-1.37
PNPLA6	0.52	0.91	0.96	0.61	0.75	-0.33	-1.38	-1.13	0.63
CXCL1	1.91	0.84	1.14	-0.29	0.19	-0.52	-0.45	-1.17	-0.69
RYR1	1.04	0.84	0.93	0.67	0.04	-0.62	-1.40	-1.83	-0.08
ATP6V0D1	0.07	1.37	0.89	0.14	0.69	-1.21	-1.24	-0.55	1.04
MLLT4	0.24	1.18	1.22	1.03	-0.70	-1.27	-0.74	-0.30	-1.34
LRG1	1.34	0.36	0.71	0.95	-0.65	-1.08	-0.89	-1.23	-0.66
GHRHR	1.10	-0.56	0.42	-0.53	-1.00	2.02	0.05	0.33	-1.21
AKT1S1	0.47	0.69	0.79	0.62	0.98	-0.09	-1.01	-0.89	0.51
STXBP2	0.58	0.96	0.99	0.37	0.65	-0.81	-1.42	-1.45	0.92
IFITM1	-1.00	-0.78	-0.43	0.66	-0.79	1.29	0.17	-1.37	1.26
C12orf75	0.81	1.06	1.02	0.83	-0.30	-1.27	-1.11	-0.59	-1.25
TRPM4	1.44	0.49	0.81	0.60	-0.84	-0.92	-0.33	-1.25	-1.10
ZFP36	0.77	1.01	1.00	0.38	0.09	-0.62	-1.11	-1.44	-1.17
XLOC_001788	-0.26	1.38	1.37	-0.84	-1.12	0.03	-0.65	-0.24	-0.98
TREM1	1.01	0.99	0.79	-0.99	0.16	-0.32	-0.82	-0.53	-1.61
TNFSF9	1.04	1.02	0.64	-0.30	-0.21	-0.06	-0.84	-1.35	-1.36
MAP2K2	1.00	0.80	0.73	0.58	0.74	-0.56	-1.05	-1.46	0.64
EEF1A1	0.76	0.86	0.62	0.47	0.56	-1.44	-0.76	-0.24	0.96
SUSD3	1.08	0.76	0.68	0.82	-0.83	-0.42	-0.43	-0.78	-1.87
ALDH3B1	0.72	0.67	0.78	0.61	0.96	-0.82	-0.96	-1.21	0.80
XLOC_l2_002033	0.10	-0.83	0.30	0.06	1.02	-0.94	1.67	-0.96	-1.32
PKN1	0.90	1.03	0.90	0.58	0.32	-0.83	-1.06	-1.27	0.79
IL21R	0.92	0.75	0.83	0.64	-1.11	0.22	-1.07	-1.57	-0.67
RIC8A	0.78	1.02	0.62	0.31	0.94	-1.09	-1.23	-1.17	0.88

LENG9	-0.96	-0.82	1.15	0.26	-0.55	1.39	-0.22	-0.65	-1.08
IL7	-0.71	0.28	-0.88	-1.31	0.15	1.64	0.85	0.80	0.47
FABP5	0.93	0.73	1.03	1.11	-0.64	-0.78	-1.15	-1.01	-1.09
SCD5	-0.31	-1.19	-0.73	-0.42	0.88	0.99	0.61	1.16	0.70
STAB1	1.21	1.01	0.84	0.60	0.56	-0.93	-1.50	-0.88	0.16
C17orf51	-0.64	-0.58	-0.95	-1.17	0.86	1.11	1.17	0.77	0.67
MKNK2	0.67	1.11	0.83	0.72	0.79	-1.08	-1.47	-0.92	0.42
VAMP2	0.34	0.99	0.93	0.28	0.92	-0.22	-1.37	-1.51	0.79
KIAA0195	0.77	0.84	0.66	0.56	0.69	-0.30	-1.10	-1.20	0.82
PGA3	1.54	0.38	0.35	1.10	0.67	-0.77	-1.67	-0.94	-0.66
LOC100270804	-0.23	-0.52	-0.51	-0.71	0.65	0.86	1.07	1.23	0.18
PLEKHG2	1.86	0.27	1.17	-0.15	-0.16	-0.96	-1.20	-0.90	-0.63
AY358259	0.49	0.40	0.88	0.06	0.65	-1.26	-0.76	-1.62	-0.40
KLF4	1.23	0.90	0.71	0.84	0.69	-1.42	-1.17	-1.19	-0.34
LSP1	0.71	0.79	0.70	0.89	0.89	-0.76	-1.65	-1.45	0.39
GNB2	0.77	0.67	0.45	0.68	1.03	-1.12	-0.88	-1.11	0.95
RILPL1	0.90	0.88	1.06	0.62	-0.73	-1.00	-0.62	-1.21	-1.07
GRINA	0.48	0.76	0.70	0.13	1.28	-0.27	-1.11	-1.07	0.81
SLC11A1	1.10	0.86	0.98	-0.11	0.71	-0.54	-0.99	-0.87	0.64
RGS14	1.06	0.97	0.64	0.59	0.47	-1.07	-1.07	-1.46	0.81
ENST00000525262	0.73	0.66	0.75	0.39	0.79	-0.61	-1.00	-1.26	1.12
RAC2	0.97	0.60	0.57	0.32	0.89	-0.61	-1.06	-1.19	1.07
NETO2	-0.66	-1.11	-1.04	-0.11	0.13	1.19	1.11	1.64	-0.23
PAX9	1.20	-0.50	0.34	-0.40	-1.14	1.93	0.06	0.40	-0.80
MSLN	1.13	0.65	1.68	0.76	-0.81	-0.83	-1.00	-0.98	-0.75
RAB40C	0.69	0.94	0.84	0.50	0.65	-0.89	-0.59	-0.89	0.69
XLOC_l2_015885	1.17	0.44	1.09	-0.66	1.09	-0.64	-1.44	-1.44	0.24
XLOC_006948	0.75	0.18	0.63	1.01	-1.07	-0.58	-1.20	-0.57	-0.87
EVL	0.85	1.07	0.93	1.01	-0.04	-1.42	-1.08	-1.40	-0.20
ADAMTS10	0.68	0.94	0.68	0.49	-1.54	-0.05	-1.02	-0.57	-1.06
XLOC_000872	1.18	-0.31	0.47	-0.49	-1.05	1.90	-0.06	0.42	-0.79
SLC2A3	0.98	1.50	1.13	0.32	0.39	-1.16	-0.94	-0.59	-0.41
NELF	0.94	1.08	1.51	0.92	-0.30	-0.69	-1.00	-1.10	-0.43
ABHD11	1.06	-0.23	0.56	-0.38	-1.06	1.74	0.01	0.64	-1.22
AB529247	1.04	-0.40	0.47	-0.34	-1.28	1.88	0.05	0.45	-0.55
ENST00000360485	-1.27	-0.67	-0.93	-0.21	0.44	1.24	0.71	1.09	0.93
ARHGDIA	1.16	0.82	0.65	0.29	0.78	-0.60	-1.42	-1.62	0.64
CTSF	-0.60	-1.19	-0.74	-0.99	1.15	1.71	0.92	0.31	0.12
FAAH	0.93	0.92	0.88	0.80	0.60	-1.26	-1.01	-1.04	0.45
CAMK1	0.90	0.49	0.81	0.58	0.96	-0.38	-1.22	-0.93	0.58
CLEC5A	0.73	1.28	1.20	0.62	-0.98	-1.36	-1.43	0.27	-0.25
NPB	1.27	-0.36	0.46	-0.31	-0.90	1.50	0.22	0.68	-1.05
TAGLN	0.64	0.84	1.05	0.39	0.80	-0.69	-1.68	-1.41	0.62
CYP27A1	-0.87	-1.28	-0.52	-1.36	-0.11	1.24	1.31	0.24	1.02
GBP4	-1.29	-0.88	-1.11	-0.94	0.31	0.89	1.68	0.54	0.64
NGFRAP1	0.20	-0.61	-0.01	-0.63	0.09	1.06	0.92	1.18	-0.01
PER1	0.45	1.16	0.63	-0.96	1.72	-0.57	-0.65	0.36	-1.08
C17orf69	-0.34	-0.59	-0.42	-0.40	-1.22	1.41	1.63	0.88	0.17
IL1RN	0.76	0.84	1.01	0.82	-0.24	-0.65	-1.42	-1.81	0.32

C5orf20	0.55	0.91	0.15	1.13	-1.46	-0.07	-1.02	-0.77	-0.87
CUEDC1	0.57	0.84	0.77	0.50	0.63	-1.25	-1.30	-1.62	0.90
LYL1	0.87	0.79	0.76	0.55	0.65	-0.76	-1.13	-1.72	0.87
VEZF1	0.73	0.92	0.74	0.51	0.42	-0.54	-1.10	-0.85	1.01
WASF1	-0.48	-0.71	-0.14	-0.69	0.10	1.32	1.36	0.94	0.11
PPT2	-0.60	-0.71	-0.87	-1.36	1.39	1.12	0.88	0.55	0.57
POU2F2	0.99	0.86	1.10	0.49	0.22	-1.00	-1.34	-1.29	0.80
TRAF4	1.25	1.01	1.04	0.85	0.26	-0.77	-0.92	-1.00	-0.29
ZNF295	1.45	0.33	1.01	-1.07	0.76	-0.55	-0.93	-1.29	-0.62
PSPH	1.10	0.63	1.32	-0.75	-1.57	-0.53	0.83	-1.14	0.46
TRNP1	0.95	1.06	1.26	0.86	-0.31	-0.86	-1.37	-1.29	-0.47
ADAM33	1.29	-0.80	0.42	-0.47	-0.96	1.93	-0.26	0.36	-1.15
HMGA1	1.03	0.92	0.64	0.78	0.69	-0.55	-1.13	-1.35	0.39
PDE4DIP	-0.74	-0.77	-1.50	-1.06	1.58	0.67	0.73	0.87	0.43
A_24_P383901	0.91	0.87	0.73	0.67	0.57	-1.69	-0.92	-1.26	0.69
XLOC_011052	0.49	0.29	0.68	1.16	-0.77	-0.99	-0.99	-1.29	-0.21
FKBP9	-1.68	-0.55	-1.08	-0.47	0.61	0.61	1.54	0.88	0.61
AP1G2	0.83	0.91	0.71	0.26	0.83	-0.44	-1.28	-1.17	0.86
HK3	0.77	0.88	0.65	0.45	0.40	-1.42	-0.44	-0.74	1.13
MAF1	0.78	0.78	0.80	0.25	1.13	-1.16	-0.94	-0.97	0.76
ENST00000411514	0.82	-0.51	1.60	1.66	-0.26	-0.74	-0.99	-0.34	-0.26
MICAL1	0.98	1.26	0.93	0.37	-0.04	-0.45	-1.20	-1.03	0.68
XLOC_010078	0.95	0.87	1.22	0.30	-0.89	-1.01	-0.94	-0.98	-0.76
XLOC_l2_006196	0.28	1.35	0.87	1.54	-0.78	-0.64	-0.85	-1.47	-0.05
FMNL1	1.07	0.82	0.62	0.27	0.77	-0.44	-1.42	-1.53	0.80
NFKB2	0.93	1.13	1.13	0.22	0.35	-0.71	-1.03	-1.11	0.60
RAI1	0.91	0.94	0.79	0.77	0.52	-0.94	-1.17	-1.44	0.64
SIRPB2	0.96	0.93	0.57	0.47	0.35	-0.50	-0.81	-0.84	0.91
CYP1B1-AS1	-0.12	-0.49	-0.55	-0.41	0.38	0.92	1.12	1.02	0.33
CCND3	0.77	0.92	0.81	0.47	0.51	-0.74	-1.58	-1.00	1.02
C13orf15	0.91	0.55	0.51	-0.73	2.01	-0.63	-0.78	-0.68	-1.25
DDX58	-0.31	0.44	0.11	-1.70	-1.76	1.00	0.44	0.02	0.83
MAPKAPK2	0.69	0.80	0.70	0.40	0.75	-0.14	-1.00	-0.89	0.77
CTTNBP2	1.10	0.60	0.88	0.95	-0.94	-1.17	-1.38	-0.42	-0.64
HPCAL1	0.84	0.83	0.77	0.50	0.66	-0.84	-0.68	-0.87	0.76
PCBP2	0.74	1.02	0.56	0.55	0.66	-0.98	-1.38	-1.10	1.03
MAGEF1	1.13	0.85	0.84	1.45	-0.71	-1.14	-1.18	-0.86	0.12
SAMD1	0.61	1.04	0.89	0.62	0.47	-0.73	-1.49	-1.59	0.74
C5orf56	-1.29	-1.29	-0.95	-0.42	0.21	1.10	1.56	0.80	0.48
C1orf21	0.04	-1.40	-0.34	-1.40	-0.20	-0.80	1.12	0.90	1.15
TIFAB	0.86	0.51	-0.25	1.27	-0.90	0.21	-0.79	-1.16	-1.20
XLOC_006774	0.61	0.40	0.59	0.66	-0.75	-0.95	-0.20	-0.98	-1.28
BRD4	0.14	0.89	0.92	0.75	0.89	-0.72	-1.67	-0.93	0.83
NEXN	-0.97	-1.61	-1.37	-0.04	0.41	1.18	0.96	0.82	0.67
AK096443	1.23	-0.57	0.44	-0.67	-0.38	1.98	-0.09	0.20	-0.82
BLVRA	-1.23	-0.37	-1.39	-1.20	0.92	1.09	0.93	0.61	0.83
SPRYD3	1.01	0.91	0.54	0.27	0.83	-0.24	-1.46	-1.33	0.73
CASP2	1.05	-0.40	0.46	-0.58	-1.01	1.99	-0.13	0.52	-0.66
SLED1	1.37	1.21	1.02	-1.44	-0.15	-0.13	-0.73	-0.45	-1.22

FCAR	0.87	1.26	1.27	-0.56	0.63	-1.37	-0.95	-1.12	-0.40
ABTB1	0.56	0.85	0.75	0.44	0.69	-0.59	-1.41	-1.77	1.01
WFS1	1.02	0.98	0.32	0.51	-0.33	-0.87	-1.31	-0.81	-1.03
CEBPA	1.01	0.74	0.62	0.96	0.31	-0.77	-1.22	-1.43	0.86
LAMC1	0.96	1.39	-0.69	0.62	-1.23	-1.09	-1.14	-0.33	0.78
SNORA57	-1.08	-1.20	-1.26	0.93	0.79	0.91	1.14	0.81	-0.55
HNRNPA1L2	0.95	1.09	0.74	0.32	0.22	-1.34	-0.78	-0.90	1.07
TMEM176A	0.02	-1.32	1.56	0.86	0.98	-0.33	-1.57	-0.23	-0.47
TUBA1A	1.01	1.25	0.94	0.38	0.52	-0.81	-1.28	-1.65	-0.21
ZNF532	-0.15	-0.36	-0.99	-0.71	0.52	0.73	1.29	1.01	0.54
GSTT1	-1.59	0.06	-0.18	-0.42	1.13	0.98	1.04	0.78	-1.49
PRSS36	1.87	-1.76	0.18	-0.84	0.26	0.74	0.55	-0.12	-0.85
KREMEN1	0.41	-1.05	-0.82	-0.81	0.64	1.02	0.82	0.71	0.84
CCDC122	-0.95	0.26	0.89	-0.92	0.88	-1.16	0.96	1.16	-1.40
XLOC_010647	0.91	-0.37	0.62	-0.42	-0.95	1.99	-0.06	0.41	-0.79
MKL2	-0.69	-0.69	-1.07	0.12	-0.72	1.25	0.82	1.15	-1.27
TMEM133	0.61	1.15	0.79	1.34	-0.96	-0.87	-1.05	-1.01	-0.75
KDM6B	0.25	1.31	1.29	0.30	0.51	-0.61	-0.98	-0.94	0.52
C17orf96	1.10	0.83	1.47	0.86	0.13	-0.82	-0.81	-0.48	-1.23
ST7L	0.97	-0.17	1.11	0.58	-0.11	-1.13	-1.17	-0.90	-0.74
STEAP4	1.40	1.09	0.67	0.11	-1.27	-1.08	-0.85	-1.11	0.28
ZG16B	0.70	0.85	0.75	0.66	-0.85	-0.09	-0.81	-1.71	-0.84
GGT5	0.60	0.68	0.77	0.16	-1.46	-0.92	-0.66	0.45	-1.20
SLC2A14	0.95	1.44	1.11	-0.92	0.37	-0.19	-0.95	-1.07	-1.22
PTPN13	1.13	0.85	0.66	0.56	-0.74	-0.82	-1.72	0.05	-1.00
SLC35B2	1.03	1.06	0.89	0.23	0.94	-1.11	-1.37	-0.52	0.16
WNT5B	1.16	1.33	0.82	0.66	-0.77	-1.27	-1.34	-0.70	-0.30
ACPL2	1.03	0.00	0.57	-0.08	-1.07	1.57	-0.16	0.62	-0.71
SRF	1.05	1.04	1.20	0.25	0.38	-1.36	-0.60	-0.25	-0.02
ATP5B	0.92	0.91	0.50	0.35	0.82	-1.45	-0.80	-0.78	0.95
RFNG	0.69	0.89	0.57	0.55	0.84	-0.85	-0.88	-1.19	0.98
LILRA2	0.49	0.74	0.76	0.78	1.01	-0.97	-1.08	-0.77	0.71
LOC407835	0.99	0.79	0.67	0.63	0.62	-0.80	-1.34	-1.64	0.75
CYP2U1	-0.25	-0.52	-0.67	-1.01	0.39	0.98	1.24	1.21	0.36
CHRNA7	-0.92	-1.11	0.21	-1.06	0.87	1.37	0.32	-1.21	0.33
PPP2R4	0.98	0.93	0.78	0.29	0.66	-0.61	-1.32	-1.41	0.82
CAPNS1	1.31	0.68	0.51	0.06	0.72	-0.33	-1.23	-1.49	0.93
ANO5	-0.86	-1.32	-0.95	-1.12	0.13	0.68	0.49	1.46	1.21
DHRS9	0.71	0.85	0.03	0.95	-0.72	-0.65	-0.61	-1.88	-0.07
ST14	-0.68	-1.17	-0.40	-0.84	1.30	0.84	-0.12	0.79	1.41
PDE4D	1.54	0.93	0.44	0.88	-0.90	-1.15	-0.99	0.73	-0.56
RN18S1	1.03	0.56	1.01	-0.65	0.94	-0.60	-1.56	-1.48	0.54
CLECL1	0.23	0.62	0.24	0.16	-1.16	0.10	-1.27	1.22	-1.48
ZDHHC18	0.98	1.32	0.76	0.29	-0.35	-0.62	-1.04	-0.84	1.01
KIAA2013	0.88	0.73	0.58	0.56	0.97	-1.20	-0.85	-1.19	0.85
TH1L	0.85	0.93	0.57	0.73	0.83	-0.91	-0.83	-0.73	0.45
SLCO2B1	1.35	0.48	0.46	1.72	-0.47	-1.13	-0.99	-0.58	-0.97
MXI1	-1.19	0.70	-0.18	-1.40	1.32	-0.37	0.99	-0.97	1.15
NLRC3	0.66	0.72	1.40	1.24	-1.23	-0.90	0.42	-0.44	-1.17

DAGLB	1.05	0.98	0.97	0.58	0.56	-1.03	-1.16	-1.02	0.40
SF3B2	0.87	0.99	0.33	0.27	0.91	-1.03	-1.41	-1.00	1.09
AQP9	-0.40	-1.32	-1.13	-1.46	0.33	0.94	0.95	1.07	0.78
MOP-1	0.87	0.41	0.50	0.13	0.47	-0.52	-0.93	-1.54	-1.10
MLF2	0.61	0.63	0.94	0.24	0.95	-0.12	-1.36	-1.62	0.83
C19orf22	0.75	0.97	1.00	0.45	0.76	-0.79	-1.44	-1.01	0.58
HSP90AB1	1.13	1.08	0.52	0.41	0.77	-0.92	-1.56	-0.79	0.53
LGALS9	0.82	0.89	0.66	0.15	0.48	-0.67	-1.24	-1.63	1.29
XLOC_014103	-0.87	0.49	1.10	-0.19	0.89	-0.76	0.09	1.03	0.28
FLJ90757	0.63	1.12	0.77	1.19	0.12	-1.80	-0.70	-0.81	0.38
LMNA	0.93	0.32	-1.12	-0.56	1.67	0.18	-0.88	0.95	-1.39
WNT6	-1.09	-0.84	-1.01	-1.04	0.40	1.15	1.37	0.41	1.12
TRIM26	1.19	0.87	0.59	0.17	0.52	-0.29	-1.18	-0.93	0.85
VAMP5	-0.95	-0.93	-0.97	-0.73	1.19	0.92	1.23	0.28	0.95
ESYT1	1.17	1.37	0.84	0.72	0.06	-1.17	-1.26	-1.17	-0.16
BCL2A1	0.93	0.62	0.82	-0.65	-0.52	-0.65	-0.56	-1.34	-0.54
SDSL	-0.33	-1.59	-1.16	-1.10	0.95	1.18	1.08	0.43	0.16
FAM118A	1.55	-0.33	1.37	-0.05	-0.45	-1.00	-0.96	1.07	-0.05
PTPN18	1.08	0.78	0.51	0.34	0.86	-0.54	-1.33	-0.88	0.81
NRBP1	0.81	0.74	0.63	0.26	1.11	-0.54	-1.27	-1.54	0.86
FAM108A1	0.72	0.74	0.72	0.79	0.66	-0.65	-0.69	-1.19	0.77
ITGB1BP1	-1.25	-1.28	-0.22	1.35	-1.00	0.31	-0.39	0.21	0.98
DGKZ	0.53	0.65	0.80	1.09	0.07	-0.87	-0.40	-0.47	0.77
FLNA	0.59	0.97	0.91	0.61	0.42	-0.09	-1.59	-1.55	0.68
FLNB	1.43	0.31	0.69	1.60	-0.42	-0.87	-1.10	-0.63	0.12
C15orf48	2.09	-0.85	0.77	0.32	-0.83	-0.35	-0.25	-0.28	-1.33
GBP3	-1.14	-0.80	-1.51	-0.56	0.80	0.49	0.97	0.80	1.36
IL3RA	0.57	0.17	0.62	0.89	0.34	-0.71	-0.91	-0.72	-1.77
LENG8	1.07	0.83	1.05	-0.12	0.47	-0.70	-0.92	0.35	0.06
SERPINB10	0.32	-0.89	1.01	1.74	-0.88	-0.77	-0.89	-0.14	1.19
A_33_P3415526	1.14	0.96	0.77	0.63	0.29	-1.62	-0.98	-1.16	0.61
FAM108C1	0.16	-0.88	-1.29	-0.66	0.76	0.20	1.18	0.93	1.05
TMEM150A	0.73	0.82	0.72	0.41	0.88	-0.68	-0.78	-0.57	0.60
DDIT4	1.01	1.28	0.30	-0.54	0.73	-0.26	-0.82	0.90	-0.81
ABCD1	0.85	0.71	0.56	0.35	0.90	-0.19	-1.19	-1.39	0.92
DMPK	1.43	0.91	1.05	1.07	-1.17	-0.30	-1.01	-0.76	-0.83
PPARG	0.81	1.18	1.35	0.44	0.28	-1.41	-1.38	-0.31	-0.91
P2RY13	1.06	0.97	0.45	0.59	0.31	-0.81	-1.77	-1.37	0.77
C11orf96	1.29	0.03	0.42	-0.88	1.75	0.67	-0.68	-0.48	-1.06
HOXA10	-0.94	-0.29	-1.02	-0.63	-0.31	0.54	1.45	0.40	1.75
NAAA	0.84	0.73	0.91	0.42	0.91	-1.64	-0.98	-0.80	0.69
VASH1	1.14	-0.78	0.76	1.31	-1.06	-0.14	-1.10	-1.03	-0.27
JUP	0.70	1.56	0.70	0.92	-0.68	-0.41	-1.21	-1.61	0.18
AK124259	0.01	0.08	0.19	2.02	0.38	-0.55	-1.21	-0.94	-1.01
MAPKAPK3	0.67	1.01	0.60	0.71	0.72	-0.70	-1.36	-1.65	0.74
GRAMD1A	1.40	0.88	0.65	0.15	0.63	-0.89	-0.70	-0.94	0.54
RHOG	1.24	0.62	0.63	0.34	0.74	-0.51	-1.10	-1.59	0.81
CD81	0.95	0.75	0.89	1.27	0.32	-0.86	-1.28	-1.53	0.05
PADI2	1.11	1.14	0.32	0.94	0.56	-0.93	-0.94	-1.22	0.36

WDR74	-0.30	-1.52	-0.63	1.15	1.36	-0.88	0.21	0.15	-0.80
LOC100506159	-1.85	-0.63	-1.38	-0.13	0.37	0.73	0.98	1.14	0.50
PRORSD1P	-0.21	-0.74	-1.01	-0.43	0.33	1.37	1.01	1.14	0.23
PRDM1	0.71	1.57	1.00	-0.12	-0.31	-0.11	-1.22	-1.25	-1.09
DHCR24	1.22	0.40	0.95	1.01	-1.00	0.70	-0.90	-0.67	-1.64
XLOC_000468	0.56	-0.29	0.59	1.03	0.05	-0.90	-0.57	-1.35	-0.95
CRTAM	-1.13	-0.98	-0.98	-0.75	0.03	0.80	1.51	0.98	1.04
RRAD	1.37	0.16	1.43	0.47	0.55	-1.31	-0.86	-1.26	-0.68
GAS6	0.86	1.55	0.63	1.29	-0.52	-1.19	-0.85	-0.13	-0.73
PYCR2	0.43	0.85	0.66	0.59	0.94	-0.74	-1.09	-1.18	1.03
MLC1	0.56	0.98	1.25	0.83	-1.42	-0.21	-0.42	-0.92	-1.37
FAM160A1	-0.48	1.69	0.88	1.28	-0.77	-0.86	0.24	-1.12	-0.91
DEF6	1.30	0.80	0.99	0.42	0.14	-1.05	-0.80	-1.11	0.73
A_33_P3216192	-1.43	-0.79	0.71	0.76	0.18	-0.98	1.37	0.81	-1.19
C20orf27	0.97	1.07	0.90	0.71	0.04	-0.80	-1.47	-1.50	0.55
ARRDC4	-1.25	-1.13	-0.57	-0.77	0.18	1.41	1.04	1.11	-0.68
NOXA1	1.12	0.90	1.13	0.45	-0.26	-0.82	-0.90	-1.88	-0.27
SEMA4A	1.07	0.84	0.75	0.30	0.32	-0.36	-0.65	-0.86	0.72
SNX9	1.29	1.28	0.62	0.34	0.02	-1.42	-0.94	-0.80	0.70
PPP1R3G	0.94	0.27	0.38	0.86	-0.93	0.65	-0.99	-1.50	-0.98
PHLDA2	0.81	-0.46	0.92	-0.81	0.93	0.59	0.90	-0.20	-0.65
IL10	1.14	0.58	1.32	1.32	-1.00	-0.08	-1.14	-0.71	-0.59
RNASE1	0.56	-0.86	-1.27	-0.64	0.52	1.71	0.46	0.22	0.70
USP5	0.90	0.90	0.89	0.59	0.40	-0.94	-1.45	-1.21	0.86
APOBEC3C	0.75	0.56	0.87	0.22	0.84	-0.64	-1.30	-1.84	0.96
CD1C	0.92	0.11	0.33	1.25	-0.83	-1.67	0.30	1.21	-0.58
XLOC_009167	-0.28	0.09	0.62	0.10	1.75	-0.05	-1.16	-1.05	-1.24
APOBEC3F	0.82	0.47	1.00	0.33	0.81	-0.55	-1.24	-1.77	0.89
C3	0.85	0.77	0.34	1.37	-0.55	-0.95	-1.45	-1.26	-0.02
ENST00000400702	0.26	0.35	1.40	0.32	-0.01	-0.78	-0.66	-1.08	-1.41
FURIN	0.72	1.07	0.79	0.50	0.60	-0.84	-0.90	-1.19	0.83
LOC100652867	0.69	1.14	1.02	0.06	-0.34	-0.18	-1.35	-1.53	-0.68
LOC100132966	0.39	-0.73	0.59	1.39	0.96	-0.86	-1.21	-1.13	-0.55
TRIM28	0.89	0.96	0.80	0.44	0.72	-0.60	-1.44	-1.62	0.59
MYADM	0.66	1.16	0.98	-0.29	1.07	-0.20	-1.11	-0.84	0.29
SRD5A3	-0.69	0.19	-0.10	-1.24	-0.46	1.07	0.78	1.43	0.62
HNRNPAB	1.10	1.20	0.60	0.18	0.67	-1.22	-1.20	-0.75	0.67
F5	-0.89	-0.15	-0.68	0.14	0.11	0.75	1.00	1.20	0.60
RTP4	-1.45	-1.14	-0.89	-0.04	-0.71	1.30	1.18	0.26	0.71
NAB2	0.49	0.30	0.59	1.01	0.64	-0.56	-1.24	-1.12	-1.43
FAM89A	0.08	1.22	1.25	1.26	-1.03	-0.52	-0.41	-1.58	-0.53
LOC100287415	1.05	1.41	1.00	0.51	-0.45	-1.29	-0.96	-0.96	-0.81
SIGLEC9	1.43	-0.52	0.18	-0.67	-0.68	2.15	-0.30	-0.16	-0.70
PTPN6	1.05	0.87	0.87	0.45	0.78	-0.86	-1.44	-1.30	0.49
CERS4	1.07	1.32	0.93	0.36	0.51	-0.15	-0.95	-1.35	-0.32
RNF167	0.40	0.62	1.49	0.75	0.33	-0.81	-1.42	-1.00	0.77
C9orf167	1.27	1.00	0.39	0.74	0.48	-1.04	-1.05	-1.62	0.49
FBXO32	-1.21	-0.75	-0.82	-0.56	0.20	1.33	1.61	0.69	0.45
MOV10	1.18	0.97	0.83	0.23	0.29	-1.09	-0.79	-1.32	0.90

POTEF	1.12	0.97	0.82	0.55	0.42	-1.50	-0.60	-0.81	0.50
TACC3	0.87	0.82	0.73	0.11	0.79	-1.31	-1.13	-1.09	1.15
CLEC4E	-1.07	-0.79	-1.10	-1.26	0.36	0.88	1.56	0.88	-0.03
SPRY1	0.75	1.07	0.58	-0.94	1.49	0.57	-1.02	-1.02	-0.34
GPR133	0.71	1.01	1.23	1.20	-1.24	-0.74	-0.59	-0.81	-1.14
NAP1L5	1.01	0.86	1.18	-0.97	0.93	-1.17	-0.88	0.44	-0.09
FLJ45248	0.91	0.18	1.11	0.62	-0.06	-1.02	-1.09	-1.26	-0.81
FAM134A	0.90	0.62	0.83	0.31	0.82	-0.61	-0.89	-1.03	0.88
CKM	0.12	0.71	0.87	0.77	-1.02	-0.69	-1.04	-1.44	0.17
A_33_P3238820	0.23	1.02	1.01	1.46	-0.82	-0.62	-0.57	-1.82	-0.12
LOC550643	-0.81	-1.55	-0.64	0.56	-0.40	0.88	0.91	0.97	-1.08
GNAS	1.01	1.04	0.98	0.21	-0.09	-1.42	-1.27	-1.22	0.86
ZNF441	-1.45	-0.57	-1.04	0.72	-1.05	0.93	0.54	0.93	-0.34
AK095730	1.01	-0.31	0.46	-0.67	-0.91	2.03	-0.07	0.34	-0.48
CH25H	1.48	-0.36	-0.01	-1.35	-0.64	1.02	1.29	0.38	-0.84
C1orf213	-0.79	-1.30	-0.81	0.30	-0.38	0.15	1.84	1.03	0.79
A_33_P3421515	0.06	-0.14	-0.01	-1.22	-1.25	1.32	0.60	1.15	-1.35
MCTP1	-1.69	0.66	1.22	0.05	-0.12	-0.75	-1.26	1.07	-0.12
MXD1	0.98	1.67	1.22	-0.74	0.39	-1.16	-0.66	-0.87	-0.74
MUC4	0.96	0.24	0.40	-1.15	-1.00	1.28	-0.44	-0.84	-0.93
XLOC_012503	-0.91	-1.60	-0.54	0.36	-0.06	1.00	1.33	1.19	0.21
KIAA0556	0.76	0.81	0.72	0.54	0.76	-0.97	-0.51	-0.76	0.68
MFNG	0.83	0.98	0.46	0.56	0.70	-1.02	-1.12	-1.48	1.01
RALY	0.97	0.73	0.68	0.41	0.34	-1.64	-0.29	-1.08	1.13
CLPTM1	0.75	0.78	0.79	0.34	0.60	-0.63	-1.04	-0.70	1.03
LOC100506312	-1.52	-1.00	-1.02	-0.43	1.43	1.11	-0.23	0.93	0.39
TUBA1C	0.95	0.98	1.02	0.43	0.81	-0.93	-1.07	-1.58	0.22
ANKRD55	0.47	0.42	1.03	1.11	-1.14	-0.28	1.24	-0.31	-1.11
POR	1.13	0.97	0.79	0.41	0.22	-1.09	-1.35	-1.45	0.78
KCNMB4	0.67	0.57	1.14	0.83	-0.82	-0.80	-0.50	-0.99	-1.41
TUSC1	-0.54	-0.75	-0.12	-1.11	1.05	0.72	0.99	0.61	0.92
PF4	-0.79	0.21	0.65	-1.51	1.72	-1.03	0.46	0.60	0.55
ORM1	0.67	1.08	0.54	0.30	-0.59	-0.98	-0.28	-0.82	-1.54
CYP1B1	-1.15	-0.51	-1.27	-0.99	0.67	0.93	0.99	1.21	0.79
SAT1	0.74	1.19	1.43	0.05	-0.68	-1.12	-0.65	-1.17	-0.74
CCDC61	1.28	-0.81	0.19	-0.65	-0.93	2.15	-0.22	0.04	-0.80
FFAR3	0.56	0.42	0.92	0.43	0.18	-0.04	-2.03	-1.17	-0.55
SLC35D2	1.03	0.87	0.48	0.54	0.50	-1.29	-0.62	-0.77	0.95
NOMO1	0.94	1.07	0.31	-0.01	0.83	-0.69	-0.95	-0.76	1.03
SPIB	0.78	0.43	1.00	1.80	-0.50	-0.85	-1.06	-1.00	-0.89
MTHFR	0.87	1.23	0.71	0.90	0.62	-1.11	-1.22	-0.91	0.14
CNN2	0.22	1.38	0.99	0.22	0.65	-0.55	-1.05	-1.46	0.81
KDM2A	1.09	1.08	0.51	0.05	0.47	-1.01	-0.61	-0.68	0.95
A_33_P3324505	0.34	-0.40	0.82	0.69	0.30	-1.40	0.02	-0.98	-1.17
LOC100507525	0.94	-0.89	0.67	-0.83	0.58	1.30	-0.58	-1.47	-0.75
HNRNPA1	0.95	1.03	0.92	0.37	0.39	-1.57	-0.64	-0.79	0.72
IRF3	0.72	0.77	0.84	0.53	0.75	-0.37	-1.49	-1.46	0.81
SMC2	-1.01	-0.47	-0.98	-0.34	-0.97	0.94	0.44	0.89	-0.42
NTNG2	-0.59	-0.71	-1.31	0.08	0.35	0.99	1.45	0.89	0.35

CTDNEP1	0.75	1.02	0.55	0.28	1.09	-0.95	-1.02	-1.07	0.80
MARK2	0.69	0.89	0.82	0.54	0.65	-0.66	-1.51	-1.40	0.91
HOMER3	-1.06	-1.10	-0.89	-0.68	1.12	1.36	0.92	0.86	0.27
GABBR1	-0.48	0.62	-0.51	0.16	1.02	0.56	-0.30	0.25	1.04
PTPN9	1.06	0.93	0.36	0.16	0.62	-0.01	-1.51	-0.94	0.90
CRIP3	1.27	0.62	0.92	1.37	-1.20	-0.91	-0.91	-0.49	-0.94
PPM1N	1.15	0.41	0.60	1.14	-0.51	-0.42	-0.67	-0.89	-1.79
GRM5	1.31	-0.09	0.51	-0.14	-1.04	1.32	-0.12	0.76	-0.76
MARCKSL1	1.07	0.53	0.97	0.72	0.87	-0.50	-1.52	-1.59	-0.07
AXIN1	0.90	1.10	1.09	0.09	0.07	-1.07	-1.12	-0.97	1.05
A_33_P3233000	0.51	-0.62	-0.71	-0.79	-0.81	2.43	-0.11	0.35	-0.61
RHOC	1.10	0.85	0.78	0.71	0.23	-1.40	-1.10	-1.32	0.77
VCPIP1	-1.11	-1.05	-0.40	-0.03	-1.28	1.36	1.16	0.84	-0.40
ARAF	0.70	0.74	0.56	0.18	0.97	-0.46	-0.67	-0.49	0.76
ROGDI	0.58	0.74	0.76	0.54	0.77	-0.15	-0.71	-1.10	0.68
AMPD2	0.82	1.23	0.82	-0.16	1.16	-1.26	-1.03	-1.02	0.40
NECAP1	0.95	0.87	0.49	-0.75	0.29	-1.18	-1.04	0.91	0.96
LOC100509498	-0.75	-0.85	-1.25	-0.28	0.42	1.44	0.89	1.30	0.22
LOC100506115	0.89	0.18	1.08	0.21	1.14	-0.93	-1.35	-0.98	0.88
CORO1B	0.67	0.56	0.84	0.80	1.02	-0.58	-0.86	-1.18	0.51
SH3BP5	0.73	1.26	0.65	0.63	0.13	-1.07	-0.99	-0.19	0.71
CSNK1D	1.01	0.83	0.98	0.22	0.73	-0.48	-1.53	-1.36	0.59
ORAI2	0.02	0.99	0.97	0.73	0.32	-1.33	-0.19	-0.84	1.02
A_33_P3235454	-1.03	-0.74	0.59	0.73	-0.18	-1.17	1.60	0.43	-1.19
LOC100507800	-0.56	-0.81	-0.99	-1.30	-0.19	0.90	1.75	0.82	0.78
PPAPDC3	0.74	-0.11	-1.27	1.03	-1.39	0.97	-1.43	0.53	0.21
NLRP1	0.73	1.36	0.71	0.65	0.25	-1.43	-1.24	-1.03	0.69
USP21	0.81	0.74	0.74	0.40	0.60	-0.30	-1.23	-0.80	0.93
SLC44A2	1.06	0.67	0.45	0.11	1.08	-1.23	-1.07	-1.00	1.06
A_33_P3362239	1.42	1.19	1.04	0.20	-0.45	-0.89	-1.02	-1.08	-0.97
RELA	0.87	1.09	0.90	-0.20	0.91	-1.38	-0.99	-0.86	0.75
PFN1P2	0.74	0.57	0.87	0.66	0.64	-0.15	-1.60	-1.79	0.63
LOC338758	0.42	0.37	1.28	0.12	0.53	-0.90	-0.71	-1.32	-1.25
A_33_P3370515	1.52	-0.65	0.31	-0.52	-0.81	2.02	-0.12	-0.37	-0.82
SLC1A5	1.04	0.94	0.72	0.38	0.63	-0.68	-1.68	-1.55	0.47
PPP4C	0.25	0.82	0.78	0.81	0.89	-0.62	-1.01	-1.53	0.90
MAP2K3	0.78	1.01	0.65	0.33	0.81	-1.04	-1.14	-1.39	0.95
FAM108B1	-0.84	-0.77	-0.23	-0.60	-1.14	1.58	1.18	1.10	-0.79
MAFG	1.11	1.00	1.20	0.49	-0.50	-1.53	-0.78	-0.73	0.68
HLA-DQB1	0.46	1.05	-1.74	-1.71	-0.11	0.31	0.85	0.58	-0.36
HNRNPU-AS1	-1.11	-0.48	-1.32	0.56	-1.11	0.20	0.58	1.74	0.05
TAGLN2	0.89	0.87	0.76	-0.09	0.73	-0.69	-1.71	-1.29	1.01
ARRDC1	0.84	0.77	0.67	0.91	0.68	-0.65	-1.24	-1.82	0.51
A_33_P3381305	1.17	1.23	1.12	0.30	-0.50	-0.90	-1.03	-1.11	-0.97
LSM3	0.28	-1.02	-0.42	-1.30	0.46	1.06	1.31	0.81	0.30
ENST00000355500	-0.73	-1.03	-0.90	-0.24	1.43	0.53	0.19	1.05	1.09
SDF4	0.71	0.76	0.65	0.14	1.13	-0.85	-0.78	-0.88	0.92
ADAM19	-0.30	-1.31	-1.53	-0.98	0.39	1.04	0.91	1.08	0.79
EML3	0.55	0.88	1.04	0.33	0.87	-0.92	-1.53	-1.35	0.76

CRNDE	0.74	0.96	0.88	-0.33	-1.07	1.55	-0.92	-0.31	-0.03
SH3GLB1	-1.00	-1.00	-0.89	-0.42	-0.58	1.16	1.30	1.31	-0.62
XLOC_002313	0.45	0.24	0.87	0.22	1.61	-0.83	-1.09	-0.87	0.82
CTDSP1	0.76	1.35	1.12	-0.10	0.56	-1.11	-0.99	-1.32	0.59
HSP90AB2P	1.10	0.95	0.53	0.45	0.82	-0.76	-1.34	-0.51	0.45
GRB2	1.07	0.99	0.78	0.05	0.59	-0.74	-1.10	-0.99	0.89
KIAA1539	0.73	0.91	0.59	0.06	0.71	-0.12	-1.17	-0.80	1.02
ARHGEF2	1.10	1.26	0.79	0.04	-0.01	-1.29	-0.77	-0.59	0.92
OLFML2B	1.10	0.34	1.41	0.50	-0.53	-0.10	-1.47	-1.10	-1.01
PI4KA	0.60	0.56	0.85	0.90	0.84	-0.54	-0.53	-0.94	0.37
XLOC_003166	-1.32	-0.13	-0.76	0.24	-1.32	1.12	-0.66	1.04	0.39
CNTD2	0.82	-0.47	-0.60	-0.65	-0.51	2.50	-0.32	-0.42	-0.67
SIRT6	0.44	0.68	0.74	0.83	0.91	-0.36	-1.22	-1.08	0.76
TMEM63C	0.40	0.72	0.42	0.72	-0.86	0.20	-0.52	-1.23	-1.51
NAGA	1.45	1.01	0.69	0.12	0.12	-0.94	-0.93	-0.66	0.75
XLOC_l2_009136	-0.25	-1.31	-0.44	-0.68	0.03	0.91	0.43	1.75	0.87
DUSP5	1.43	0.41	0.53	-0.78	1.41	-0.97	-1.21	-1.07	-0.27
NFKBID	0.87	1.64	1.31	-0.22	0.10	-0.91	-1.26	-0.87	0.12
DCTN1	0.96	0.91	0.67	0.17	0.68	-0.27	-1.77	-1.43	0.77
ACCS	-0.41	-0.96	-1.00	-0.28	0.20	1.07	1.30	0.41	1.20
UTF1	0.90	0.39	0.38	0.56	-0.50	-0.04	-0.86	-1.62	-0.96
LDLRAP1	0.81	0.81	0.95	0.51	0.35	-0.87	-0.32	-0.49	0.49
PLP2	1.03	0.56	0.69	0.50	0.96	-0.43	-1.30	-1.76	0.57
HIST1H2BK	-1.22	-1.18	-0.66	-0.86	0.01	1.41	1.50	0.75	-0.13
COPS7A	1.00	0.80	0.62	0.48	0.69	-0.81	-1.04	-1.52	0.94
HIF1A	-0.46	-1.27	0.39	-1.18	-0.38	1.18	1.29	1.23	-0.95
ST13	0.83	0.98	0.45	0.35	0.66	-1.13	-1.41	-0.96	1.20
IKZF1	0.86	0.53	0.54	0.76	-0.78	-0.86	-0.76	0.64	1.02
DOPEY1	0.84	-0.74	0.16	-0.35	-1.26	2.30	-0.04	0.23	-0.70
GNG11	0.75	1.19	0.36	0.74	0.99	-1.09	0.02	-1.12	-0.15
C1D	-0.71	1.05	0.34	-1.27	1.56	-0.88	-0.72	-0.60	1.27
TUBB2A	1.20	1.28	1.58	-0.62	0.20	-0.50	-0.55	-0.49	-1.04
CALCOCO1	0.94	0.82	0.67	0.41	0.44	0.24	-1.69	-1.33	0.71
FLJ38717	0.31	-0.48	0.44	0.93	0.74	-1.14	-0.09	-1.49	-0.88
CLIC2	-0.72	-0.78	-0.45	-0.52	0.27	1.42	0.95	1.02	0.55
PTAR1	-0.90	-0.68	-1.04	0.25	-1.19	1.15	0.15	1.42	-0.42
ENST00000383834	-0.32	-0.99	0.63	0.97	1.48	-0.63	-0.16	-0.75	-1.42
AK123993	-1.02	1.32	-1.32	-0.99	-0.47	0.43	-0.19	1.26	-0.21
FRY-AS1	-1.65	-0.73	-0.71	-0.45	-0.11	1.09	1.52	0.97	0.58
WDR33	-0.96	-0.55	-1.12	0.38	-1.15	1.30	-0.07	1.50	-0.34
SLC7A5	1.32	0.99	0.95	0.66	0.19	-0.62	-0.15	-0.46	-1.15
NFXL1	-1.57	1.05	0.80	1.18	-0.87	-0.96	0.49	0.81	-0.02
BAMBI	1.94	0.51	-0.38	0.08	-1.13	-0.14	0.26	1.04	-0.97
GPAM	-1.47	-0.61	-0.73	1.01	-0.83	1.08	-0.38	0.61	-0.26
SNORD49A	0.41	0.51	0.36	1.28	-0.22	-1.16	-1.18	-0.95	-0.69
XLOC_l2_007271	0.79	1.12	0.80	0.32	0.47	-1.37	-0.87	-0.88	0.97
TTYH3	0.59	0.67	0.59	0.53	1.12	-0.53	-1.42	-1.02	0.93
RHOBTB2	0.90	1.15	1.15	0.94	-0.57	-1.20	-1.01	-1.19	-0.57
MAN2C1	1.02	0.81	0.39	0.64	0.90	-1.25	-1.27	-0.68	0.75

ZNF185	-0.27	-1.23	-0.68	-1.67	1.10	0.79	0.93	0.80	0.74
TPM3	0.81	1.16	0.98	-0.07	0.25	-0.99	-1.32	-1.04	-0.91
CASP9	1.09	-0.27	0.44	-0.05	-1.20	1.54	0.08	0.74	-0.76
HIP1	0.57	1.00	0.99	0.95	0.63	-1.69	-0.99	-0.68	0.23
XLOC_003007	-1.25	-0.29	-1.29	-0.83	0.34	1.09	1.06	0.13	-0.47
CANT1	0.70	0.54	0.76	0.50	0.53	-0.29	-0.55	-0.55	0.76
HCG26	-1.58	-0.91	-0.78	-0.04	-0.18	1.12	1.24	1.41	0.17
PI4KAP1	0.91	0.85	0.74	0.50	0.88	-0.67	-0.90	-0.81	0.44
ZBTB11	-1.00	-0.84	-0.70	0.17	-1.28	1.04	0.81	1.36	-0.63
RAB7B	1.13	0.61	0.17	0.75	-1.02	0.20	-1.10	0.41	-1.92
A_33_P3213518	-0.11	1.01	0.17	1.73	-0.80	-1.17	-0.62	-0.74	-0.70
LAGE3	1.40	-0.39	0.47	-0.26	-0.93	1.48	0.01	0.67	-1.02
AMOT	1.34	0.71	1.09	1.00	-1.46	0.01	-0.17	-0.50	-1.20
A_33_P3261024	-1.08	-1.16	-0.77	0.20	-0.02	0.74	1.66	1.30	0.06
ZNF615	-1.06	-0.75	-0.89	-0.07	-0.99	0.98	1.42	0.95	-0.68
POLL	0.71	0.84	0.71	0.78	0.58	-0.63	-1.17	-1.62	0.86
DYSF	0.96	0.77	0.93	0.92	0.05	-1.09	-0.78	-0.87	0.74
XLOC_001265	0.63	-0.07	0.63	0.23	0.09	-1.27	-0.80	-1.26	-0.24
IFIT5	-1.20	-1.17	-0.96	-0.29	-0.54	1.70	1.09	0.56	0.09
TMEM64	-1.11	-0.32	-0.54	-1.15	1.02	0.97	1.29	0.87	0.25
TAGAP	0.69	0.23	0.77	0.71	0.70	-0.61	-0.94	-1.62	-1.19
LOC100129617	-0.97	-0.57	0.87	-0.32	1.20	1.08	-1.36	0.75	0.56
XLOC_003501	-0.69	-1.27	-0.79	-0.30	-0.45	1.30	1.32	1.18	-0.90
SETD5	1.12	1.18	0.43	0.28	0.47	-1.06	-1.34	-1.20	0.92
XLOC_005851	-0.99	-0.56	-0.34	-0.72	0.39	0.49	1.63	0.45	1.20

Supplemental table 5: Full list of signature genes. Genes to be used in the signature were identified as being significantly differentially expressed (p<0.05), greater than 1.5 fold differentially expressed in monocytes, and greater than 1.5 fold differentially expressed in T cells in the same direction as in monocytes.

	Log2 Fold Change T (AvF)	Log2 Fold Change Mono (AvF)
FCGBP	-2.3465	-6.0025
HBG1	-4.713	-5.295833333
SOCS3	-3.001	-4.585
CD69	-1.9915	-3.990833333
BTG2	-1.28	-3.9275
IGF2BP3	-5.6695	-3.62
MAF	-1.613	-3.539166667
FOS	-4.0595	-3.365833333
JUP	-2.729	-3.106666667
IGFBP2	-4.487	-3.0525
TNF	-1.5585	-2.619166667
C3AR1	-1.177	-2.383333333
CAMK1	-2.2125	-2.21
C17orf96	-1.6505	-2.199166667
TYMS	-7.3245	-2.178333333
PLAG1	-1.313	-2.174166667
ZG16B	-1.3775	-2.133333333
TUBA1C	-1.2325	-2.131666667
XLOC_006948	-1.3575	-2.116666667
SNX27	-0.919	-2.013333333
RGS1	-5.2325	-1.928333333
SGK1	-3.232	-1.8175
SLC29A1	-1.9035	-1.8075
CBX8	-1.751	-1.765833333
MLC1	-2.6675	-1.765
PIEZO1	-0.988	-1.755833333
SERPINF1	-5.2865	-1.749166667
CTNNA1	-1.3695	-1.711666667
PDE4D	-1.845	-1.656666667
YBX1	-0.7565	-1.6525
CTSC	-1.3805	-1.626666667
MATK	-1.961	-1.5925
EWSR1	-1.4315	-1.56
PDE6G	-3.6885	-1.56
BMF	-1.861	-1.555
XLOC_002323	1.289	1.536666667
RECK	1.1995	1.550833333

KLHDC7B	1.7905	1.5525
A_19_P00811234	1.014	1.5525
SP140	0.962	1.605
TCEAL5	4.177	1.616666667
MAFIP	1.4465	1.6175
ARMCX4	2.21	1.649166667
ACACB	3.231	1.663333333
SARM1	2.467	1.705833333
SELM	4.3975	1.711666667
RBM43	1.165	1.731666667
MB21D2	0.821	1.74
DDB2	0.997	1.7525
PCBP4	2.2105	1.766666667
KLF9	3.7715	1.776666667
CELA1	2.07	1.783333333
MYOM1	1.7455	1.8025
ENST00000485253	1.5855	1.815833333
RHOXF1	2.073	1.961666667
LONRF3	5.1575	1.994166667
MT1F	2.7725	2.050833333
PLA2G16	3.0085	2.135
BLVRA	2.293	2.164166667
XLOC_l2_009136	2.847	2.216666667
NTNG2	1.9215	2.2825
A1BG	3.434	2.299166667
LOC100509498	1.8205	2.299166667
GBP5	4.2005	2.308333333
ANKRD20A2	2.685	2.323333333
PAM	1.179	2.351666667
TRIM7	2.9795	2.3525
FGFR1	2.2505	2.4075
NFIA	1.959	2.409166667
C17orf51	1.7415	2.490833333
FCRLB	3.596	2.601666667
FBXO32	1.274	2.76
CTSF	1.6185	2.785
MIRLET7BHG	4.737	2.946666667
C5orf56	1.023	2.975833333
CLEC2B	1.218	3.03
ZNF618	2.2765	3.4575
HSBP1L1	2.0225	3.655833333
LOC100131733	1.329	4.075

Publishing Agreement

It is the policy of the University to encourage the distribution of all theses, dissertations, and manuscripts. Copies of all UCSF theses, dissertations, and manuscripts will be routed to the library via the Graduate Division. The library will make all theses, dissertations, and manuscripts accessible to the public and will preserve these to the best of their abilities, in perpetuity.

Please sign the following statement:

I hereby grant permission to the Graduate Division of the University of California, San Francisco to release copies of my thesis, dissertation, or manuscript to the Campus Library to provide access and preservation, in whole or in part, in perpetuity.

_____   3/21/14
Author Signature   Date